



| | Correlation between different micro-structural parameters with physical/mechanical properties of polyethylene blown films |
|-------------------------|--|
| Auteur: Author: | Shokoh Fatahi |
| Date: | 2006 |
| Туре: | Mémoire ou thèse / Dissertation or Thesis |
| Référence: Citation: | Fatahi, S. (2006). Correlation between different micro-structural parameters with physical/mechanical properties of polyethylene blown films [Thèse de doctorat, École Polytechnique de Montréal]. PolyPublie. https://publications.polymtl.ca/7767/ |

Document en libre accès dans PolyPublie Open Access document in PolyPublie

| URL de PolyPublie: PolyPublie URL: | https://publications.polymtl.ca/7767/ |
|--|---------------------------------------|
| Directeurs de recherche: Advisors: | Pierre Lafleur, & Abdellah Ajji |
| Programme: Program: | Non spécifié |

UNIVERSITÉ DE MONTRÉAL

CORRELATION BETWEEN DIFFERENT MICRO-STRUCTURAL PARAMETERS WITH PHYSICAL/MECHANICAL PROPERTIES OF POLYETHYLENE BLOWN FILMS

SHOKOH FATAHI DÉPARTMENT DE GÉNIE CHIMIQUE ÉCOLE POLYTECHNIQUE DE MONTRÉAL

THÈSE PRÉSENTÉE EN VUE DE L'OBTENTION DE DIPLÔME DE PHILOSOPIAE DOCTOR (GÉNIE CHIMIQUE) MAI 2006

© Shokoh Fatahi, 2006.



Library and Archives Canada

Branch

Published Heritage

395 Wellington Street Ottawa ON K1A 0N4 Canada Bibliothèque et Archives Canada

Direction du Patrimoine de l'édition

395, rue Wellington Ottawa ON K1A 0N4 Canada

> Your file Votre référence ISBN: 978-0-494-20825-0 Our file Notre référence ISBN: 978-0-494-20825-0

NOTICE:

The author has granted a nonexclusive license allowing Library and Archives Canada to reproduce, publish, archive, preserve, conserve, communicate to the public by telecommunication or on the Internet, loan, distribute and sell theses worldwide, for commercial or noncommercial purposes, in microform, paper, electronic and/or any other formats.

AVIS:

L'auteur a accordé une licence non exclusive permettant à la Bibliothèque et Archives Canada de reproduire, publier, archiver, sauvegarder, conserver, transmettre au public par télécommunication ou par l'Internet, prêter, distribuer et vendre des thèses partout dans le monde, à des fins commerciales ou autres, sur support microforme, papier, électronique et/ou autres formats.

The author retains copyright ownership and moral rights in this thesis. Neither the thesis nor substantial extracts from it may be printed or otherwise reproduced without the author's permission.

L'auteur conserve la propriété du droit d'auteur et des droits moraux qui protège cette thèse. Ni la thèse ni des extraits substantiels de celle-ci ne doivent être imprimés ou autrement reproduits sans son autorisation.

In compliance with the Canadian Privacy Act some supporting forms may have been removed from this thesis.

While these forms may be included in the document page count, their removal does not represent any loss of content from the thesis.

Conformément à la loi canadienne sur la protection de la vie privée, quelques formulaires secondaires ont été enlevés de cette thèse.

Bien que ces formulaires aient inclus dans la pagination, il n'y aura aucun contenu manquant.



UNIVERSITÉ DE MONTRÉAL

ÉCOLE POLYTECHNIQUE DE MONTRÉAL

Cette thèse intitulée:

CORRELATION BETWEEN DIFFERENT MICRO-STRUCTURAL PARAMETERS WITH PHYSICAL/MECHANICAL PROPERTIES OF POLYETHYLENE BLOWN FILMS

présentée par: <u>FATAHI Shokoh</u>
en vue de l' obtention de diplôme de : <u>Philosophiae Doctor</u>
a été dûment acceptée par le jury d'examen constitué de :

- M. PATIENCE Gregory S., Ph. D., président
- M. LAFLEUR Pierre G., Ph. D., membre et directeur de recherche
- M. AJJI Abdellah, Ph. D., membre et codirecteur de recherche
- M. DUBOIS Charles, Ph. D., membre
- M. MUSA R. Kamal, Ph.D., membre

Dedicated

То

My children Ashkan , Mahan and my brother Firouz

ACKNOWLEDGEMENTS

I would like to express heartfelt gratitude to my research and thesis director Professor Pierre G. Lafleur and co-director Dr. Abdellah Ajji for providing me an opportunity to study under their supervision. Indeed, I am very indebted to them for their guidance, cooperation, financial support and kind understanding throughout my study at the École Polytechnique de Montréal and the Industrial Materials Institute in Boucherville.

I would like to express my sincere gratitude to the other Professors and technical staff of the Chemical Engineering Department at the École Polytechnique de Montréal and at the Industrial Materials Institute, Boucherville, for their help in different aspects.

I would also like to thank Mr. Nick Virgilio for helping me to translate abstract and the extended abstract into French. Finally special thanks also goes to my children, Ashkan, and Mahan for their patience and understanding, my brother Firouz for his encouragement in accomplishment of my study.

RÉSUMÉ

Plusieurs chercheurs ont effectué des travaux sur la structure moléculaire du polyéthylène (PE), sur sa mise en forme et sur ses propriétés afin de prédire la performance de films de PE préparés par soufflage. Cependant, il n'existe présentement aucun modèle ou approche qui permet de prédire quantitativement, en relation avec la microstructure et le développement de la morphologie, les propriétés des films de PE préparés par soufflage. Aucune étude systématique sur la relation entre les paramètres microstructuraux des films (cristallinité, dimension des cristallites et orientation, etc.) et leurs propriétés mécaniques et physiques n'a encore été effectuée.

Trois familles de PE différents, incluant le polyéthylène linéaire basse densité (LLDPE), deux polyéthylènes hautes densités (HDPE) et un polyéthylène basse densité (LDPE) ont été utilisés pour la préparation des films soufflés. En contrôlant les conditions de la mise en forme des films, différentes structures ont été obtenues, permettant ainsi de réaliser une étude sur les paramètres structuraux. Il existe plusieurs techniques permettant de caractériser la structure des films: la biréfringence, la diffraction des rayons X aux grands et petits angles (WAXD, avec les figures de pôles, et SAXS), la microscopie à force atomique (AFM), la microscopie électronique à balayage (SEM) et la spectroscopie infrarouge (FTIR). Ces techniques ont été utilisées

pour caractériser la morphologie des films et pour déterminer et calculer les paramètres structuraux.

En premier lieu, la morphologie et l'orientation des films de PE ont été étudiées par WAXD, SEM, AFM, FTIR et mesures de la biréfringence. Les micrographies obtenues au SEM montrent la surface des films et des coupes dans les directions machine et transversale. Elles ont été comparées aux images obtenues au AFM. Il a été observé que la morphologie de la surface est en continuation avec la morphologie de volume du film.

L'orientation des régions cristallines et amorphes contrôle la structure et les performances des films soufflés. Il est donc très important de pouvoir caractériser l'orientation des zones cristallines et amorphes des films. L'orientation uniaxiale est généralement caractérisée par le facteur d'Hermans. Les paramètres d'orientation des films ont été mesurés par FTIR, XRD et biréfringence. Ils ont de plus été déterminés pour les phases cristallines et amorphes. Les mesures par FTIR ont été réalisées en transmission suivant la technique du film incliné. Un des avantages de la technique FTIR est qu'elle peut donner des informations non seulement sur la phase cristalline, comme la diffraction des rayons X, mais aussi sur la phase amorphe.

La calorimétrie différentielle à balayage (DSC), la diffraction des rayons X aux petits (SAXS) angles et la méthode des figures de pôles ont été utilisées pour déterminer le taux de cristallinité, la taille des cristaux, l'épaisseur des lamelles, la longueur moyenne des couches cristallines et amorphes, et la distance moyenne séparant les

cristallites. Les caractéristiques mécaniques importantes, incluant la résistance à la déchirure (Elmendorf), les propriétés à l'impact et les propriétés en tension dans les directions machine et transverse ont été mesurées. De plus, les propriétés optiques, notamment la transparence et la clarté, ont été mesurées. En utilisant un protocole expérimental statistique et une modélisation à plusieurs variables, ces propriétés ont été corrélées aux paramètres microstructuraux tels que le taux de cristallinité, la taille moyenne des cristallites, l'épaisseur des lamelles et les facteurs d'orientation d'Herman. Par la suite, un modèle mathématique permettant de corréler les paramètres microstructuraux aux propriétés mécaniques des films a été établi.

La dernière partie de ce travail a été d'établir un modèle fondamental/structural établissant une relation entre les paramètres microstructuraux et le module en tension des films. Un modèle pour le module en tension est proposé et est corrélé à quelques paramètres structuraux incluant la cristallinité, les facteurs d'orientation pour l'axe cristallin c et la phase amorphe, l'épaisseur des lamelles et la taille des cristaux. Les modules mesurés et calculés ont été comparés et montrent une concordance raisonnable.

Les effets des paramètres de la mise en forme (TUR, BUR et FLH) sur les propriétés mécaniques et les paramètres microstructuraux des films de PE ont été étudiés. Un protocole expérimental statistique a été utilisé pour étudier les effets majeurs liés aux paramètres microstructuraux et aux propriétés des films de PE, et ce pour différentes conditions de mise en forme. Un total de 43 essais ont été réalisés (incluant 10

différents échantillons de LLDPE, 15 échantillons de LDPE et 18 échantillons de HDPE), avec 3 variables indépendantes (TUR, BUR et FLH). Un total de 12 variables dépendantes (réponses) ont été étudiées, incluant le taux de cristallinité, la longueur des cristaux, l'épaisseur lamellaire, la taille des cristaux dans les directions (110) et (200), la rugosité et les facteurs d'orientation pour les phases cristalline (axes cristallins a et b) et amorphe dans les directions machine et transverse. Les résultats montrent que des changements dans les paramètres de soufflage, tels que le taux de gonflage (BUR), le taux d'étirage (TUR), et la hauteur de figeage (FLH) ont un effet sur les paramètres microstructuraux, la cristallinité et les propriétés mécaniques.

ABSTRACT

Several authors have investigated polyethylene molecular structure, processing and property relationships with the goal of predicting the end use performance of blown films. However, at present, a model or approach does not exist to quantitatively predict blown film properties in conjunction with their microstructure and morphology development. No systematic investigation and fundamental understanding on the interrelations between films structural parameters (crystallinity, crystallite dimensions and orientation etc.) and mechanical/physical properties has been carried out. In this thesis, a wide range of PE materials, including LLDPE, two different HDPEs and LDPE were used for preparation of the blown films. Then, by changing processing conditions, different structures for these blown films were produced and their structural parameters investigated. Different techniques for characterizing films structure were used. They include birefringence, wide angle X-ray diffraction (WAXD), small angle Xray scattering (SAXS), atomic force microscopy (AFM), X-ray pole figure analysis, scanning electron microscopy (SEM) and infrared spectroscopy. These techniques were used for the determination and calculation of structural parameters and the morphology

of the films.

SEM images of the film plane surface (MT) and cross section slices in TN and MN planes were made and compared with AFM images. It was observed that the surface morphology was a reflection of the bulk morphology.

The orientation of the crystalline and amorphous phases controls the structure and performance of the blown films. It is thus very important to be able to determine orientation characteristics of the blown films. The uniaxial orientation is generally described by the Herman's factor. The orientation parameters of the films were measured by FTIR, XRD and birefringence. They were determined for both crystalline and amorphous phases.

The FTIR measurements were made in transmission with the use of the tilted film technique. An advantage of the infrared technique is that it can give information not only on the crystalline phase, like X-ray diffraction, but also on the amorphous phase. Differential scanning calorimetry, WAXD pole figure and SAXS techniques were used to determine the degree of crystallinity, crystal sizes, lamellar thickness, the average length of the crystal and amorphous layers, and average inter-crystallite separation in the amorphous region. Finally, key mechanical properties including Elmendorf tear strength, dart drop impact, tensile properties (modulus, strength and elongation) in both MD and TD and optical properties such as haze and clarity have been measured. By using the statistical design of experiments and multivariate modeling, these properties were correlated to the microstructural parameters including the degree of crystallinity, the average size of the crystallites, lamellar thickness and

Herman's orientation factors. Then a mathematical model was performed to correlate these structural parameters and measured tensile properties of the blown films.

Establishing fundamental /structural model between structural parameters and tensile modulus of blown films was the final objective of this work. A model for the tensile modulus was proposed and correlated to some structural parameters including crystallinity, orientation factors for crystalline c-axis and amorphous phase, lamellar thickness and crystal size. The measured modulus and calculated one were compared and a reasonable agreement was found between them.

The effect of processing parameters (TUR, BUR, and FLH) on the mechanical properties and micro-structural parameters of the PE films was determined. A statistical design of experiment was used to study the major effects between the micro-structural parameters and the properties of the polyethylene films with process conditions. The experiments consisted of 43 test runs (including 10 different samples for LDPE, 15 samples for LDPE and 18 samples for HDPE) involving 3 independent variables. The independent variables are TUR, BUR and FLH and there are 12 dependent variables (responses) including crystallinity, crystal length, lamellar thickness, crystal size in (110), crystal size in (200), roughness, orientation factors for crystalline (a axis, b-axis) phase and amorphous phase in machine and transverse direction. Results show that changes in the blown film process parameters, such as take up ratio, blow up ratio and frost line height have an effect on structural parameters, crystallinity and mechanical properties.

CONDENSÉ EN FRANÇAIS

L'étude de la structure des films de polyéthylène (PE) a débuté au début des années 1950. Durant cette période, plusieurs études ont porté sur la compréhension de l'interaction complexe existant entre les paramètres de la mise en forme, de la structure et des propriétés durant le soufflage de films. Quelques-unes de ces études ont porté plus précisément sur le développement de l'orientation moléculaire et de la morphologie dans les films soufflés. D'autres ont davantage étudié les effets des paramètres de la mise en forme sur les propriétés des films soufflés. En ce qui concerne le PE, les effets de copolymère de l'éthylène sur les propriétés des films ont été étudiés. Quelques études ont, quant à elle, tenté de corréler les propriétés mécaniques des films avec la cinématique et la dynamique du procédé. Relativement peu d'études ont examiné et modélisé les propriétés des films soufflés en corrélation avec la microstructure et le développement de la morphologie. Si l'on considère la littérature portant sur ce sujet, il est clair qu'il y a des lacunes concernant la compréhension fondamentale au niveau de la relation entre la structure moléculaire et les propriétés des films soufflés. Pour établir des corrélations entre les propriétés mécaniques/physiques et les caractéristiques de la microstructure pour des films de PE, trois polymères, soient le polyéthylène basse densité (LDPE), le polyéthylène basse densité linéaire (LLDPE) et le polyéthylène haute densité (HDPE), ont été utilisés dans ces travaux. Une série de films soufflés ont été préparés en variant les conditions de mise en forme.

Dans le premier article, les paramètres de structure ont été définis par XRD, DSC et FTIR. Les résultats obtenus ont été analysés et comparés entre eux afin de déterminer la précision de chacune des méthodes. Les facteurs d'orientation d'Hermans ont été déterminés par la méthode des figures de pôles et par dichroïsme infrarouge.

Le dichroïsme infrarouge est une technique quantitative importante permettant de déterminer les fonctions d'orientation cristalline et amorphe. Ces mesures permettent d'obtenir rapidement, quantitativement et séparément les fonctions d'orientation cristalline et amorphe.

Dans les polymères polycristallins, la région cristalline est composée de cristallites, dont les dimensions peuvent être déterminées à partir de mesures de la diffraction des rayons X aux petits (SAXS) et grands (WAXD) angles de Bragg. Les informations à l'échelle nanométrique sont révélées par SAXS. Cette technique a permis d'obtenir la longue période (L) et la longueur moyenne des cristallites. Un autre avantage de la diffraction des rayons X est la possibilité, en principe, d'obtenir la distribution de l'orientation de la phase cristalline par la méthode des figures de pôles.

Le contenu cristallin et l'épaisseur des lamelles, obtenus respectivement par DSC et la méthode des figures de pôles, ont été sélectionnés pour analyse des données. Les propriétés en tension (modules ainsi que résistance et élongations au seuil

d'écoulement et à la rupture), la résistance à la déchirure (Elmendorf), la résistance à l'impact, la turbidité et la clarté ont été mesurées.

Un protocole expérimental statistique a été utilisé pour étudier les effets majeurs reliés aux paramètres microstructuraux et aux propriétés des films de polyéthylène. Le protocole suivi a consisté en 22 essais (incluant 4 échantillons de LLDPE, 8 échantillons de LDPE et 10 échantillons de HDPE) impliquant 12 variables indépendantes. Les informations obtenues à travers cette étude statistique ont permis de déterminer les effets des paramètres microstructuraux sur les propriétés. Il a été montré que certains paramètres, tels que la cristallinité et les facteurs d'orientation, ont un effet sur la plupart des propriétés mesurées. En se basant sur l'analyse expérimentale statistique, il a été observé que les propriétés en tension, les propriétés optiques et les propriétés à l'impact sont dépendantes des différents paramètres de la microstructure. Les résultats d'analyse de modélisation statistique montrent que le module dans la direction machine, les élongations au seuil d'écoulement et à la rupture dans les directions machine et transverse, la résistance au seuil d'écoulement en tension et les propriétés optiques (notamment la turbidité et la clarté) sont corrélés au taux de cristallinité, aux facteurs d'orientation pour les phases cristalline (axes a et b) et amorphe dans les directions machine et transverse, à l'épaisseur des lamelles et à la rugosité.

Dans le deuxième article, différents films obtenus par soufflage ont été mis en forme en changeant trois paramètres d'opération importants, soient le taux de gonflage (BUR), le taux d'étirage (TUR), et la hauteur de figeage (FLH). Le travail principal a

consisté à comprendre et à caractériser en détails la morphologie des films de PE soufflés. La morphologie a été caractérisée par microscopie électronique à balayage (SEM) et par microscopie à force atomique (AFM). Le MEB utilise les électrons provenant de la surface de l'échantillon pour générer des images de celle-ci, ce qui permet d'obtenir des informations reliées à la microstructure. Plus récemment, la microscopie à force atomique s'est révélée une technique d'analyse de surface particulièrement efficace. Elle est maintenant régulièrement employée pour étudier la morphologie des surfaces d'homopolymères. La microscopie à force atomique ne nécessite pas l'emploi d'agents chimiques tels que ceux utilisés pour la microscopie électronique en transmission (TEM), ni de gravures chimiques telles qu'utilisées pour la microscopie électronique à balayage. Comparativement à la microscopie à force atomique à contact permanent, la microscopie à force atomique à contact intermittent (« tapping mode AFM ») nécessite une force moindre, permet de limiter les dommages causés à la surface et élimine les problèmes de traînée dus aux forces latérales. L'effet des paramètres de la mise en forme (TUR, BUR et FLH) sur les propriétés morphologiques et mécaniques des films de PE ont été étudiés par SEM, AFM (en contact intermittent), DSC, SAXS et WAXD.

La résistance en traction, de même que les propriétés à l'impact et en tension dans les directions machine et transverse, ont été mesurées. Il est montré que ces propriétés sont influencées par l'orientation des lamelles. Pour certains échantillons de HDPE, la résistance à l'impact est nulle. Ils n'ont pas déchiré dans la direction transversale, et ce pour un pendule de masse maximale. Ce résultat est une conséquence de

l'augmentation de l'orientation dans les films après l'augmentation du TUR au cours de la production.

Le premier article montre que les propriétés mécaniques peuvent être corrélées aux paramètres microstructuraux tels que les fonctions amorphe et d'orientation, la cristallinité et la taille des cristallites. Dès lors, les propriétés mécaniques telles que le module d'Young, l'élongation à la rupture et la résistance maximum en tension ont été obtenues pour 44 films différents. Les mesures ont été comparées aux résultats des modèles mathématique et structurel à chaque étape. Dans le troisième article, un modèle permettant de relier les caractéristiques de la microstructure au module en tension a été développé. Le module en tension, qui est relié à la rigidité du matériau, a été calculé à partir de la pente initiale de la courbe de la déformation en fonction de la contrainte dans les limites de la zone élastique d'étirement.

La modélisation a été effectuée en combinant une technique de modélisation statistique (design statistique d'expériences et modélisation multivariable) avec une modélisation fondamentale.

Le modèle utilisé pour prédire le module en tension résulte d'une combinaison entre une modélisation empirique et une modélisation fondamentale/structurelle. L'approche empirique inclut un protocole expérimental statistique et une modélisation multivariable. Une modélisation multivariable, avec l'incorporation des paramètres de structure, a été utilisée pour développer un modèle permettant de prédire les propriétés des films de PE soufflés.

Un modèle du module de tension est suggéré et corrélé aux paramètres de la microstructure des films de PE tels que la cristallinité, l'épaisseur lamellaire, la taille des cristaux, la longueur moyenne des lamelles cristallines, la longue période(L) et les facteurs d'orientation pour l'axe-c cristallin et la phase amorphe. Les résultats montrent qu'il y a une relation satisfaisante entre les modules mesurés et calculés.

TABLE OF CONTENTS

| DEDICATION. | IV |
|--|-------|
| ACKNOWLEDGEMENTS | V |
| RÉSUMÉ | VI |
| ABSTRACT | X |
| CONDENSÉ EN FRANÇAIS | XIII |
| TABLE OF CONTENTS | XIX |
| LIST OF TABLES | XXIV |
| LIST OF FIGURES | XXV |
| NOMENCLATURE | XXVII |
| CHAPTER 1. INTRODUCTION AND OBJECTIVES | 1 |
| 1.1. Introduction | 1 |
| 1.2. Objectives | 3 |
| CHAPTER 2. LITERATURE REVIEW | 5 |
| 2.1. Polyethylene Types in Film Forming Processes | 5 |
| 2.2. The Structure of Polyethylene Blown Films | 8 |
| 2.3. The Relation Between Mechanical/Physical Property & Structure | 12 |
| 2.3.1. Influence of Degree of Crystallization on Mechanical Properties | es13 |

| 2.3.2. Dart Drop Impact Resistance | . 14 |
|---|------|
| 2.3.3. Elmendorf tear strength (MD and TD) | .15 |
| 2.3.4. Tensile Properties | .16 |
| 2.3.5. Haze | .17 |
| 2.3.6. Shrinkage | .18 |
| 2.4. Processing - Structure -Property Relationships in Polyethylene Blown Films | .19 |
| CHAPTER 3. ORGANIZATION OF THE ARTICLES | .26 |
| CHAPTER 4.CORRELATION BETWEEN STRUCTURAL PARAMETERS AND | |
| PROPERTY OF PE BLOWN FILMS | .28 |
| 4.1. Abstract | .29 |
| 4.2. Introduction. | .30 |
| 4.3. Experimental | .33 |
| 4.3.1. Materials | .33 |
| 4.3.2. Film Preparation. | .33 |
| 4.3.3. Morphological Observations. | .35 |
| 4.3.3.1. Scanning Electron Microscopy | .35 |
| 4.3.3.2. Atomic Force Microscopy. | .37 |
| 4.3.4. Wide-Angle X-Ray Diffraction (WAXD) | .41 |
| 4.3.5. Small Angel X-Ray Scattering (SAXS) | 42 |
| 4.3.6. Infrared Dichroism Using FTIR Spectroscopy | 45 |
| 4.3.7. Differential Scanning Calorimetry. | 46 |

| 4.3.8. Birefringence. | 46 |
|--|----|
| 4.4. Results and Discussion. | 48 |
| 4.4.1. Orientation Measurement. | 48 |
| 4.4.2. Crystal Size and Lamellar Thickness Measurement | 54 |
| 4.4.3. Mechanical Property Measurements. | 56 |
| 4.4.4. Design of Experiment | 58 |
| 4.5. Conclusions | 64 |
| 4.6. References. | 65 |
| CHAPTER 5. : INVESTIGATION ON THE STRUCTURE AND PROPERTIES OF | |
| DIFFERENT PE BLOWN FILMS | 69 |
| 5.1. Abstract | 70 |
| 5.2. Introduction. | 71 |
| 5.3. Backgrounds. | 72 |
| 5.4. Experimental | 74 |
| 5.4.1 Materials. | 74 |
| 5.4.2 Experimental Conditions. | 74 |
| 5.5. Results and Discussion. | 75 |
| 5.5.1 Scanning Electron Microscopy | 75 |
| 5.5.1.1. Surface and Bulk Images | 75 |
| 5.5.1.2. Scanning Electron Microscopy and the Effects of Process Condition | 81 |
| 5.5.2 Atomic Force Microscopy (AFM) | 82 |
| 5.5.3. Measured Properties and the Effect of Process Conditions | 88 |

| 5.5.4. Structural Characteristics and the Study of the Major Effects by Design of | |
|---|-----|
| Experiment. | 91 |
| 5.6. Conclusions | 98 |
| 5.7. References. | 99 |
| CHAPTER 6. CORRELATION BETWEEN DIFFERENT MICROSTRUCTURAL | |
| PARAMETERS AND TENSILE MODULUS OF VARIOUS POLYETHYLENE | |
| BLOWN FILMS | 101 |
| 6.1 Abstract | 102 |
| 6.2. Introduction | 103 |
| 6.3.Experimental | 106 |
| 6.3.1.Materials | 106 |
| 6.3.2 Experimental Conditions | 106 |
| 6.3.3. Crystalline content and lamellar thickness measurements | 107 |
| 6.3.4. Wide & small angle X-ray diffraction | 107 |
| 6.3.5. Mechanical Properties Measurements | 108 |
| 6.4. Results and Discussion | 109 |
| 6.4.1. Orientation Determination and Morphological Study of the Blown Film | 109 |
| 6.4.2. The Relation Between Tensile Properties & Structure | 111 |
| 6.4.3. Modeling Analysis | 112 |
| 6.4.3.1. Statistical Modeling | 114 |
| 6.4.3.2. Formulation of the Structural/Fundamental Model | 114 |
| 6.4.2.2 Evaluation of the Model | 110 |

| 6.5. Conclusions |
|---|
| 6.6. References |
| CHAPTER 7. GENERAL DISCUSSION140 |
| CHAPTER 8. CONCLUSIONS AND RECOMMENDATIONS142 |
| 8.1 Conclusions |
| 8.2 Recommendations for Future Work |
| CHAPTER 9. SCIENTIFIC CONTRIBUTIONS146 |
| REFERENCES 147 |
| APPENDIX 164 |

LIST OF TABLES

| Table 2.1. | The key features of different types of PE film resins |
|------------|---|
| Table 4.1. | Specification of materials |
| Table 4.2. | Process condition for selected samples |
| Table 4.3. | Independent variables |
| Table 4.4. | Dependent variables61 |
| Table 4.5. | Correlation between structure parameters and properties of blown PE films using |
| | effects chart62 |
| Table 5.1. | The specification of materials74 |
| Table 5.2. | Process condition for selected samples |
| Table 5.3. | Mechanical properties and process conditions for different PE films92 |
| Table 5.4. | Correlation between process conditions and polymer specifications in blown |
| | LDPE film95 |
| Table 5.5. | The correlation between process conditions and structure parameters of PE blown |
| | films using effects chart |
| Table 6.1. | The specification of the materials |
| Table 6.2. | XRD results of HDPE films |
| Table 6.3. | Process condition for selected samples |
| Table 6.4. | The measured structural parameters for HDPE127 |
| Table 6.5. | The measured structural parameters for LLDPE |
| Table 6.6. | The measured structural parameters for LDPE129 |

LIST OF FIGURES

| Figure 1.1. | A schematic illustration of the blown film process | .3 |
|--------------|---|----|
| Figure 2.1. | Schematic representation of the shish-kebab morphology | 12 |
| Figure 2.2. | Morphologies produced by crystallization under stress | 12 |
| Figure 2.3. | Tie molecules in polymer chain. | 13 |
| Figure 4.1. | Schematic of effects of the structure and processing conditions on the | |
| | mechanical properties | 32 |
| Figure 4.2. | SEM images of blown PE films (Machine Direction [†] , | |
| | Transverse Direction→) | 36 |
| Figure 4.3. | AFM images of the surfaces of blown films. | 38 |
| Figure 4.4. | 3D surface plot analysis of AFM height images of blown films | 39 |
| Figure 4.5. | The surface roughness of the samples measured by AFM | 40 |
| Figure 4.6. | SAXS intensity distribution curves for LLDPE, LDPE, and HDPE films4 | 14 |
| Figure 4.7. | Birefringence in MD, TD, ND | 47 |
| Figure 4.8. | Measured orientation functions from two FTIR and WAXD techniques | 50 |
| Figure 4.9. | Amorphous orientation functions obtained using crystallinity from DSC and | |
| | WAXD techniques. | 53 |
| Figure 4.10. | Measured lamellar thickness from two different equations | 55 |
| Figure 4.11. | Measured mechanical properties | 57 |
| Figure 5.1. | Crystalline morphology of surface of different PE blown films | 77 |
| Figure 5.2. | Comparison between surface and bulk morphologies of different PE films | |

| | $MD\uparrow, TD\rightarrow)$ | 1 |
|--------------|--|-----|
| Figure 5.3. | Morphological characteristics of PE films with different structure using | |
| | SEM83 | 1 |
| Figure 5.4. | Height and phase images of different PE films83 | 3 |
| Figure 5.5. | 3D surface plot analysis of AFM height images of blown films8 | 5 |
| Figure 5.6. | Atomic force microscopy results8 | 7 |
| Figure 5.7. | Photographs of the TD tear strength failure samples ((TD↑, MD→)90 | 0 |
| Figure 5.8. | Response surface for f_{T_b} ; TUR and BUR as independent variables98 | 3 |
| Figure 6.1. | WAXS profiles for PE blown films | 0 |
| Figure 6.2. | Schematic illustration of crystallite | 1 |
| Figure 6.3. | Measured strain at yield | 2 |
| Figure 6.4. | Measured tensile modulus | 3 |
| Figure 6.5. | Measured tensile strength | ,4 |
| Figure 6.6. | Arrangement of the polymer chains in (a) a polyethylene single crystal and | |
| | (b)View along the C-direction1 | 35 |
| Figure 6.7. | The folded chain mode in PE | 36 |
| Figure 6.8. | Crystalline lamella | 131 |
| Figure 6.9. | Takayanagi models for polymer blends1 | 38 |
| Figure 6.10. | The series-parallel (a) and parallel- series (b) | 39 |
| Figure 6.11. | Predicted and measured modulus of different PE films1 | 4(|

NOMENCLATURE

Aa Area under amorphous hump

A_c Area remaining under the crystalline peaks

E_c Tensile modulus of the crystalline region(C)

Ea Tensile modulus in the amorphous region (A)

E_{ic} Modulus value for the PE crystal

E_{ia} Modulus value of the amorphous region for PE

E_{MD} Calculated tensile modulus in MD

E_{TD} Calculated tensile modulus in TD

f Herman's orientation function

f_c Crystalline orientation function

f_{am} Amorphous orientation function

fM_a _(WAXD) Orientation function for crystalline a-axis along MD from

WAXD techniques

fM_a_(IR) Orientation function for crystalline a-axis along MD from FTIR

techniques

fT_a_(WAXD) Orientation function for crystalline a-axis along TD from

WAXD techniques

| fT_a_(IR) | Orientation function for crystalline a-axis along TD from FTIR |
|------------------------|--|
| | techniques |
| fM_b_(WAXD) | Orientation function for crystalline b-axis along MD |
| | from WAXD techniques |
| fM_b_(IR) | Orientation function for crystalline b-axis along MD |
| | from FTIR techniques |
| fT_b_(WAXD) | Orientation function for crystalline b-axis along TD |
| | from WAXD techniques |
| fT_b_(IR) | Orientation function for crystalline b-axis along TD |
| | from FTIR techniques |
| fM_amorph_(WAXE | Orientation function for the amorphous phase along MD |
| | from WAXD techniques |
| fM_amorph_(IR) | Orientation function for the amorphous phase along MD |
| | from FTIR techniques |
| fT_amorph_(WAXD | Orientation function for the amorphous phase along TD |
| | from WAXD techniques |
| fT_amorph_(IR) | Orientation function for the amorphous phase along TD |
| | from FTIR techniques |
| $\Delta 	ext{H}^\circ$ | Heat of fusion of 100% crystalline |
| I | Dart impact strength |
| I_{ref} | Dart impact strength at the reference condition |
| K | Constant value for (110) and (200) planes |

ℓ Lamellar thickness

L Long spacing period

L_c Crystal length

L_t Transverse dimension of crystallites

M Machine direction

N Normal direction

n_M Refractive indices for the machine direction

n_N Refractive indices for the normal direction

n_T Refractive indices for the transverse direction

 Δn Birefringence

 Δn_a° Intrinsic birefringence values for the amorphous phases

 Δn_c° Intrinsic birefringence values for the perfectly oriented

crystalline

 Δn_{form} Form birefringence

 Δn_{MN} Difference in refractive indices between the machine and

normal directions

 Δn_{MT} Difference in refractive indices between the machine and

transverse directions

 Δn_{TN} Difference in refractive indices between the transverse and

normal directions

P Average size of the crystalline regions

Prog T° Processing temperature

Prog Tores Processing temperature at the reference condition

Q Extruder output rate

Q_{ref} Extruder output rate at the reference condition

R₀ Die radius

R_f Final bubble radius

s Scattering vector

T Transverse direction

T Melt temperature

 T_{ref} Melt temperature at the reference condition

 T_{110} Average crystallite size in (110)

 T_{200} Average crystallite size in (200)

T_f Melt temperature

Tf° Melt temperature of 100% crystalline

V₀ Final bubble velocity

V_f Melt velocity at the die

X_c Degree of crystallinity

X_{C mass} Crystalline mass fraction

Greek letters

Λ Average dimension of crystallites

Angle between a-axis and Machine or Transverse or Normal direction

| β | Angles between b-axis and Machine or Transverse or Normal direction |
|--------------|--|
| β | Full width at half maximum |
| λ | Wavelength (m) |
| λ | Volume fraction of crystalline phase parallel to the applied tensile |
| | stress |
| δ_{e} | Basal surface free energy |
| ρς | Density of the crystalline phase |
| γ | Angles between c-axis and Machine or Transverse or Normal direction |
| Θ | Bragg's angle |
| θ | Angle between the chain axis and the chosen reference axis |
| Φ | Volume fractions of crystalline phase perpendicular to the applied |
| | tensile stress |
| ν | Volume fraction of the crystalline region |

Abbreviations

FLH

| AFM | Atomic force microscopy |
|-------------|--|
| BUR | Blow up ratio |
| BUR_{ref} | Blow up ratio at the reference condition |
| DDR | Draw down ratio |
| DSC | Differential scanning calorimetry |
| | |

Frost line height

FLH_{ref} Frost line height at the reference condition

FTIR Fourier Transform Infrared

HDPE High density polyethylene

LCB Long Chain branching

LDPE Low density polyethylene

LLDPE Linear low density polyethylene

MD Machine direction

M_N Number-average molecular weight

M_W Weight-average molecular weight

MWD Molecular weight distribution

ND Normal direction

PE Polyethylene

SAXS Small angel X-ray scattering

SCB Short chain branching

SCBD Short chain branching distribution

SEM Scanning electron microscopy

TD Transverse direction

TUR Take up ratio

WAXD Wide angle X-ray diffraction

CHAPTER 1

INTRODUCTION AND OBJECTIVES

1.1 Introduction

Polyethylene film is one of the most consumed polymeric materials today and most PE films are produced by a tubular blowing process. The film blowing process is used to produce polymer film since 1940. In this process (schematically illustrated in Figure 1.1) the molten polymer is extruded upward through an annular die to form a film, orientation is produced in the hot, amorphous material by the action of a velocity gradient. Then polymer melt undergoes shear deformation inside a tubular die and the polymer chains reorient themselves upon exiting from the die. The final die gap is much larger than the desired thickness of the film, and in addition the polymer swells on exit. The molten tube of polymer is inflated with air, forcing it to expand into the shape of a bubble. Air is simultaneously blown onto the film to cool and crystallize the polymer. The point at which the polymer crystallizes is known as the frost line height (FLH). The film continues to cool until it is collapsed by a frame then it is drawn up by a nip roller. The nip roller produces an airtight seal for the bubble and also serves to provide the axial tension to draw the film upwards. Then, the tubular bubble is subject to a biaxial stretching, which is realized by stretching the bubble along the machine direction (MD) with a take-up device and along the transverse direction (TD) by bubble expansion. The morphology produced being affected by the temperature of

the melt leaving the extruder, the ratio of the tube diameter to the die diameter (BUR),

the draw down ratio (DDR) and the freeze line height. Many parameters including

molecular orientation, polymer characteristics and the equipment characteristics (such

as die gap) also influence the morphology development of blown films. For example it

has been shown that controlled molecular orientation can result in greatly improved

physical and mechanical properties, such as tensile modulus, tensile strength, fracture

toughness and thermal stability. Therefore, characterization of film morphology is

crucial for finding relationships between structure and property.

Since the same polymer running at different conditions on the same equipment result

in a variation of film properties and optical properties, so changes in the blown film

process parameters, including cooling which influences frost line height (FLH), have

an impact on final film properties. FLH is the distance from the die where all

acceleration in film surface velocities are zero. This is where the bubble has stopped

expanding and reached its final film thickness.

DDR= Die gap
Film thickness XBUR

TUR=DDR/BUR

 $BUR=R_f/R_0$

 $TUR=V_f/V_0$

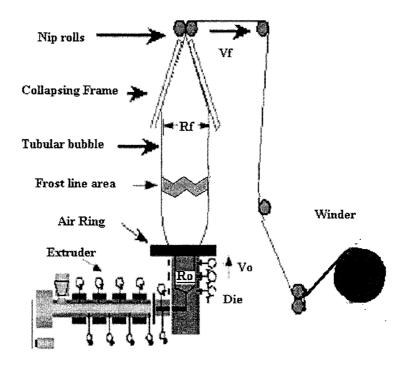


Figure 1.1. A schematic illustration of the blown film process

1.2 Objectives

In recent years, many investigations have been reported concerning very complex relationships between processing, structure and property in film blowing. The development of molecular orientation and morphology in blown films has been investigated extensively in recent years. Some researchers have attempted to correlate the mechanical properties of blown films with the kinematics and dynamics of the process. But few studies focused on the modeling of mechanical properties of blown film in terms of the microstructure and morphology development in the films. A model, providing the means for predicting the final product properties, is still not

available. The goal of this research project is to establish a model using different types of polyethylene (LLDPE, HDPE, LDPE) at different process conditions, between final properties and film microstructure. Then to achieve this goal, the objectives of the research work can be summarized as:

- To evaluate the effect of the process conditions on the microstructure of produced films.
- To correlate different micro-structural parameters with mechanical and physical properties of polyethylene (LLDPE, HDPE, and LDPE) films.
- To establish a model to predict mechanical and physical properties of the polyethylene films based on the microstructure developed during the process.

Secondary objectives are:

- To study the morphology, crystallization and orientation of polyethylene films obtained using different DDR, BUR, and FLH.
- To measure the different micro-structural parameters of the different polyethylene films.
- To determine the physical and mechanical properties of the films that will be produced at different process conditions.
- To compare the experimental data to the calculated one.

CHAPTER 2

LITERATURE REVIEW

The goal of studying the film blowing process, as in most polymer processing operations, is to obtain a maximum production rate with optimal physical and mechanical properties. Ultimate film properties are controlled by molecular orientation and stress-induced crystallization. Many parameters influence the morphology development of blown films in a very complex way. These parameters include the molecular structure, molecular orientation, polymer characteristics (such as molecular weight, molecular weight distribution and branching) and the equipment characteristics (such as die gap) as well as processing variables (such as DDR, BUR, and FLH).

2.1. Polyethylene types in film forming processes

There are four major types of polymers used to make PE films: LDPE, HDPE, LLDPE and Metallocene PE (MPE). These polymers differ from the amount of short chain branching (SCB) and long chain branching (LCB) occurring along the backbone of the molecule. SCB is particularly effective at lowering the crystallinity of the product. For

all PEs, the main parameters that govern their processing characteristics are their molecular weight (MW) and molecular weight distribution (MWD). In general PEs with higher MW or narrower MWD are more difficult to process but have better mechanical properties. In addition to MW effects, the different structures of LDPE and LLDPE especially the LCB in LDPE give further changes in their rheological response. There are main differences in processing these three types of PE. Less energy is required to extrude LDPE due to its lower viscosity at typical extrusion shear rates but LLDPE gives superior mechanical properties to LDPE due to SCB, which lowers the crystallinity of the polymer. As more equipment is adapted to make its processing more economic, the use of LLDPE is spreading. Tough films made from high molecular weight HDPE require quite different processing equipment and conditions for optimum performance and output. This product dominates specific applications such as thin carrier bags, food packing, typewriter ribbons and coextruded liners. Typical performance criteria for such HDPE films are stiffness, tensile strength, puncture resistance, resistance to tear propagation and barrier resistance. A summary of the major applications for blown film processing and the property differences between the three classes of PE are given in Table 2.1.

Table 2.1. The key features of different types of PE film resins

| Material | | Structure | | Processing | Properties | | | | |
|----------|--------|-----------|------|---|--|-----------|--------------------------|--|--|
| | MWD | SCB | LCB | Elle Waspier | Mechanical | Optical | Heat sealing | | |
| LDPE | Broad | Some | High | Excellent-high output from ; good bubble stability and low power requirements | Good | Excellent | Low seal temperatures | | |
| LLDPE | Narrow | High | None | Good drawdown for thin films but processing more difficult than LDPE | Excellent impact, tear, stiffness and puncture | Good | Good hot tack | | |
| HDPE | Broad | Low | Low | Good drawdown and bubble Stability but high power and pressure requirements | Excellent impact and stiffness Poor MD tear | Poor | High seal temperature | | |

Metallocene catalyzed polyethylenes are reported to have superior properties over conventional polyethylenes, principally due to their narrow molecular weight distribution and more uniform co-monomer distribution. However, these polymers are generally more difficult to process in film extrusion than LDPE and LLDPE. Wong et al. (1998) studied PEs with different molecular structures (LDPE, LLDPE, Metallocene). Their results showed that, LLDPE has the higher energy consumption during extrusion and LDPE the lowest. The range of FLH at which bubble stability exists can be used to evaluate the processability of the material in film blowing. For

LDPE this range is the widest and the narrowest range for MPE. In 1998 Sukhadia examined three LLDPE type resins made using chromium, metallocene and Ziegler Natta catalysts and observed that the metallocene resin had the narrowest processing window exhibiting the lowest bubble stability, highest extruder pressures and motor loads and lowest output rate for the onset of melt fracture. The blown films from this resin, however, had the best optical properties, excellent impact strengths and good tear strength. Seungoh et al. [2003] studied the bubble stability regions using an in line scanning camera. They obtained the effect of long chain branching and breadth of molecular weight distribution on the bubble instability of metallocene and Ziegler Natta catalyzes PEs (LLDPE, HDPE, LDPE, MPE). They observed that the LDPE shows the most stable processing window and the branched metallocene PEs having certain levels of LCB show better bubble stability than other PEs having broader MWD, implying that the presence of LCB plays a more important role than the broadening of the MWD.

2.2. The structure of polyethylene blown films

In this section, research work on the relationship between structure and properties and also the processing- structure- property relationships will be reviewed. However, in doing so, it is necessary to focus first on the published work on the morphology and different structures in PE blown films.

The study of the structure of extruded PE films started in the 1950s. Holmes et al. (1953) studied the structure of melt-extruded low-density polyethylene (LDPE) blown films and concluded that the a-axis of the crystal unit cell lies along the extrusion direction. This finding was confirmed by Aggarwal et al. (1959) who concluded that the crystallographic a-axis in PE blown film is oriented along the machine direction (MD), while the b -and c -axes are randomly distributed in the plane perpendicular to the a -axis. In 1954, Keller proposed that the crystal b-axis in PE blown films has a preferred orientation perpendicular to the MD while the a- and c-axes are randomly distributed with cylindrical symmetry. He postulated that there was row nucleation occurring with high molecular weight chains forming the backbone in the MD with radial growth in the b direction and the a- and c-axes rotating about that growth direction. Using the method of pole figures for high-density polyethylene (HDPE) extruded films, Lindenmeyer and Lustig (1965) found support for the row structure. In 1967 Keller and Machin further modified the model of "row nucleation" based on the level of stress for both LDPE and HDPE extruded films and suggested that the row nucleated structure is similar to the "shish-kebabs" (Figure 2.1) crystallized from the stirred solution state. According to the modified model, two major crystallization processes take place depending upon the magnitude of the stress in the melt, namely "low-stress" and "high-stress" crystallizations. Under low-stress conditions, the lamellae grow radially outward in the form of twisted ribbons, with the crystallographic b-axis parallel to their growth axis. As a result of this lamellar growth process, the a-axis of the crystal unit cell is oriented preferentially along the MD of the blown film. This texture is referred to as the Keller/Machin I (Figure 2.2a) morphology or a-texture. Under high-stress conditions, the radially grown lamellae extend directly outward without twisting. The folded chains (c-axis) within the lamellae remain parallel to the extended microfibers, resulting in the c-axis oriented preferentially along the MD. This is referred to as the Keller/Machin II (Figure 2.2b) morphology or c-texture. The Keller/Machin I morphology is the most commonly observed morphology in PE blown films .The Keller/Machin II morphology has been observed only in HDPE blown films.

Kwack et al. (1988) developed the crystalline structure of LDPE and LLDPE blown films by using WAXS, LALS, and SEM. They used the applied stresses S_{11f} and S₃₃₆, that were expressed in terms of DDR, BUR, and the pressure difference across the film of the bubble, to interpret the crystalline axes orientation in the films. It was found that the S_{11f} is an important process parameter for the crystalline axes orientation and that the biaxial stresses ratio (S_{11f} / S_{33f}) appears to be a determining factor in the distribution of fibrillous nuclei, crystalline texture and film anisotropy. Dormier et al. (1989) presented their finding of a dual crystalline texture in HDPE films. In one texture the c-axis is predominantly oriented along the transverse direction. The b-axis then orients along the machine direction and the a-axis along the machine direction. The a-axis and b-axis then randomly orient in the plane perpendicular to the machine direction.

Fruitwala et shirodkar (1994) determined the crystalline structure of HMW-HDPE and LLDPE films by WAXS and TEM. Their results support Keller 's model of row nucleation. HMW-HDPE generates high stress (due to its high viscosity), leading to c-structure. The LLDPE resin, with its lower viscosity, generates a-structure. The c-structure was found to be predominant in HDPE whereas a-structure was found to be present in the LLDPE blown films.

In 2001 Lu et al. observed an orthogonally-oriented, dual crystalline texture in HDPE films using transmission electron microscopy, small-angle X-ray scattering and infrared dichroism. In one row oriented texture, the lamellae are stacked along the machine direction; while in the other, the lamellae are stacked along the transverse direction. There was an increasing tendency toward a single MD stacked lamellar texture as the neck height decreased. The higher the neck height, the longer time available for the MD chain orientation introduced in the die to relax, and thus fewer extended chains remain to serve as nucleating point to form the MD oriented lamellar stacks. They mentioned that since the relaxation of polymer chain orientation during the film blowing process plays an important role in the structure formation of blown films, the resin melt relaxation time have a significant influence on the crystalline texture of blown films.

In 2002 Krishnaswamy and Sukhadia observed the Keller/Machin I structure for different LLDPE. Their characterization results indicate that all of the blown films display significant orientation of the a-axis in the crystalline phase along the MD and b-axis has strong orientation along the film normal direction. The c-axis isn't as

strongly oriented. In brief, the LLDPE blown film microstructure was described as a parallel array of lamellae with their long axes along the TD normal plane.

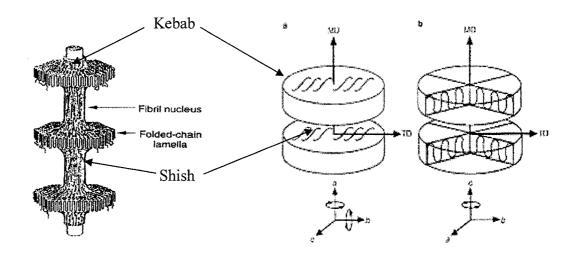


Figure 2.1. Shish-kebab morphology

Figure 2.2. Morphologies produced by crystallization under stress:

- a) Keller/Machin I morphology produced under low stress conditions;
- b) Keller/Machin II morphology formed under high stress conditions

2.3. The relation between mechanical/physical property & structure

The final properties of a product, produced from semicrystalline polymers, are to a great extend determined by their structure, which itself is established during processing of that product. The most severe effects of structure on the material

properties are discussed here. Since resistance to tear propagation, resistance to impact failure, tensile and optical properties are the most important mechanical and physical properties for blown film, this review is limited to these properties.

2.3.1. Influence of degree of crystallization on mechanical properties

It is a well-established and proven fact that a lamellar crystal is the fundamental structural form by which polymers crystallize. Schematic of a model, showing the surface of a lamella, interlamellar region and tie chains between the lamella is shown in Figure 2.3.

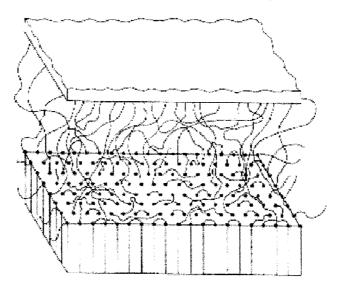


Figure 2.3. Tie molecules in polymer chain (Flory, P.J. J. Amer. Chem. Soc. 1962,84,2857.)

A semicrystallline material is generally brittle and has a low strength at temperatures below its $T_{\rm g}$. There are a number of possible reasons for this. It may be that the

crystallites impose strain on the amorphous region, or voids may be created during the crystallization process, or the crystallites may act as stress concentrators. It is known that chain ends and low molecular weight chains collect in the amorphous region. Since the strength of semicrystalline polymers comes primarily from the tie molecules between lamellae, the presence of chain ends and low molecular weight chains in the inter-lamellar region may reduce the number of tie molecules, and hence the strength of the polymer.

An increase in crystallinity is usually related to an increase in modulus and tensile strength at yield, but a decrease in the elongation at yield and break. In general some effects of the crystallization on the mechanical properties are:

- Strength and stiffness increases with increasing crystalline fraction.
- Amorphous regions provide impact toughness.
- High free volume fraction increases mobility and then dissipates the energy.
- Resistance to solvent increase with the crystallinity.

2.3.2. Dart Drop impact resistance

The dart impact strength is the energy that causes plastic film to fail under specified conditions of impact of a free-falling dart. This energy is expressed in terms of the

weight (mass) of the missile falling from a specified height that would result in 50% failure of the specimens tested.

Lu et al. (2001) show different results from studying a series of HDPE films. In these films, dual crystalline texture consisting of two row – oriented crystalline textures (an MD- stacked row crystalline texture and a TD- stacked row crystalline texture) was found. They noted that TD-stacked lamellar texture can withstand more load than the MD-stacked lamellar texture and the MD-oriented lamellar stacks are indeed relatively weak in dart impact compared to the TD-oriented lamellar stacks. It means a larger number of MD -oriented lamellar stacks are needed to gain the same strength as a small number of TD-oriented lamellar stacks. Therefore, in HDPE films with dual crystalline texture, the number of the MD- oriented lamellar stacks is the more important feature for the dart drop impact resistance.

However a good balance in structure and mechanical properties between the MD and TD usually give a high dart impact.

2.3.3. Elmendorf tear strength (MD and TD)

Tear strength is a measure of the resistance to tear propagation on a specimen with a pre-cut slit.

Fruitwala et Shirodkar (1994) correlated the Herman orientation function for the "b" axis with the tear properties of both LLDPE and HMW-HDPE films.

Lu et al. (2001) studied a series of HDPEs and reported that the trend in tear strength can be correlated to the feature of dual crystalline texture. In films with dominant MD-stacked lamellar texture, tear strength in the TD is higher than in the MD and in films with dominant TD-stacked lamellar texture, MD tear strength is much higher than the TD tear strength.

2.3.4. Tensile properties

Babel et al. (1996) determined the orientation for LDPE and LLDPE films by using Polarized infrared radiation. Their results indicated a correlation between the strain/strain rate and the dichoric ratio in 3D surface plot. Also they obtained the surface plot for impact strength against the strain and strain rates and they concluded that the dichroic ratio might be used to predict the properties of the film.

In 2000 Lu et al. studied two different LLDPE films by using stalk and non-stalk bubble configuration; one film possessed more randomly oriented lamellar texture. They mentioned that lamellar twisting may not be necessary for the formation of attexture, suggesting that the row orientation model of Keller/Machin may need some adjustment. They reported also that in films having more random lamellar orientation, the tensile behaviours in the MD and TD are similar to each other compared with other films. They also observed that the stress-strain curves for the MD stretching of both films show double yielding phenomena. The modulus (both the MD and TD) and the

yield stress at the second yield point of films with more random lamellar orientation are much lower.

Lu et al. (2001) studied the correlation between the dual crystalline texture of HDPE and the mechanical properties. They considered a Laminate Composite model for hard crystalline and soft amorphous phases that stacked along the MD. The results showed that TD tensile modulus is higher than the MD tensile modulus, because the majority of the lamellae are stacked perpendicular to the MD. In films with more biaxial orientation, similar modulus in the MD and TD are observed.

2.3.5. Haze

The gloss and haze in LLDPE films can be related to crystal size. If the film is cooled rapidly after extrusion and blowing (decreasing the FLH), the crystals will be smaller and the film will show higher gloss and lower haze. Haze is the percentage of the total transmitted light which, in passing through the specimen, is scattered from the incident beam.

Smith et al. (1996) used atomic force microscopy for PE films and studied the correlation between the haze, roughness and surface morphology. The results showed that the haze is related primarily to the surface roughness and can be reduced by lowering the frost line.

Johnson et al. (2001) applied atomic force microscopy (AFM) and small angle light scattering (SALS) techniques and found that the optical haze in LLDPE blown films, is adversely affected by enhanced surface roughness caused by the formation of spherulitic superstructures in PE having low melt elasticity characteristic. In another paper, they found that high haze in PEs blown films can be caused by very different surface roughness mechanisms having unique origins. Their results show that the total haze exhibits a parabolic relationship with the logarithm of the recoverable shear strain parameter, γ_{∞} . At low γ_{∞} , spherulitic superstructures were formed. As γ_{∞} increases, a fibril row-nucleated stacked lamella texture was developed and film exhibited lower haze. At much higher values of γ_{∞} , the resins possessed high melt elasticity, inducing a very fine-scale, elasticity-driven surface roughness that once again increased haze. Then both very low and very high melt elasticity has been a major factor in producing high haze in PE blown films.

2.3.6. Shrinkage

Patel et al. (1994) found a good correlation between MD shrinkage and Δ_{13} (difference in refractive indices between machine and normal direction) for LLDPE films. But no correlation was found between birefringence and shrinkage data on three LDPE blown films fabricated under nearly identical conditions. Lu et al. (2002) characterized the morphology of LDPE, LLDPE and their blends by using TEM, SAXS, IR dichroism

and thermal shrinkage techniques. The percentages of thermal shrinkages for the three films produced showed that both MD and TD shrinkages of LLDPE film are extremely small. LDPE film has a very large thermal shrinkage in the MD and a small shrinkage in the TD. The blend has a moderate shrinkage in the MD. They concluded that thermal shrinkage is mainly a measure of chain extension in the amorphous phase. Ajji et Zhang (2002) investigated the relationships between orientation the amorphous phase of LDPE on the shrinkage property. They assumed that shrinkage came from the amorphous phase (the amorphous region orients to the MD since MD shrinkage is higher than TD shrinkage), so they observed a correlation of MD shrinkage with birefringence and also global orientation function ($f_{global, MD}$ - $f_{global, TD}$). Haudin et al. (2003) studied the shrinkage properties of two types of LDPE blown films. They did not observe a good correlation between the orientation of the amorphous phase and shrinkage. In this study, shrinkage is more related to the orientation of the crystalline phase.

2.4. Processing - structure -property relationships in polyethylene blown films

Primary molecular parameters such as molecular weight, molecular weight distribution (MWD), type and amount of short chain branching (SCB) and short chain branching distribution (SCBD) affect processing, final film structure/morphology and properties of blown films.

The same polymer processed at different operating conditions on the same equipment result in a variation of the ultimate properties of the product. For example in the blown film process, parameters including cooling which influences frost line height, will have an impact on final film properties.

The effect of processing parameters (TUR, BUR, FLH) on the morphologies and mechanical properties of HDPE films was determined with using DSC, SAXS and Infrared Dichroism by Simpson et Harrison (1993). Their results showed that the structures for blown films are row nucleated structures with lamellae that have normals oriented in the MD in an amorphous field that has predominant chain axis orientation in the MD. As TUR was increased, the row nucleated structures became more perfectly aligned in the MD. There were no significant changes in morphology with increasing FLH. They applied composite theory in the form of a rule of mixtures to define the effect of morphology on modulus. Yield stress was higher in the MD because there were more tie chains and it took more energy to deform a crystal, along the chain direction. Higher yield strain in the MD can be attributed to the relaxed amorphous material in the MD that must be extended before crystal deformation starts. Patel et al. (1994) reported that in LLDPE films, MD tear increased with a decrease in the die gap and an increase in BUR. Increasing BUR would lead to less MD orientation leading to higher MD tear and conversely a higher DDR and lower BUR leads to lower MD tear. They also showed that dart impact increased with an increase in die gap and with an increase in BUR (Higher BUR would lead to more balanced orientation as well as to a higher degree of planar orientation therefore increasing dart impact).

Butler et al. (1994) studied the effect of process conditions on LLDPE film properties. They reported that dart impact increases with increasing BUR and FLH and the most dramatic improvement in tear was noted at high FLH. Kim et al. (1997) investigated the effect of morphological features of different HDPE on mechanical properties under various processing conditions. They observed an increasing dart impact strength with an increase in BUR (a more balanced MD/TD strength) and with an increase in molecular weight. Increasing BUR leads to a better balance of tear strengths in the MD and TD. With investigating the morphology of the failure regions by using SEM, they found that dart drop impact resistance of the films is significantly dependent on the presence of the network structure of lamellar stacks and the level of interconnectivity of the lamellar stacks. The tearing and tensile deformation behaviour of the films was also influenced by the orientation distribution of the lamellar stacks, as well as their interconnections.

Sukhadia (1998) examined different types of HDPE and LDLPE (LDLPE is a low density linear polyethylene resin which is different from conventional LLDPE resins due to its much broader MWD) via TEM, WAXS, and Infrared Dichroism. His results showed that Melt Index, density and molecular weight were ineffective in the prediction of the performance of the films. Under the same processing condition, resins with longer melt relaxation times had a greater degree of lamellar stacking and high level of molecular orientation (either a-axis or c-axis). He concluded that an

optimum structure for blown films should be such that the resin exhibits low zero shear viscosity and low relaxation times and thus the PE should contain a minimum level of long chain branching and very few or no high molecular weight tails. A good balance of lamellar orientation and molecular orientation with no predominant a-axis or c-axis orientation (well balanced structure) provided for the optimal balance of key film properties.

Ajji et al.(1998) studied the effect of processing condition on mechanical properties of polyethylene films (LLDPE and LDPE and metallocene PE). They investigated the effects of BUR and TUR on tensile properties and shrinkage and measured the birefringence and IR dichroism to characterize the orientation of the films at different process conditions. Their results showed for LDPE that the TD tensile modulus can be related to crystalline phase organization. Lamellar orientation in TD became more perfect with an increase of TUR. Increasing BUR caused disorder in lamellar stacks producing a drop in TD modulus due to imperfect lamellar orientation.

They also studied the correlation between the structure of different polyethylene and their properties. They reported tear strengths and tensile strengths in the MD and TD directions for LDPE, HDPE and different grades of LLDPE. LLDPE samples differed in terms of comonomer (Butene or Octene comonomer) and catalyst (Ziegler-Natta or Metallocene). They observed that increasing DDR for LDPE results in higher MD tear strength over TD, but in LLDPE the trends is opposite. Increasing ratio of MD/TD tear strength as DDR increases was interpreted as due to interlocked twisted lamella, but the spherulite structure in LLDPE caused balanced tear strength. They showed that

increasing DDR, increases LDPE anisotropy in tensile properties. The increasing ratio of MD/TD tensile strengths with increasing of DDR in LDPE and HDPE is related to a fibrillar structure that isn't present in LLDPE samples.

The effect of polymer specification and processing conditions on the orientation and mechanical properties of LLDPE and LDPE were presented by Ghaneh Fard et al. (1999). Their results showed that the impact resistance of the LDPE and LLDPE were significantly improved with increasing the ratio BUR/DDR. Die gap, extrusion temperature and polymer flow rate did not have any effect on this property. For LLDPE, MD and TD modulus decreased with increasing DDR and for LDPE, the modulus also decreased with increasing DDR at high BUR. At low BUR, with increasing DDR, TD modulus increased while MD modulus was not affected. At high BUR, with increasing DDR, TD modulus decreased, while the MD modulus remained constant. The extrusion temperature and FLH did not significantly influence the modulus. But for LLDPE, the modulus decreased with increasing polymer flow rate. They observed significant variations of birefringence along the TD and MD without noting any correlation between the birefringence and the tensile modulus. They concluded there are many other structural factors, besides total orientation, such as degree of crystallinity, the structure of crystalline and non-crystalline region and crystallite thickness that could affect the ultimate properties of films.

Chai et al. (2000) studied the effects of FLH, BUR, output rate and melt temperature on LLDPE (with different MWD) film properties. They quantified the effects of processing conditions on the film properties and determined predictive models for film

dart impact strength and optical haze using the following equations (I_{ref} and $Haze_{ref}$ are the impact strength and Haze at the reference conditions):

$$I = I_{ref} \times (FLH/FLH_{ref})^{0.13} \times (BUR/BUR_{ref})^{1.38} \times (Q/Q_{ref})^{-0.36} \times (T/T_{ref})^{0.30} \tag{2.1}$$

$$Haze=Haze_{ref}\times (FLH/FLH_{ref})^{0.68}\times (BUR/BUR_{ref})^{0.10}\times (Q/Q_{ref})^{-0.72}\times (Prog\ T\circ/Prog\ T\circ_{ref})^{-0.30}$$
 (2.2)

The results of tear strength did not show good correlation with processing conditions. The impact strength was the most sensitive property to polymer MWD and process conditions changes. They also found that as the molecular weight distribution narrowed the sensitivity of impact strength to process conditions increased.

The influence of processing conditions on the performance of HMW-HDPE blown films was investigated in relation to their molecular orientation characteristics by Krishnaswamy (2001). He observed that dart impact increases with increasing draw-down ratios (decreasing film thickness) and MD tear resistance increases with decreasing draw down ratio(increasing film thickness). He reported that the MD tear resistance of these films increased with increasing FLH and the TD tear resistance decreased with increasing FLH.

Johnston et al. (2003) used various LLDPE with different density and comonomer and their results showed that decreasing the cooling rate had the general effect of reducing modulus in both the TD and MD. They noted that the modulus of blown film is

affected more by the density of the sample rather than by the comonomer type used in production of LLDPE. Stress at maximum load decreased as the cooling rate was decreased and young 's modulus of the samples increased with density. Another point was related to the effect of the cooling rate on crystallinity; as the cooling rate was decreased, crystallinity of the film increased until the cooling rate was low enough that the rate of draw became the controlling factor and the level of crystallinity started to decrease.

Godshall et al. (2003) have investigated the structure of different HDPE films (different MW and MWD) using WAXS, SAXS and FESEM at different processing conditions. They reported that increasing FLH leads to relaxation of MD oriented chains before crystallization and increases the number of TD oriented chains. The orientation of the MD stacked material that is determined by the relaxation behaviour can be controlled by FLH. Increasing the DDR increased the stress and produced more TD stacked material. Increasing FLH increased the MD and decreased the TD tear strength. The impact strength increased with increasing FLH. At low output rate the polymer chains can relax prior to crystallization leading to higher impact strength.

CHAPTER 3

ORGANIZATION OF THE ARTICLES

The objective of this work was to developed practical, predictive model for rapid estimation of film mechanical and optical properties. A series of blown films were produced at different processing conditions.

By measuring experimentally the physical and mechanical properties, the relationships between important mechanical and optical properties including dart impact strength, tensile properties, tear strength, and haze with morphological features of blown films was studied. In the first article a statistical analysis was used to determine the effects of structure parameters on each property. The structural parameters were determined by studying the morphology and orientation of different polyethylene films. The orientation, crystalline content, crystal size and lamellar thickness were characterized for the films at different process conditions. WAXS pole figure technique was used to determine the orientation of the crystal phase (Herman's factors) and the amorphous orientation functions were calculated from the birefringence measurements. The measurement of lamellar thickness, crystal size, the long spacing and the length of the crystallites were accomplished by DSC, WAXD and SAXS techniques.

Based on the results of statistical technique a good correlation was observed between structure and properties. A model for the prediction of properties using structural parameters such as crystalline content, orientation functions for crystalline a-axis along MD and TD, b-axis along MD and TD, amorphous along MD and TD, crystal size and lamellar thickness roughness was found.

Since the study of PEs blown film structure can provide the knowledge about structure formation during film blowing and in turn, the effect of processing conditions on film properties. Therefore, investigation on the structure of PE blown films is the focus of the second article where the structure and morphology of various melt-extruded polyethylene blown films were studied. The orientation of lamellae and lamellar stacks and the morphology of the films were characterized by SEM, AFM and X-ray diffraction.

From the first article it was found that the statistical approach requires more test runs to determine the desired factor effects and response surfaces. For example, it is not possible to relate the dart impact strength on crystallinity and there is no explanation for the case of dependency of the tensile strength at break in MD on roughness. Therefore in the third article the set of experimental runs was increased two times (44 test runs) to improve the predictions. Modeling used for predicting tensile modulus includes empirical modeling, using statistical design of experiments and multivariate modeling, and fundamental/structure modeling approaches. Based on the statistical modeling, equations were found that relate the structural parameters including the crystalline content, lamellar thickness, crystal length, orientation factors for crystalline and the amorphous phase along MD & TD to the tensile moduli.

Then a model was developed to show how each of the structural parameters selected contributes to the magnitude of changes of the tensile properties tested.

CHAPTER 4

FIRST ARTICLE

CORRELATION BETWEEN STRUCTURAL PARAMETERS AND PROPERTY OF PE BLOWN FILMS

Shokoh Fatahi¹, Abdellah Ajji² and Pierre G. Lafleur¹

¹École Polytechnique de Montréal, Chemical Engineering Departement CREPEC

CP 6079,Succ. Centre-ville, Montréal ,Québec, H3C 3A7 Canada
²Industrial Materials Institute, NRC, 75 Boul. De Mortagne, Boucherville Québec, QC, J4B 6Y4 Canada.

Journal of PLASTIC FILM & SHEETING, October 2005, Vol. 21, 281

Correspondence concerning this article should be addressed to Shokoh Fatahi.

4.1. Abstract

Our objective in this study is to develop models which relate detailed structural parameters to performance, providing the means for predicting final films properties. In this work we used different types of polyethylene (LLDPE, HDPE, and LDPE) at different process condition in the film blowing process. The morphology of films was studied using X-ray diffraction, SEM, AFM, FTIR, and birefringence measurements. Herman's orientation factors of the films were determined via both WAXD pole figures and infrared dichroism. DSC, WAXD and SAXS were used to determine microstructural parameters including the degree of crystallinity, lamellar thickness, crystal size, length of crystal and long spacing. By using the statistical design of experiments, a correlation between mechanical properties including tensile properties, Elmendorf tear, dart impact and optical properties such as haze and clarity was obtained with the microstructural parameters.

KEY WORDS: microstructure, mechanical properties, optical properties, physical properties, blown films, LLDPE, LDPE, HDPE, crystallinity, morphology, modeling, effects of processing variables.

4.2. Introduction

Polyethylene (PE) blown film is one of the most important polymeric products today. Because of the commercial significance of PE in blown film applications, PE film manufactures have been aggressive in improving film properties and reducing manufacturing cost to become more competitive in the global market.

It is known that in the film blowing process, the primary molecular parameters are coupled with processing conditions to produce the final film morphology, which in turn determines the final film properties. In addition to these primary molecular parameters, the molecular orientation imparted during blown film is known to have a major effect on the mechanical properties of films. Therefore, characterization of film morphology is crucial for finding the structure and property relationships.

Process variables in the blown film process include:

- Temperature of the melt leaving the die
- Die gap
- Blow up ratio (BUR), defined as the ratio of final film-tube diameter to die diameter
- Take up ratio (TUR), defined as the ratio of film velocity at the nip roll to average velocity of film leaving the die
- Frost line height and cooling conditions

Figure 4.1 shows the schematic of the effects of molecular structure and processing induced secondary film structure (morphology and molecular orientation) on the mechanical properties of PE blown films.

Since the same polymer run at different conditions on the same equipment result in a variation of film properties and optical properties, so changes in the blown film process parameters, including cooling which influences frost line height, have an impact on final film properties.

Physical and mechanical properties of polyethylene are known to be strongly influenced by morphology, such as molecular orientation, size, shape and characteristics of crystalline domains. Therefore fundamental structure – property (S-P) relationships in PE blown films are important to blown-film manufacturers. Understanding of the S-P relationships should enable film manufacturers to predict the physical and mechanical properties of films and to determine the processing conditions or resin properties required for achieving certain film properties.

A number of studies have been reported in recent years concerning the interrelations among processing, film structure and physical properties of the films -and it has been well-recognized that the properties of blown films are greatly influenced by structure development during their fabrication. But from the various literature studied on this subject, it seemed that this field lacked the full development of relating the molecular structure to the properties of blown films. Therefore, it was decided to start this work aimed at a fundamental understanding of the structure-property relationships in polyethylene blown films with a goal to establish a model for predicting final film

properties of different types of polyethylene (LLDPE, HDPE, LDPE) in the film blowing process [1-16].

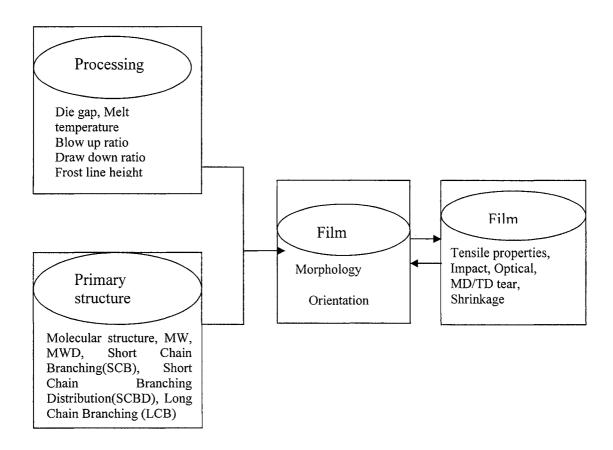


Figure 4.1. Schematic of effects of the structure and processing conditions on the mechanical properties.

4.3. EXPERIMENTAL

4.3.1. Materials

HDPE, LDPE, and LLDPE are investigated. The materials were provided by Dow Plastics Company and NOVA with the specifications listed in Table 4.1.

Table 4.1. Specification of materials.

| GRADE | MFI (g/10 min) | Density (g/cm3) | Mw | Mw/ Mn | Manufacturer |
|-----------------------|-------------------|--------------------|---------|--------|-------------------------|
| LDPE 503A | 1.9 | 0.923 | 80,900 | 5.02 | Dow Plastics Company |
| LLDPE-Octene FP 120-A | 1.0 | 0.92 | 103,200 | 3.38 | Nova Company |
| HDPE 58A | 0.41 | 0.957 | 193,885 | 12.94 | Dow Plastics Company |

4.3.2. Film preparation

PE blown films with different structures were produced at two locations. A 45 mm diameter killion single screw extruder with a helical annular die (outer diameter of 63.5 mm and a gap of 3 mm), a dual lip air ring and take up equipments was used in the École Polytechnique of Montreal for all the HDPE and LDPE samples. The mass flow rate was maintained around 2.5 kg/hr by adjusting screw speed. For the LLDPE

samples, we used a Brampton Engineering blown film extrusion line (die diameter of 101.6 mm and die gap of 1.1 mm) equipped with air cooling and using five extruders at the Industrial Materials Institute (IMI) of the National Research Council of Canada in Boucherville, Quebec. A mass flow rate of around 20 kg/h was maintained by adjusting the screw speeds of the five extrudes which were maintained at the same temperature.

The process conditions for these films are summarized in Table 4.2. The preparation of films with different structures was based on changing the process conditions, particularly varying the take up ratio (TUR) and the blow up ratio (BUR) for each type of polyethylene, while maintaining a stable bubble.

Table 4.2. Process condition for selected samples.

| | LLDPE1 | LLDPE5 | LLDPE9 | LLDPE10 |
|----------|--------|--------|--------|---------|
| TUR | 22 | 15 | 22 | 30 |
| BUR | 2.1 | 3 | 2.1 | 1.5 |
| FLH (in) | 10 | 12 | 17.2 | 10 |

| | LDPE0 | LDPE3 | LDPE5 | LDPE7 | LDPE10 | LDPE11 | LDPE12 | LDPE13 |
|----------|-------|-------|-------|-------|--------|--------|--------|--------|
| TUR | 30.5 | 20 | 30.5 | 42 | 42 | 52.5 | 42 | 64 |
| BUR | 1.7 | 1.92 | 1.5 | 1.29 | 1.47 | 1.6 | 1.64 | 1.5 |
| FLH (in) | 7.5 | 9 | 6 | 5 | 9 | 7 | 5 | 6 |

| | HDPEln | HDPE2 | HDPE2n | HDPE4n | HDPE5 | HDPE6n | HDPE7n | HDPE8 | HDPE9n | HDPE10n |
|---------|--------|-------|--------|--------|-------|--------|--------|-------|--------|---------|
| TUR | 30.5 | 42 | 42 | 64 | 64 | 85.5 | 96.5 | 107.5 | 107.5 | 107.5 |
| BUR | 1.35 | 1.05 | 1.15 | 1.25 | 0.88 | 1 | 1.08 | 0.9 | 0.88 | 0.82 |
| FLH(in) | 6 | 5.5 | 6 | 6 | 5.5 | 6 | 6 | 7 | 6.5 | 6.5 |

4.3.3. Morphological observations

4.3.3.1. Scanning electron microscopy

Molecular orientation and structure development during film blowing have a major effect on mechanical and physical properties of polyethylene films, therefore comprehensive and detailed morphological characterization of PE blown films was the core work. The film samples were observed using field emission gun-scanning electron microscopy (FEG-SEM). As an example, the SEM images for one sample of each different type of polyethylene films (LLDPE, LDPE, and HDPE) are shown in Figure 4.2. The PE films specimens were etched by soaking for 20 min in a 0.7% solution of potassium permanganate in a mixture of 65% vol sulfuric acid and 35% vol orthophosphoric acid.

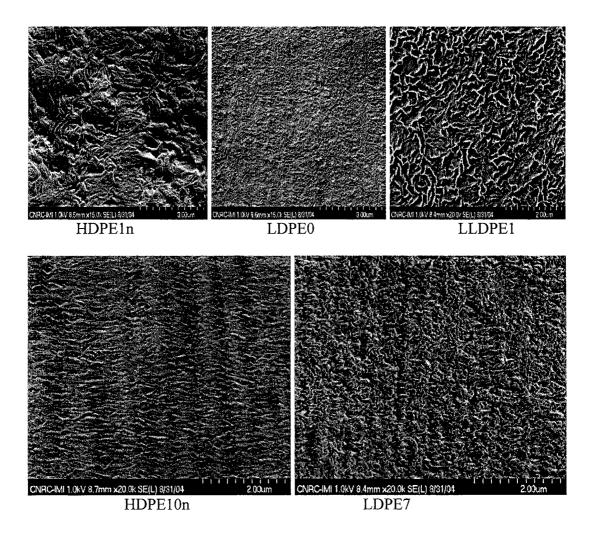


Figure 4.2. SEM images of blown PE films (Machine Direction↑, Transverse Direction→).

4.3.3.2. Atomic Force Microscopy

The surface morphologies of films were evaluated using Digital Instrument Nanoscope IV Scanning Probe Microscope operated in multimode (Veeco Metrology Group). It was used for quick determination of surface roughness of the film and to find the images of the different structures in the various blown films. Tapping modes of AFM were used to observe surface morphology (topography) of the films at room temperature. The AFM images can accumulate three types of images such as height and phase and amplitude types. In the phase images, brighter regions represent the hard crystalline phase and the darker regions usually represent soft amorphous phase.

Typical surface images and 3D images are shown in the Figure 4.3 and Figure 4.4 for LDPE, LLDPE, and HDPE. The surface roughness of the samples was determined by AFM and is shown in Figure 4.5. The surface roughness of the HDPE films was generally higher than LDPE and LLDPE.

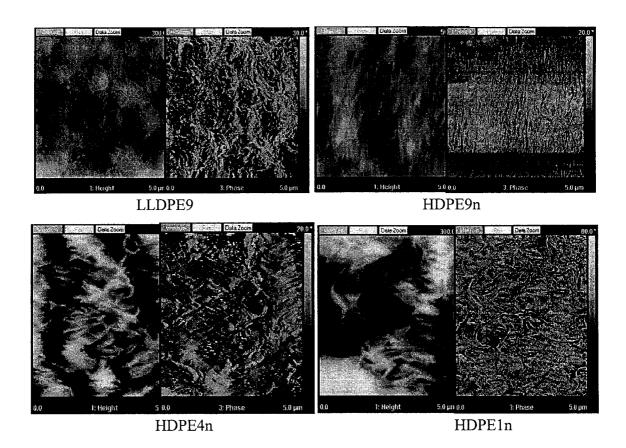


Figure 4.3. AFM images of the surfaces of blown films.

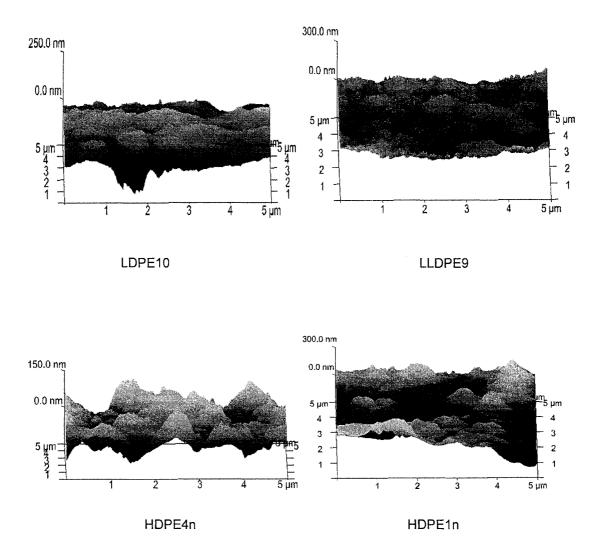


Figure 4.4. 3D surface plot analysis of AFM height images of blown films.

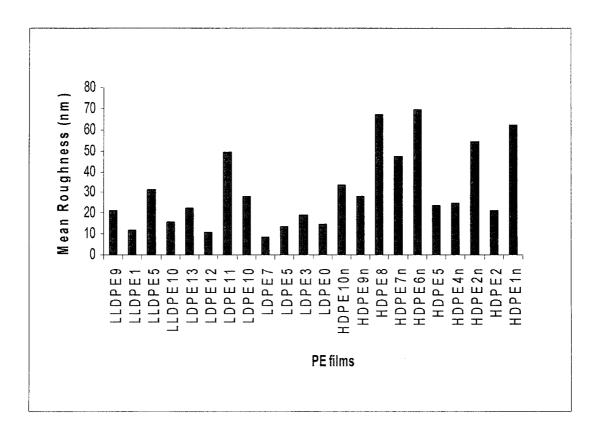


Figure 4.5. The surface roughness of the samples measured by AFM.

4.3.4. Wide-angle X-ray diffraction (WAXD)

WAXD is a useful technique for understanding oriented semi-crystalline polymers and it was used for the determination of the crystal size and crystal orientation. The use of wide-angle X-ray pole figures allows one to obtain considerable information regarding the orientation of specific crystalline axes or planes. The average size of the crystalline regions (*P*) was determined by using Scherrer formula:

$$P=0.89\lambda/\left(\beta\cos\Theta_{110}\right) \tag{4.1}$$

Where β is the full width at half maximum, Θ is the Bragg's angle, and λ is the wavelength. The transverse dimension of crystallites is calculated by:

$$L_{t}=0.94\lambda/\left(\beta\cos\Theta_{200}\right) \tag{4.2}$$

The crystalline mass fraction or degree of crystallinity is obtained through:

$$X_{\text{C mass}} = A_c / (A_a + A_c) \tag{4.3}$$

A_a: Area under amorphous hump and A_c: Area remaining under the crystalline peaks

The WAXD experiments were performed using a Bruker D8 Discover apparatus. The instrument with a Cu- K_{α} radiation (wavelength of 1.54 Å) was operated at 40 KV and 40 mA. From the WAXD pole figure technique (the (110) and (200) reflections were used), the orientation parameters, the degree of crystallinity (X_c), the average crystallite size in (200) and (110) were determined. WAXD pole figure technique was used to obtain quantitative information about crystal orientation.

4.3.5. Small angel X-ray scattering (SAXS)

SAXS is an effective tool for studying the crystalline structure in polymers at angles very close to the main beam, typically <2°. SAXS measures the distance between PE crystal centers, which is in the range of hundreds of angstrom units. Most frequently the only cooperative reflections that usually appear in the SAXS patterns occur as a consequence of the periodic arrangement of crystal lamellae along the chain-axes (c-axis) direction. This is because there is considerable disorder in crystal matching in the other two directions from crystallite to crystallite. Since the long spacing measures the distance between crystal centers, it includes the non-crystalline phase between the crystals in the c-axis direction as well. In fact the intensity of the SAXS is inversely proportional to the square of the electron density difference between the crystalline and non-crystalline regions.

The SAXS intensity distribution curves for different PE samples are shown in Figure 4.6. SAXS was carried out to determine Long spacing (L), the length of the crystallites and the average length of the amorphous layer. The well-known Bragg relation is used:

$$s = (2 \sin \Theta)/\lambda \tag{4.4}$$

$$\lambda = 1.54 \text{ Å}$$

Where λ is the wavelength and s is the scattering vector. Direct application of Bragg law to the maximum of the scattering curve (Figure 4.6) yields the long spacing L= 1/

s (at maximum point of scattering curve), where L is the average length of the crystalline layer plus the amorphous layer. The average crystal length follows from the knowledge of L and percentage crystallinity of the polymer, typically:

Crystal Length=
$$L \times (Volume fraction crystallinity)$$
 (4.5)

SAXS results indicate that the samples crystallized with a stacked lamellar morphology, with the lamellar normals oriented parallel to MD. The existence of the randomly oriented lamellar has been seen in the LDPE and LLDPE samples.

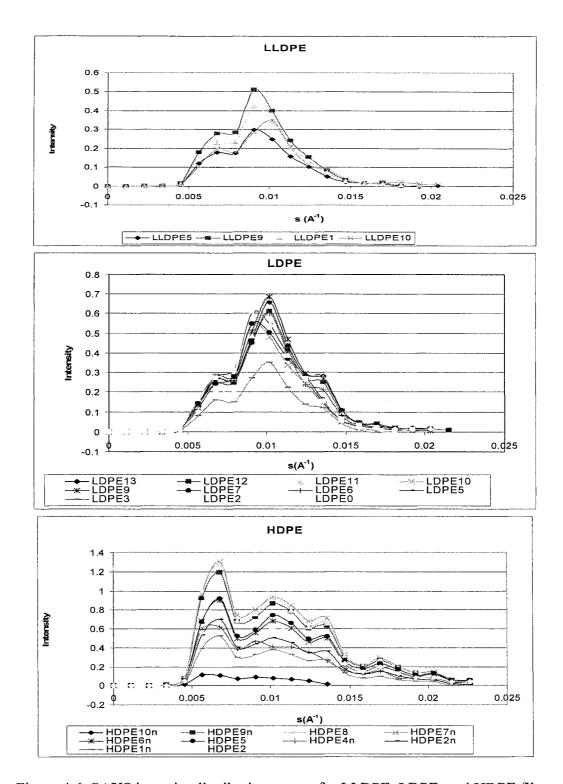


Figure 4.6. SAXS intensity distribution curves for LLDPE, LDPE, and HDPE films.

4.3.6. Infrared dichroism using FTIR spectroscopy

Infrared dichroism obtained from polarized FTIR spectroscopy is a technique for the determination of crystalline a-, b-, c-axes and amorphous orientation functions for polyethylene. The uniaxial orientation is generally described by the Herman's factor:

$$f = (3 \cos^2 \theta) - 1/2 \tag{4.6}$$

Where θ is the angle between the chain axis and the chosen reference axis (usually the machine direction). Most samples have a certain degree of symmetry with three orthogonal directions designated as machine (M), transverse (T), and normal (N). For polyethylene, the orientation functions for the a, b, and c crystallographic axis are defined as:

$$f_a = (3\cos^2\alpha - 1)/2$$
 (4.7)

$$f_b = (3\cos^2\beta - 1)/2$$
 (4.8)

$$f_c = (3\cos^2 \gamma - 1)/2$$
 (4.9)

Where α , β , γ are the angles between the unit whose orientation is of interest (a-axis, b-axis or c-axis) and a reference axis (M, T or N). The three crystallographic axes are perpendicular such that:

$$f_a + f_b + f_c = 0$$
 (4.10)

A Nicolet 170SXFTIR (Magna-IR 860) was used to obtain the raw spectra at a resolution of 2 cm⁻¹ with an accumulation of 128 scans using both a normal and tilted

incidence. A deconvolution procedure was then applied in the 720-730 cm⁻¹ spectral region to determine the dichroic ratios and orientation functions [17-18].

The Herman's orientation functions were calculated using both the Pearson VII and Lorentzian equations in HDPE/LDPE samples, and Pearson in LLDPE samples at the region between 690 and 760 cm⁻¹ [19,20]. This band could be decomposed by peak deconvolution techniques into three peaks. Two narrow peaks at 730 and 720 cm⁻¹ arise from crystalline structure and a broader peak at 723 cm⁻¹ arises from the amorphous phase.

4.3.7. Differential scanning calorimetry

Thermal analysis was performed using a Perkin-Elmer Pyris-7. The percentage of crystallinity of samples were obtained from DSC results were be used as independent variables in the modeling. The heat of fusion of 100% crystalline PE was taken as 289 J/g [21] and the heating rate used was 10° C/min.

4.3.8. Birefringence

Birefringence is a measure of the total molecular orientation of a system. It is defined as the difference between the different refractive indices for the machine, transverse and normal direction. $\Delta n_{MT} = n_M - n_T$, $\Delta n_{MN} = n_M - n_N$ and $\Delta n_{TN} = n_T - n_N$. The technique we use for its measurement is the multiwavelength polarized white light

technique and light is directed through at least two beams at different angles. Figure 4.7 shows the results for birefringence in M,T, N directions. It is obvious that HDPE films have higher birefringence than that LDPE and LLDPE films that is due to the increase of the orientation due to increasing of TUR in production of HDPE films.

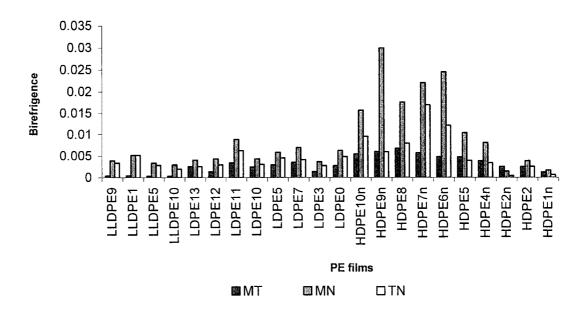


Figure 4.7. Birefringence in MD, TD, ND.

4.4. Results and discussion

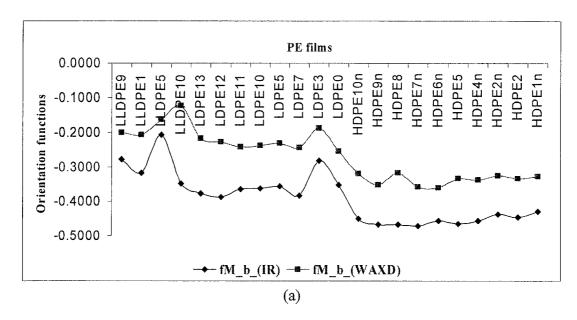
4.4.1. Orientation measurement

The orientation in both crystalline and amorphous phases is important in determining the mechanical properties of PE blown films. SEM was used to observe the orientation of lamellae and lamellar stacks directly. Further, the WAXD pole figure technique was used to obtain quantitative information about crystal orientation. Fourier transform infrared (FTIR) dichroism experiments were performed to compare with the WAXD results. The calculated Herman's functions for crystalline a-, b-, c-axes and amorphous phase are shown in Figure 4.8. It is obvious from Figure 4.8(a) that the orientation function obtained from FTIR had a quite similar trend for all samples when it is compared with WAXD results, but the values from IR were higher than those from the WAXD pole figure technique. The amorphous orientation functions from FTIR technique were not reasonable (Figures 4.8(e), (f)), because the amorphous orientation should be more oriented in MD. In this work, the Herman's factors that were obtained from WAXD pole figure technique were considered in statistical data analysis and the amorphous orientation functions were calculated from:

$$\Delta n = X_c f_c \Delta n_c^{\circ} + (1 - X_c) f_{am} \Delta n_{am}^{\circ} + \Delta n_{form}$$
 (4.11)

Where Δn is the birefringence of the polymer, f_c and f_{am} are the crystalline and amorphous orientation functions, Δn_c° and Δn_a° are the intrinsic birefringence values

for the perfectly oriented crystalline and amorphous phases, X_c is the crystal weight fraction, and Δn_{form} is the form birefringence due to the distortion of the electric field of the light wave at the anisotropic phase boundary. Δn_{form} is generally neglected, since it is just 5-10 % of the total birefringence [22]. In the case of polyethylene, the value Δn_c° =0.058 was determined; Δn_{am}° values were found at various sources in the literature.



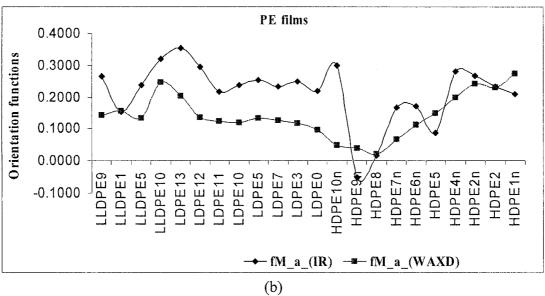
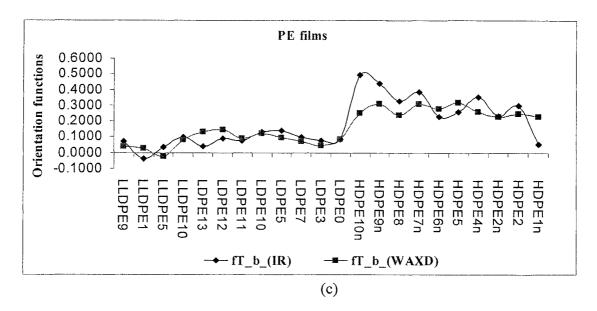


Figure 4.8. Measured orientation functions from two FTIR and WAXD techniques: (a) Orientation factors of crystalline b-axis in MD; (b) Orientation factors of crystalline a-axis in MD; (c) Orientation factors of crystalline b-axis in TD; (d) Orientation factors of crystalline a-axis in TD; (e) Orientation factors of amorphous phase in MD; and (f) Orientation factors of amorphous phase in TD.



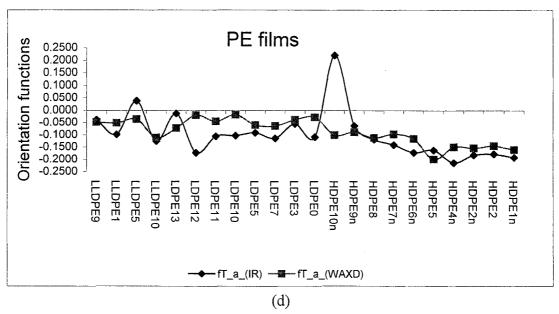
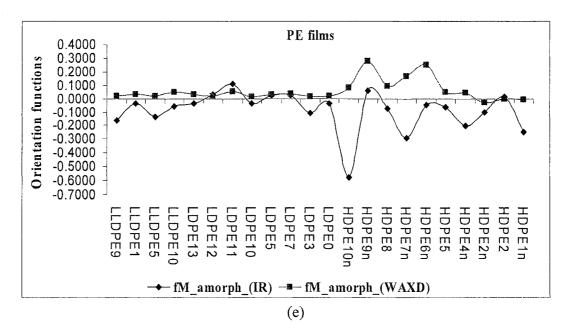


Figure 4.8. Continued



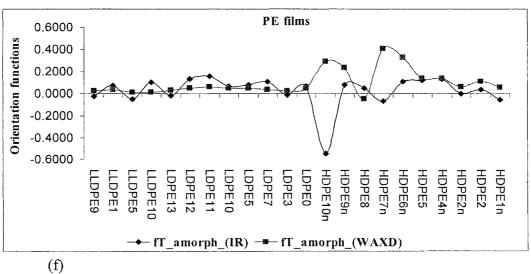


Figure 4.8. Continued

The crystalline contents were obtained by DSC and WAXD techniques and they were used in Equation (4.11) to calculate the amorphous orientation factors for MD and TD. The results are shown in Figure 4.9.

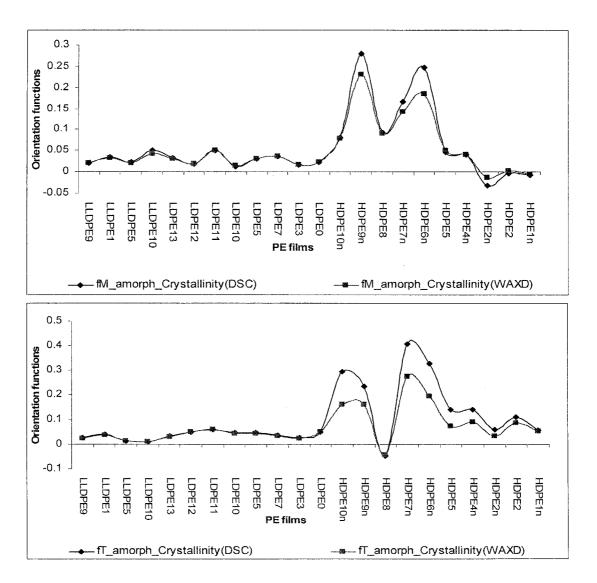


Figure 4.9. Amorphous orientation functions obtained using crystallinity from DSC and WAXD techniques.

4.4.2. Crystal Size and Lamellar Thickness Measurement

Lamellar thickness and its distribution are important morphological characteristics of semicrystalline polymers. The measurement of dimension of crystal and lamellar thickness were accomplished by SAXS, WAXD and DSC techniques, because the melting temperature of polymer crystals is related to lamellar thickness.

The Gibbs-Thomson equation (simplified) and Wunderlich equation applied to obtain the thickness of lamellae at melt temperature [21,23].

$$\ell = 2\delta_{e} T f^{\circ} / (\Delta H^{\circ} \rho c (T_{f}^{\circ} - T_{f}))$$
(4.12)

$$\ell = 414.2 \times 0.627/(414.2 - Tf)$$
 (4.13)

 T_f and ℓ are respectively the melt temperature (°K) and the thickness of lamellae, and δ_e is the basal surface free energy (one of the hypotheses is that the amount of δ_e for all samples including - LDPE, LLDPE, and HDPE - are constant at 90 erg/cm²), $\Delta H^\circ = 289 \text{J/g}$ (Heat of fusion of 100% crystalline), $\rho c = 0.995$ g/cm3 (the density of the crystalline phase), $Tf^\circ = 418.7^\circ \text{K}$ (melt temperature of 100% crystalline).

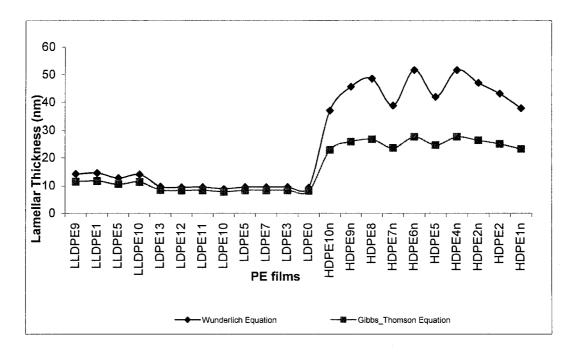
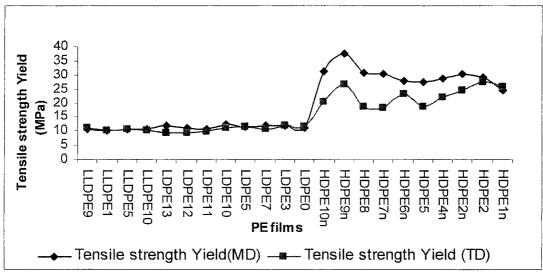


Figure 4.10. Measured lamellar thickness from two different equations.

Figures 4.9 and 4.10 show that in the HDPE case, the gap between the results (orientation factors and lamellar thickness) from different methods is bigger than LLDPE and LDPE cases.

4.4.3. Mechanical property measurements

The tensile properties of the films were evaluated according to ASTM D 882-02 using an Instron tensile testing machine at room temperature. The mechanical properties were measured in MD and TD directions for Young's modulus, elongation at break, elongation at yield, tensile strength at break and tensile strength at yield. The tear strength (MD and TD tear resistance) of films was measured according to ASTM D1922. The haze was measured according to ASTM D 1003. The impact resistance of the films was evaluated in accordance with ASTM D1709-98. Some mechanical properties measured for the PE films are shown in Figure 4.11.



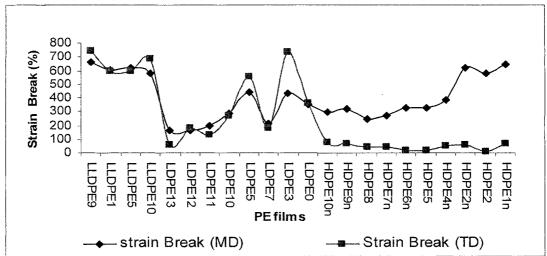


Figure 4.11. Measured mechanical properties.

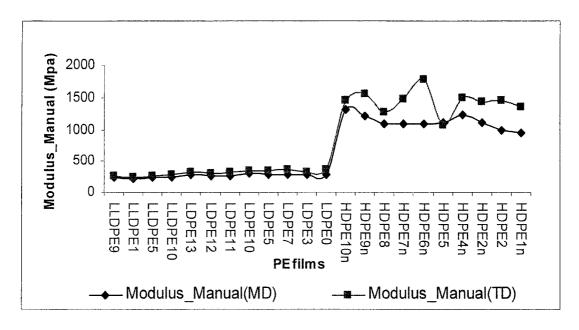


Figure 4.11. Continued

4.4.4. Design of experiment

A statistical design of experiment was used to study the major effects between the micro-structural parameters and the properties of polyethylene films. The experiment consisted of 22 test runs (including 4 different samples for LLDPE, 8 samples for LDPE, 10 samples for HDPE) involving 12 independent variables. The independent variables and dependent variables (responses) are shown in Tables 4.3 and 4.4 respectively. These test data were used to generate equations to describe the factor effects on each of the mechanical and physical properties.

A stepwise Regression approach was used and each response was regressed against all independent factors. The results of stepwise regression summary are shown in Table 4.5. Table 4.5 indicates which structure parameters caused a statistically significant (>95%) effect on the properties of the PE films. The parameters are listed down the left side of the table. The properties are listed across the top of the table. If a coefficient is listed on the line of a parameter, then that parameter has a significant effect on the corresponding property. These coefficients can be used to predict the individual film properties.

Based on the effects chart, it is obvious that there are correlations between the properties such as the Modulus in MD and TD; Tear strength in TD, tensile strength at break in MD and TD, tensile strength at yield in MD and TD, strain at break in MD and TD, strain at yield in MD and TD, haze and clarity with structural parameters including the crystalline content, lamellar thickness, orientation parameters for crystalline a-axis along MD, b-axis along MD and TD, the amorphous phase along MD and TD. For example, Table 4.5 shows that dart impact strength depends mainly on the lamellar thickness and orientation of the b-axis along MD and TD, a-axis along MD. The modulus in TD, the tensile strength at yield in MD and TD, haze and clarity are affected by the crystallinity.

Table 4.3. Independent variables.

| | Gystallirity | Cystallinity Crystal length (Lc) | landlar Thickness | Gystal size(110) | Cystal size(200) | | ff a (WWD) | (WWXD) | IT b (WWXD) 1 | Manuph (WWD) | Ma (WAX) fla (WAX) fly (WAX) fly | Ruginess |
|-------------|--------------|----------------------------------|-------------------|------------------|----------------------|--------|------------|---------|---------------|--------------|--|----------|
| GHIII | 37.75 | 377 | 1422 | 3639 | 3059 | 0.1410 | -00481 | -02005 | 0.0373 | 60200 | 0024 | 21.4 |
| IIII | 41.43 | 416 | 1455 | 3617 | 3037 | 01550 | -00511 | -02055 | 0020 | 00340 | 00000 | 11.7 |
| HIPES | 3831 | 338 | 1276 | 3683 | 31.05 | 01320 | -00338 | -0.1620 | -00020 | 00221 | 00125 | 31.5 |
| HINE 100 | 40.70 | 363 | 1403 | 39.77 | 3266 | 02420 | -01110 | -01230 | 00810 | 00200 | 60100 | 159 |
| UNE | 3991 | 355 | 973 | 4016 | 31.66 | 02040 | -00059 | -02160 | 01283 | 00318 | 0.0323 | 221 |
| 117902 | 3992 | 360 | 925 | 3428 | 3038 | 01360 | -00168 | 1/220- | 0.1434 | 16100 | 00488 | 109 |
| HEREIT | 39.13 | 348 | 1976 | 37.43 | 3279 | 01240 | -004/6 | -02406 | 0000 | 00514 | 9000 | 49.5 |
| OGHIII | 4230 | 424 | 830 | 3648 | 32.78 | 01200 | -00178 | -02374 | 01179 | 00132 | 000 | 282 |
| OHII | 4123 | 414 | 196 | 4071 | $\mathfrak{B}\Theta$ | 01260 | -00638 | 02730 | 00087 | 0.0338 | 00067 | 84 |
| IINES | 4123 | 414 | 196 | 3963 | 31.50 | 01330 | -00997 | -02315 | 00039 | 00301 | 191010 | 13.5 |
| EHII | 4509 | 326 | 196 | 3236 | 3288 | 01160 | -00384 | -0.1866 | 00451 | 00171 | 95700 | 192 |
| OHI | 37.73 | 418 | 938 | 3611 | 3203 | 00068 | -00079 | 4520- | 93300 | 00238 | 3000 | 144 |
| HYFOR | 72.59 | 1225 | 37.0I | 49.68 | 37.85 | 00400 | -01000 | -03180 | 0220 | 00798 | 81620 | 33.6 |
| HTFBh | 68.38 | 656 | 4500 | 4678 | 3636 | 00938 | -00888 | -03331 | 03084 | 16220 | 02345 | 280 |
| нж | 7021 | 984 | 4854 | 47.19 | 3803 | -00235 | -0.1120 | -03170 | 93050 | 00935 | -00475 | 67.2 |
| HHE | 6873 | 196 | 3885 | 4648 | 35.85 | 00067 | -0000 | -03574 | 16020 | 01667 | 04071 | 468 |
| HFF | 71.28 | 1001 | 51.76 | 21.00 | 41.05 | 01130 | -01160 | -03-00 | 89/20 | 02481 | 03222 | 69.4 |
| HIRS | 1269 | 696 | 4200 | 469 | 3819 | 0.1480 | -01990 | -03343 | 03152 | 00474 | 0.1411 | 236 |
| HTHE | 71.77 | 1008 | 51.76 | 4073 | 3688 | 01980 | -01500 | -03377 | 98570 | 00414 | 0.1411 | 246 |
| HIME | 2065 | 166 | 47.07 | 4868 | 39.56 | 02430 | -01540 | -03257 | 19770 | -0032 | 000 | 545 |
| HHZ | 69:69 | 9.73 | 4316 | 4673 | 3230 | 0230 | -0.1450 | -03339 | 05460 | -00084 | 01033 | 21.3 |
| HTFI | 69:69 | 926 | 37.91 | 430 | 33.50 | 02740 | -01600 | +0220- | 02280 | 69000- | 0000 | 621 |
| | | | | | | | | | | | | |

Table 4.4. Dependent variables.

| | MD Tensile | : MD strain | MD Tensile MD strain MD Tensile MD strain | MD strain | | MD Modulus | TD Tensile TD strain | TD strain | TD Tensile | TD strain | | TD Modulus | DART | Tear strength | - 1 | Haze | Clarity |
|---------|------------|-------------|---|-----------|--------|------------|----------------------|-----------|------------|-----------|--------|------------|--------|---------------|------|------|---------|
| | strength | @Yield | strength | Break | (N | (MPa) | strength | @Yield | strength | @Break | (M) | (MPa) | impact | Ø | | % | % |
| | Yield(MPa) | % (| Break(MPa) | % (| Manual | Automati | Automatic Yield(MPa) | % | Break(MPa) | % | Manual | Automatic | 500 | m#/6 | mn/8 | | |
| LLDPE9 | 10.5 | 14.0 | 31.9 | 9.659 | 235.7 | 232.1 | 10.9 | 13.7 | 29.4 | 746.9 | 261.2 | 255.9 | 296.0 | 16.1 | 28.2 | 9.7 | 98.8 |
| LLDPE1 | 10.1 | 13.4 | 30.0 | 601.2 | 223.2 | 217.9 | 10.1 | 12.6 | 18.2 | 596.9 | 245.7 | 246.9 | 336.0 | 14.8 | 27.2 | 6.4 | 97.9 |
| LLDPES | 5 10.5 | 13.3 | 23.4 | 621.7 | 233.7 | 234.2 | 10.5 | 14.1 | 17.9 | 593.1 | 264.3 | 258.6 | 480.0 | 17.3 | 24.2 | 8.2 | 0.66 |
| LLDPE1 | 10.5 | 12.0 | 38.5 | 576.0 | 241.4 | 227.2 | 10.3 | 10.7 | 20.8 | 687.4 | 277.4 | 278.5 | 174.0 | 8.9 | 29.6 | 5.2 | 9.66 |
| LDPE13 | 11.9 | 12.1 | 14.5 | 164.8 | 286.7 | 221.5 | 9.1 | 4.6 | 4.9 | 8.09 | 329.2 | 326.9 | 15.8 | 7.3 | 8.2 | 6.3 | 91.2 |
| LDPE12 | 11.0 | 11.9 | 16.3 | 166.3 | 259.7 | 201.0 | 9.2 | 6.4 | 5.4 | 176.5 | 312.9 | 312.0 | 4.0 | 9.4 | 7.4 | 9.9 | 92.0 |
| LDPE11 | 10.7 | 12.4 | 14.2 | 9.961 | 256.0 | 194.2 | 9.8 | 8.9 | 5.0 | 132.0 | 324.1 | 326.4 | 8.9 | 7.2 | 8.9 | 6.5 | 90.3 |
| LDPE10 | 12.1 | 11.9 | 10.1 | 283.4 | 298.1 | 251.5 | 10.8 | 8.1 | 7.6 | 265.6 | 349.1 | 346.7 | 11.8 | 9.6 | 12.1 | 6.4 | 91.9 |
| LDPE7 | 11.7 | 12.6 | 12.8 | 210.1 | 290.3 | 224.1 | 10.6 | 7.9 | 5.2 | 176.1 | 361.9 | 362.2 | 13.9 | 12.3 | 9.5 | 7.0 | 91.0 |
| LDPES | 11.2 | 13.2 | 16.4 | 441.7 | 274.4 | 222.4 | 11.2 | 9.3 | 11.1 | 551.9 | 347.7 | 346.5 | 22.3 | 28.3 | 21.6 | 6.4 | 93.7 |
| LDPE3 | 11.6 | 14.6 | 10.3 | 431.6 | 289.0 | 283.5 | 11.9 | 11.8 | 14.6 | 737.7 | 333.3 | 326.1 | 49.5 | 4.9 | 8.1 | 9.4 | 92.4 |
| LDPE0 | 10.9 | [4.] | 12.3 | 353.6 | 280.2 | 217.1 | 11.3 | 9.3 | 8.7 | 361.4 | 354.4 | 354.5 | 38.5 | 8.7 | 10.8 | 9.6 | 86.4 |
| HDPE101 | 31.1 | 4.8 | 58.3 | 293.3 | 1303.7 | 1185.6 | 20.4 | 2.2 | 14.9 | 9.02 | 1444.7 | 1519.6 | 0.0 | 9.0 | 6.7 | 54.5 | 34.9 |
| HDPE9n | 37.5 | 0.9 | 71.4 | 318.3 | 1222.2 | 1113.0 | 26.4 | 3.2 | 17.1 | 64.8 | 1553.6 | 1371.5 | 0.0 | 0.7 | 12.2 | 51.3 | 34.7 |
| HDPE8 | 30.9 | 6.0 | 44.2 | 243.7 | 1094.9 | 933.2 | 18.6 | 2.3. | 12.2 | 36.8 | 1275.5 | 1279.2 | 0.0 | 0.3 | 9.3 | 58.1 | 33.0 |
| HDPE7n | 30.2 | 5.3 | 46.7 | 273.2 | 9.8601 | 1047.9 | 18.3 | 2.0 | 8.8 | 41.5 | 1481.4 | 1537.2 | 0.0 | 0.3 | 16.1 | 58.4 | 32.5 |
| HDPE6n | 1 27.8 | 4.7 | 38.5 | 324.8 | 1085.7 | 1112.7 | 23.0 | 1.6 | 16.4 | 13.5 | 1782.7 | 1799.5 | 0.0 | 0.4 | 16.0 | 63.3 | 26.0 |
| HDPE5 | 27.4 | 5.0 | 35.1 | 327.0 | 1109.2 | 1096.3 | 18.6 | 2.7 | 12.2 | 15.9 | 1074.6 | 1090.2 | 0.0 | 0.7 | 13.1 | 71.3 | 19.5 |
| HDPE4n | 28.5 | 4.5 | 46.8 | 382.7 | 1226.1 | 1229.6 | 22.0 | 2.4 | 12.0 | 48.2 | 1489.2 | 1498.8 | 0.0 | 0.3 | 29.6 | 65.2 | 24.9 |
| HDPE2n | 30.2 | 6.5 | 44.2 | 621.6 | 1112.9 | 1107.9 | 24.4 | 2.4 | 16.8 | 54.2 | 1441.1 | 1461.4 | 1.3 | 0.5 | 38.3 | 74.4 | 16.0 |
| HDPE2 | 29.1 | <i>L</i> .9 | 47.5 | 582.8 | 987.7 | 1009.3 | 27.5 | 2.6 | 21.4 | 6.7 | 1453.0 | 1468.2 | 3.8 | 0.7 | 24.3 | 9.07 | 17.8 |
| HDPE1n | 24.6 | 6.5 | 31.3 | 645.2 | 953.5 | 1015.3 | 25.7 | 2.8 | 16.4 | 1.19 | 1356.2 | 1363.4 | 3.7 | 0.4 | 17.8 | 72.9 | 15.6 |
| - | | | | | | | | | | | | | | | | ĺ | İ |

Table 4.5. Correlation between structure parameters and properties of blown PE films using effects chart.

| Clarity | | | -0.62 | | | | | | | 0.33 | | | | |
|---|---|--|---------------|---------------------|--------------------|-------------------|-------------------|-------------|-------------|-------------|-------------|------------------|------------------|-----------|
| Haze (| | | 0.46 | | | | | | | -0.21 | | -0.12 | | |
| trength | | TD | | | 1.86 | | | 0.46 | | | -0.93 | | | |
| Tear st | | MD TD | | | | | | | | | | | | |
| DART | impact | | | | 1.59 | | <i>LL</i> '0- | -0.4 | | 0.61 | -1.47 | | 0.33 | |
| snInpo | (OI | AUT | 0.69 0.61 | | 0.67 0.27 0.3 | | | 0.19 0.15 | 0.32 0.26 | | | | 0.11 | |
| M | | Mar | 0.69 | | 0.27 | 0.14 | | 0.19 | 0.32 | -0.1 | | 0.11 | | |
| Strain (6 | Break | (TD) | | | 19.0 | | | | | 0.71 | -0.71 | | | |
| Tensile | strength Yield strength Break (TD) impact | Break(TD) | | | 1.88 | | 6.0- | | | | -1 | | | |
| Strain @ | Yield | (TD) | | | 0.46 | | | -0.27 | | | -1 | | | |
| Tensile Strain @ Tensile Strain @ Modulus DART Tear strength Haze Clarity | strength | Yield(TD) | 0.91 | | | | | 0.31 | | | | | | |
| snIn | D) | AUT | | 0.4 | 0.22 | | | | | | | | 60.0 | |
| Modulus | M) | Man | | 0.64 | 0.23 | | | | | · | 0.16 | | | |
| Strain | Break | (MD) | | | | | | 0.54 | | | | | | |
| Tensile | strength Break (MD) | Break(MD) (MD) Man AUT Yield(TD) (TD) Break(TD) (TD) Man AUT | | | 1.12 | | -0.57 | | | 0.64 | | | | -0.27 |
| Strain | @Yield | (MD) | -0.74 | | | | | | | | -0.34 | | | |
| Tensile | strength (ayYield | Yield(MD) (MD) | 1.1 | | | | | | | | | | | |
| | | ; | Crystallinity | Crystal length (Lc) | Lamellar thickness | Crystal size(110) | Crystal size(200) | fM_a_(WAXD) | fT_a_(WAXD) | fM_b_(WAXD) | fT_b_(WAXD) | fM_amorph_(WAXD) | fT_amorph_(WAXD) | Roughness |

From statistical study concerning a set of independent values and a corresponding set of dependent values, it was found some functional form that will relate the dependent values to the independent values. The main approach in these studies is to select linear relationships as the functional form for the properties that show a linear relationship. A linear equation or mathematical model explicitly defining the dependent variables (properties) is obtained of the form:

Property=
$$A + B(X1) + C(X2) + ...$$

Where B, C,.. are regression coefficients and A is a pure constant . X1, X2, ... are the independent variables. For example, Modulus (Aut) can be calculated by this equation using Table 4.5:

Modulus (TD) =
$$(A + 0.61 \times Crystallinity) + (0.3 \times Lamellar thickness) +$$

 $(0.15 \times fM \ a) + (0.26 \times fT \ a) + (0.11 \times fT-amorph)$

From Tables 4.3 and 4.4, it is obvious that the information gained through the statistical study can be used to determine the effects of parameters on each property, but it should be pointed out that the statistical approach was based on a limited set of experiments (22 test runs) and thus are not definitive. For example in the case of dependency of tensile strength break at MD on roughness and the independency of Dart impact strength on crystallinity, there is no explanation. Although it is generally accepted that the effects chart could provide guidance to develop practical, predicative

models for the estimation of PE film properties, it is clear that it requires more test runs at commercial production levels to determine the desired factor effects that are under study.

4.5. Conclusions

A systematic investigation provided fundamental understanding on the interrelations between polyethylene films structural parameters (crystallinity, crystallite dimensions and arrangement, orientation etc.) and physical properties. There are different techniques for characterizing the film structure including birefringence, WAXD, SAXS and AFM, X-ray pole figure analysis, SEM, and infrared radiation. These techniques were used for determination and calculation of structural parameters and the morphology of the films.

By changing the processing conditions and producing different structures for LDPE, LLDPE, and HDPE blown films, the study of structural parameters was combined and with measuring the physical and mechanical properties (tensile property, tear strength, dart impact strength, haze and clarity), so that models for each property were defined.

Statistical analysis showed that parameters such as lamellar thickness, crystallinity and orientation factors have a significant effect on majority film properties. Tear strength, dart impact strength, tensile and optical properties are

important in many film applications; and based on the statistical technique it was observed that many of these properties correlate with various structure parameters (crystalline content, orientation functions for crystalline a-axis along MD and TD, b-axis along MD and TD, amorphous along MD and TD, lamellar thickness and roughness).

4.6. References

- 1. Lu, J., Zhao, B. and Sue, H.-J. (1999). ANTEC Proceedings, pp. 1768–1774.
- 2. Krishnaswamy, R.K. and Sukhadia, A.M. (2000). Polymer, 41(26): 9205–9217.
- 3. Krishnaswamy, R.K. (2001). Structure-property Relationships in HMW-HDPE Blown Films, In: *ANTEC Proceedings*, pp. 111–115.
- 4. Babel, A.K., Nagarajan, G. and Campbell, G.A. (1996). *ANTEC Proceedings*, pp. 2112–2119.
- 5. Lu, J. and Sue, H.-J. (2000). J. Materials Sci., **35**(20): 5169–5178.

- 6. Patel, R.M., Butler, T.I., Walton, K.L. and Knight, G.W. (1994). *Polymer Engineering and Science*, **34**(19): 1506–1514.
- 7. Simpson, D.M. and Harrison, I.R. (1993). *ANTEC Proceedings*, pp. 1206–1209; also (1994). A Study of the Effects of Processing Prarameters on the Morphologies and Tensile Modulus of HDPE Blown Films: Application of Composite Theories on a Molecular Level to Characterize Tensile Modulus, *J. Plas. Film & Sheeting*, **10**(4): 302–325.
- 8. Kim, Y.-M., Kim, C.-H., Park, J.-K., Lee, C.-W. and Min, T.-I. (1997). *J. Appl. Polym. Sci.*, **63**(3): 289–299.
- 9. Sukhadia, A.M. (1998). ANTEC Proceedings, pp. 160-168.
- 10. Godshall, D., Wilkes, G., Krishnaswamy, R.K. and Sukhadia, A.M. (2003). *Polymer*, **44**(18): 5397–5406.
- 11. Haudin, M.J., Piana, A., Monasse, B. and Gourdon, B. (2003). *Ann. Chim. Sci. Mat.*, **28**(1): 91–107.

- 12. Krishnaswamy, R.K. and Sukhadia, A.M. (2002). *ANTEC Proceedings*, pp. 2395–2399; also (2005). The Influence of Solid-state Morphology on the Dart Impact Strength of LLDPE Blown Films, *J. Plas. Film & Sheeting*, **21**(2): 145–158.
- 13. Ajji, A. and Zhang, X. (2002). ANTEC Proceedings, pp. 1651–1655.
- 14. Lu, J. and Sue, H. (2002). J. Polymer Sci. (Physics Edition), 40(6): 507–518.
- 15. Ghaneh-Fard, A. (1999). Effects of Film Blowing Conditions on Molecular Orientation and Mechanical Properties of PE Films, *J. Plas. Film & Sheeting*, **15**(3): 194–218.
- 16. Chai, K.C., Selo, J.-L. and Osmont, E. (2000). Influence of Molecular Weight Distribution on LLDPE Blown Film Processing Conditions and Property Sensitivity, In: *ANTEC Proceedings*, pp. 331–335.
- 17. Zhang, X.M., Verilhac, J.M. and Ajji, A. (2001). Polymer, 42(19): 8179–8195.
- 18. Cole, K.C. and Ajji, A. (2000). In: Ward, I.M., Coates, P.D. and Dumoulin, M.M. (eds), *Characterization of Orientation in Solid Phase Processing of Polymers*, Carl Hanser Verlag, Munich.

- 19. Heuvel, H.M. and Huisman, R. (1985). J. Appl. Polym. Sci., 30(7): 3069–3093.
- 20. Cole, K.C., Legros, N. and Ajji, A. (1998). SPE Conference Proceedings on Orientation of Polymers, pp. 322–334.
- 21. Hoffman, D.J. and Miller, L.R. (1997). Polymer, 38(13): 3151-3212.
- 22. Stein, R.S. (1963). Newer Methods in Polymer Characterization, Chap. IV, Wiley-Interscience, New York.
- 23. Hohne, G.W.H. (2002). Another Approach to the Gibbs-Thomson Equation and the Melting Point of Polymers and Oligomers, *Polymer*, **43**(17): 4689–4698.

CHAPTER 5

SECOND ARTICLE

INVESTIGATION ON THE STRUCTURE AND PROPERTIES OF DIFFERENT PE BLOWN FILMS

Shokoh Fatahi¹, Abdellah Ajji² and Pierre G. Lafleur¹

¹École Polytechnique de Montréal, Chemical Engineering Departement

CREPEC

CP 6079,Succ. Centre-ville, Montréal ,Québec, H3C 3A7 Canada
²Industrial Materials Institute, NRC, 75 Boul. De Mortagne, Boucherville Québec, QC, J4B 6Y4 Canada.

Accepted on the Journal of International Polymer Processing, 2006.

Correspondence concerning this article should be addressed to Shokoh Fatahi.

5.1. Abstract

Molecular orientation and structure development during film blowing have a major effect

on mechanical and physical properties of polyethylene films. In this work the structures and

morphology of three different polyethylene blown films; linear low-density polyethylene

(LLDPE), low-density polyethylene (LDPE), and high density polyethylene (HDPE) were

studied. A series of blown films were produced at different process conditions. The orientation

of lamellae and lamellar stacks and the morphology of the films were characterized by SEM,

AFM and X-ray diffraction. SEM images of the film plane surface (MT) and cross section

slices in TN and MN planes were made and compared with AFM images. It was observed that

the surface morphology reflects a continuation of the bulk morphology for the cases studied.

Changes in the blown film process parameters, such as take up ratio, blow up ratio and frost

line height have an effect on structural parameters, crystallinity and mechanical properties.

KEY WORDS: microstructure, mechanical properties, blown films, LLDPE, LDPE,

HDPE, crystallinity, morphology, effects of processing variables.

5.2. Introduction

The goal of studying the film blowing process, as in most polymer processing operations, is to obtain a maximum production rate with optimal physical and mechanical properties. Ultimate film properties are controlled by film microstructure, developed under molecular orientation and stress-induced crystallization. Many parameters influence the morphology development of blown films in a very complex way. These parameters include the molecular structure, molecular orientation, polymer characteristics (such as molecular weight, molecular weight distribution and branching) and the equipment characteristics (such as die gap) as well as processing variables (such as DDR, BUR, and FLH).

As part of an effort toward better understanding of fundamental properties-structureprocessing (P-S-P) relationships in PE blown films, it is necessary to focus first on the
characterization of morphology and different structures in PE films by variety of microscopic
techniques. Because different morphologies result in different mechanical properties,
therefore, detailed characterization of film morphology is the key step in the investigation of
fundamental P-S-P relationships. The results of the morphological characterization are used to
determine how the film structure affects the mechanical properties. The investigation is also
aimed at understanding how processing conditions affect microstructure and ultimately the
final properties of the films. In this research work, we are concerned with PE films structure
characterization as well as the relationships between structure, properties and process
parameters in those films [1-10].

5.3. Backgrounds

In this section, some research works about the relationship between structure and properties are reviewed. Lu and al. (1999) used two different films of LLDPE, one film was made by using a low stalk bubble geometry (this film possesses a significant higher lamellae orientation than the other film) while the other film was blown by using a high stalk bubble configuration [11]. They reported that as crystalline orientation decreases, the difference between the tear strength in MD and TD decreases and dart impact increases (dart impact is related to the balance of mechanical properties between MD and TD). They also noted that the modulus of low stalk configuration film is higher because of higher crystalline content. The effect of orientation in LLDPE blown films on tear strength was investigated by Krishnaswamy et Sukhadia (2000) [12]. Their results indicated that the TD tear strength was high when the crystalline lamellae were relatively straight and oriented closer to the film TD. The MD tear resistance was higher when the non-crystalline chains were closer to equi-biaxial in the plane of the film. Orientation of the non-crystalline chain segments in these blown films suggested that inter-lamellar shear plays an important role in determining the MD tear strength of the films. Lu et al. (2001) obtained different results from studies on a series of HDPE films [13]. In these films, dual crystalline texture consisted of two row-oriented crystalline textures (an MD- stacked row crystalline texture and a TD- stacked row crystalline texture) was found. They noted that TD-stacked lamellar texture can withstand more load than the MD-stacked lamellar texture and the MD-oriented lamellar stacks are indeed relatively weak in dart impact compared to the TD-oriented lamellar stacks. It means a larger number of MD -oriented lamellar stacks are needed to gain the same strength as a small number of TD-oriented stacks.

So in HDPE films with dual crystalline texture, the number of the MD- oriented lamellar stacks is more important for the dart drop impact resistance. They reported also that the trend in tear strength can be correlated to the feature of dual crystalline texture. In films with dominant MD-stacked lamellar texture, tear strength in the TD is higher than in the MD and in films with dominant TD-stacked lamellar texture, MD tear strength is much higher than the TD tear strength. Krishnaswamy in 2001 determined the effect of micro-structural deformations on the tear resistance of HDPE [14]. He changed the morphology of the film by reducing the relative amount of the lamellar stack oriented orthogonal to the film MD (by increasing FLH) which resulted in lower TD tear resistance. Ajji and Zhang (2002) studied the correlation of tear resistance of LDPE films with orientation and reported that higher orientation along MD (a-axis orientation) or TD (b-axis orientation) and degree of row structure would give higher TD tear strength [15]. Krishnaswamy and Sukhadia (2002) used different LLDPE resins and reported that dart impact increases as the lamellar orientation in the blown film becomes more random [16]. The orientation factors of the LLDPE films were determined from Fourier Transform Infra-Red (FTIR) spectrometer equipped with a polarizer. They also found that the degree of lamellar orientation was dependent on both resin characteristics and processing condition and they increased the degree of lamellar orientation with increasing DDR/BUR ratio.

5.4. Experimental

5.4.1 Materials

A wide range of PE materials, including an LLDPE, two different HDPEs and an LDPE are investigated. The materials were provided by Dow Plastics Company, NOVA Chemicals, Petromont and Union Carbide with the following characteristics.

| Resin | GRADE | Comonomer | MFI (g/10 min) | Density (g/cm3) | M w (kg/mol) | M _w /M _n | Manufacturer |
|-------|------------|-----------|-------------------|--------------------|-----------------|--------------------------------|----------------------|
| LDPE | 503A | • | 1.9 | 0.923 | 80900 | 5.02 | Dow Plastics Company |
| LLDPE | FP 120-A | Octene | 1.0 | 0.920 | 103200 | 3.38 | Nova Company |
| HDPE | 58A | - | 0.41 | 0.957 | 193885 | 12.94 | Dow Plastics Company |
| LDPE | LF-Y-819-A | | 0.75 | 0.920 | 189200 | 9.10 | Nova Company |
| HDPE | DMDF 6200 | | 3.40 | 0.955 | | - | Petromont |

Table 5.1. The specification of materials.

5.4.2 Experimental conditions

A 45 mm killion single screw extruder with a helical annular die (outer diameter of 63.5 mm and a gap of 3 mm), a dual lip air ring and take up equipments was used at the École Polytechnique of Montreal. The mass flow rate was maintained around 2.5 kg/hr by adjusting screw revolution. Additional PE blown films with different structures were produced by changing the process conditions, using an extrusion line (die diameter of 101.6 mm and die gap of 1.1 mm) from Brampton Engineering equipped with five extruders at the Industrial Materials Institute (IMI). The process conditions for the films of interest in this paper are

summarized in Table 5.2 (The nomenclature of the films is based on changing the process condition particularly increasing TUR for each type of polyethylene).

5.5. Results and Discussion

5.5.1 Scanning electron microscopy

The morphology of PE films was observed with a low voltage microscope FEG-SEM S-4700 (Field Emission Gun Scanning electron microscopy) from Hitachi. Etching was employed for some of the samples by soaking for 20 min in a 0.7% solution of potassium permanganate in a mixture of 65 ml sulfuric acid and 35 ml orthophosphoric acid. Etched samples were examined using Jeol JSM-6100 scanning electron microscope.

5.5.1.1. Surface and bulk images

Typical morphologies of the surface of the various polyethylene films with different processing conditions are shown in Figure 5.1. Different morphologies are observed for LDPE, LLDPE, and HDPE blown films. The non-twisted row-nucleated structure was only found in HDPE, twisted lamellae were observed for LDPE and a spherulitic structure for LLDPE films. These observations are in a good agreement with other results in literature [17].

Table 5.2. Process condition for selected samples.

| Resin: LLDPE-Octene FP 120-A | ctene FP 120-A | | | | | | | |
|------------------------------|----------------|--------------|-----------------|----------|-----------------|------------|-------------|----------------|
| | LDPE0 | LDPE3 | LDPES | LDPE7 | LDPE10 | LDPE11 | LDPE12 | 2 LDPE13 |
| TUR | 30.5 | 20 | 30.5 | 42 | 42 | 52.5 | 42 | 64 |
| BUR | 1.7 | 1.92 | 1.5 | 1.29 | 1.47 | 1.6 | 1.64 | 1.5 |
| FLH (in) | 7.5 | 6 | 9 | 5 | 6 | 7 | 5 | 9 |
| Resin:LDPE 503a | la la | | | | | | | |
| | LDPE1imi | ni LDPE2imi | imi LDPE3imi | | LDPE4imi LD | LDPE5imi] | LDPE6imi | LDPE7imi |
| TUR | 26.2 | 21.9 | 22 | | 21.1 | 17.04 | 17.44 | 17.48 |
| BUR | 1.7 | 2 | 2 | 2 | 2.1 | 2.5 | 2.5 | 2.5 |
| FLH (in) | 4 | 8.5 | 7 | (A | 25 | 11 | 12.5 | 14 |
| Resin: LDPE LF-Y-819-A | -Y-819-A | | | | | | | |
| | HDPE1n HD | HDPE2n HDPE2 | CZ HDPE4n | HDPES | HDPE6n F | HDPE7n H | HDPE8 HDF | HDPE9n HDPE10n |
| TUR | 30.5 | 42 42 | 49 | 49 | 85.5 | | 107.5 10 | 7.5 107.5 |
| BUR | 1.35 | 1.15 1.05 | 1.25 | 0.88 | 1 | 1.08 | 0.9 | 0.88 0.82 |
| FLH(in) | 9 | 6 5.5 | 9 | 5.5 | 9 | 9 | 7 6. | 6.5 6.5 |
| Resin: HD58A | | | | | | | | |
| | HDPE1imi | HDPE2imi | HDPE3imi | HDPE4imi | HDPE5imi | HDPE6imi | ni HDPE7imi | ni HDPE8imi |
| TUR | 24.27 | 22.81 | 15.6 | 16.15 | 12.76 | 12.8 | 10.5 | 10.43 |
| BUR | 1.5 | 1.6 | 2 | 2 | 2.5 | 2.5 | က | 3 |
| FLH (in) | 29 | 20 | 24 | 19 | 18 | 26 | 16 | 29 |
| Resin: HDPE DMDF 6200 | MDF 6200 | | | | | | | |

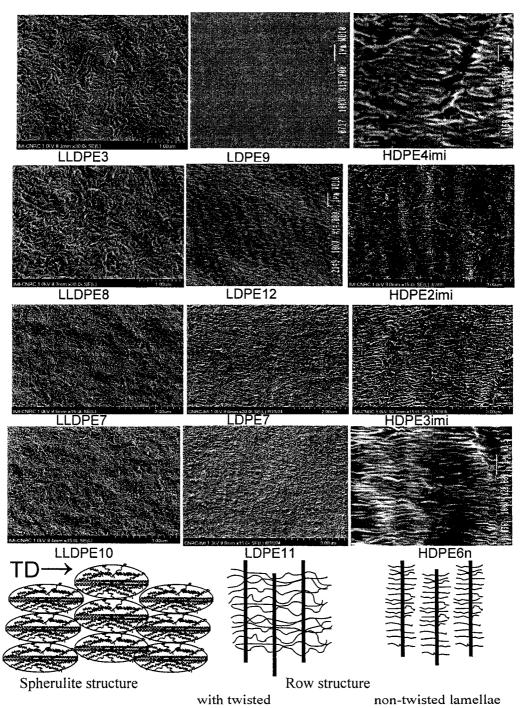
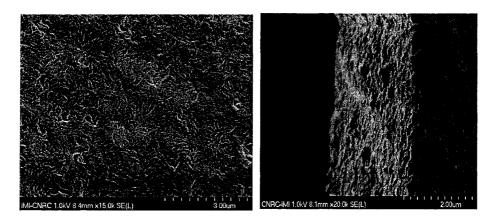


Figure 5.1. Crystalline morphology of surface of different PE blown films.

The interior morphology of polyethylene blown films was determined by examination of the cross section of the films in the two different directions. Cross section slices in MN and TN planes were prepared using a cryogenic ultra-microtome, Leica ULTRACUT with freeze cooling system attachment, at -100 °C. SEM images of the film plane surface (MT) and cross section slices in TN and MN planes are shown in Figure 5.2.

The differences in morphology between different PE blown films are the result of materials characteristics and processing conditions. By comparing the cross section images with surface images of different PE films, it was observed that the surface morphology reflects a continuation of the bulk morphology and the morphology of the inside and outside of the films has the same profile. This is because the films are thin (the average thickness of the all of the films is $27 \, \mu m$) so the difference in temperatures between the surface and the interior of the films is small during film blowing process. Therefore we have same crystallization behavior (nucleation and growth of crystallites) in the surface and bulk of the blown films.



Surface image of LLDPE9

SEM image of LLDPE9_CrossSection_MD

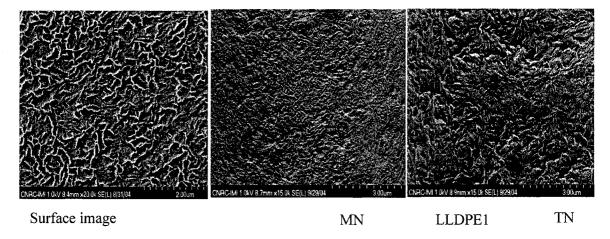


Figure 5.2. Comparison between surface and bulk morphologies of different PE films (MD \uparrow , TD \rightarrow).

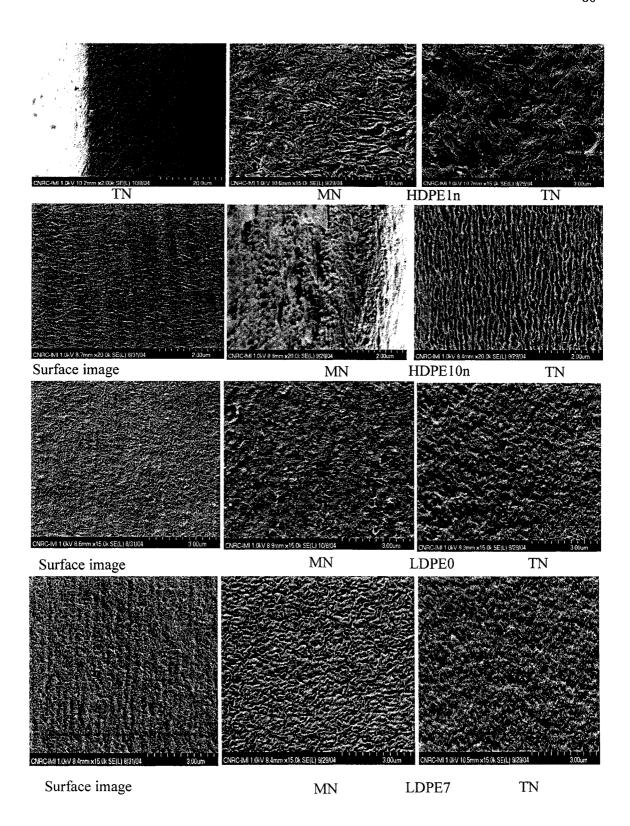


Figure 5.2. Continued

5.5.1.2. Scanning electron microscopy and the effects of process condition

The effect of processing parameters (TUR, BUR, FLH) on the morphologies of HDPE films was determined using SEM (Figure 5.3). The results show that the structures of the blown films are row-nucleated structures with lamellae that have normals oriented in the MD in an amorphous field that has predominant chain axis orientation in the MD. As TUR was increased, the row-nucleated structures became more perfectly aligned in the MD.

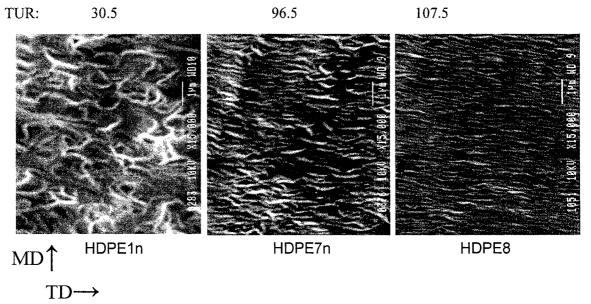


Figure 5.3. Morphological characteristics of PE films with different structure using SEM.

5.5.2 Atomic Force Microscopy (AFM)

The surface morphology and roughness of the films were evaluated using Atomic Force Microscopy. It was used for quick determination of surface roughness of the film and to evaluate the differences in structure between the various blown films. Tapping mode AFM was used to observe surface morphology (topography) of the films at room temperature. The AFM images are of three types: height, phase and amplitude. In the phase images, brighter regions represent the hard crystalline phase and the darker regions usually represent soft amorphous phase. In principle, the height image should reflect the sample topography, while phase images are well-known to show morphological structures (Figure 5.4). The AFM height images of the surfaces of films (3 Dimension images) are shown in Figure 5.5. The surface roughness of the samples was determined using those height images (Figure 5.6). The surface roughness of the HDPE films was higher than that of LDPE and LLDPE films. Comparison of the SEM images with the AFM images demonstrates that at the lamellar crystalline level, the AFM images generally confirmed morphological and crystalline structures deduced from Scanning Electron Microscopy.

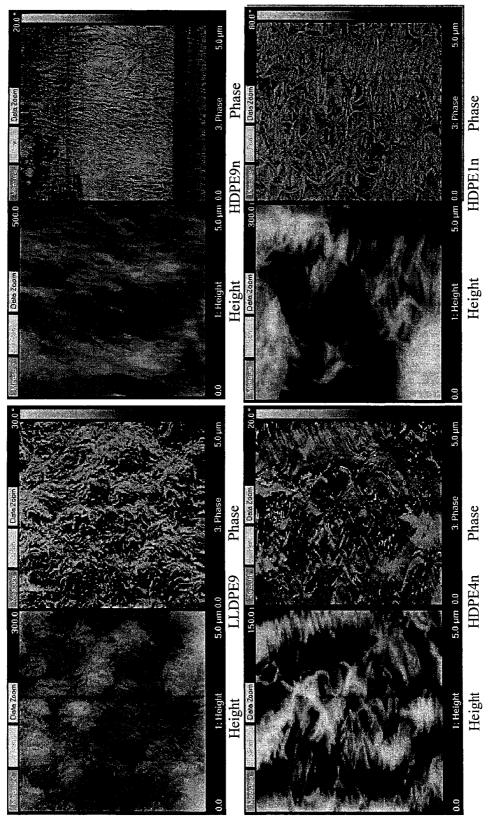
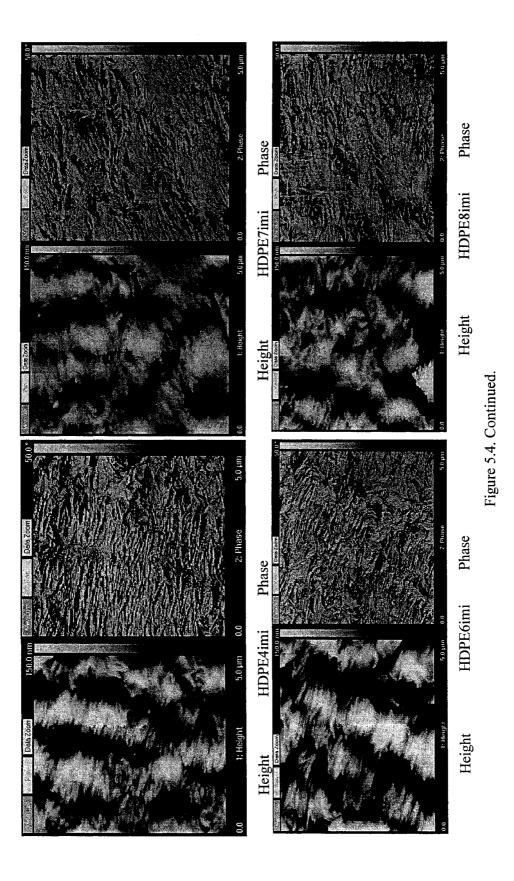


Figure 5.4. Height and Phase images of different PE films.



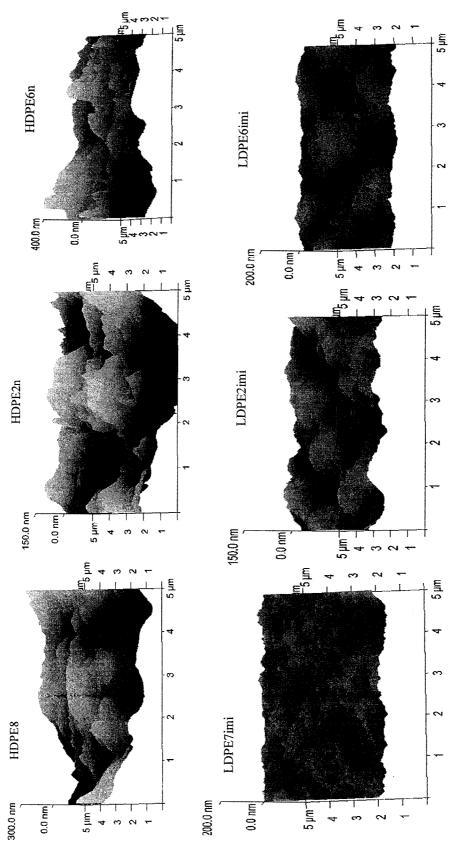
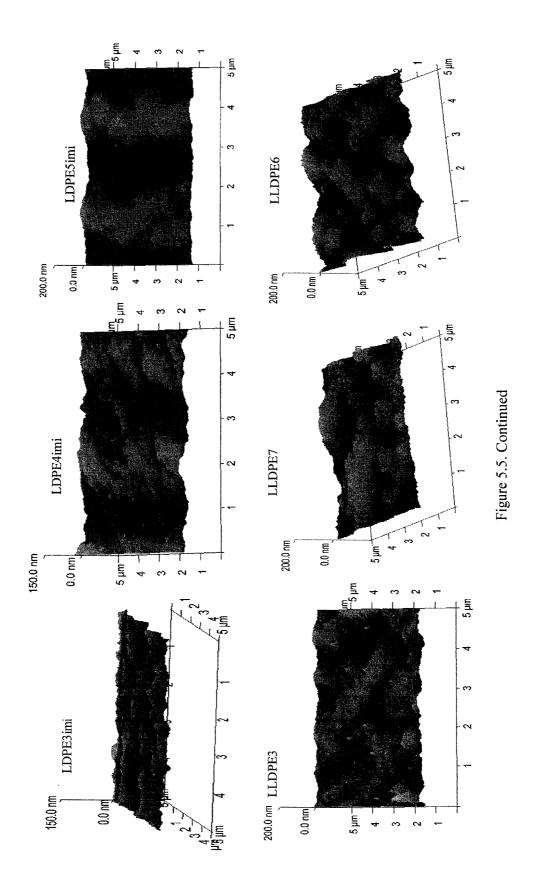


Figure 5.5. 3D surface plot analysis of AFM height images of blown films



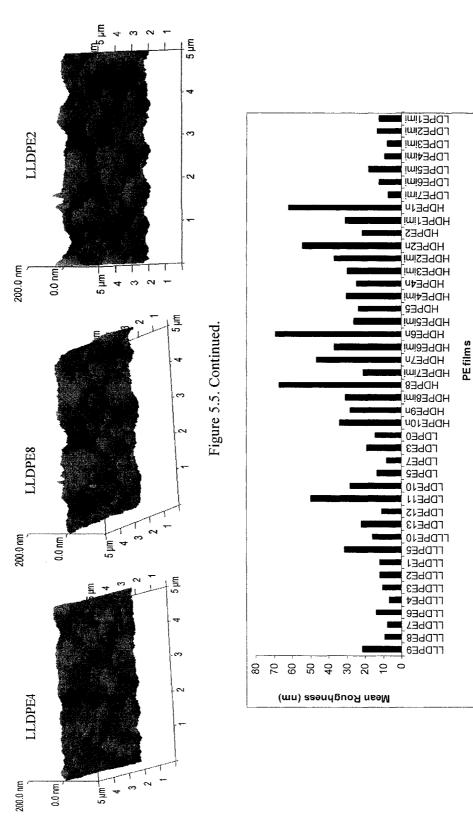


Figure 5.6. Atomic Force Microscopy results.

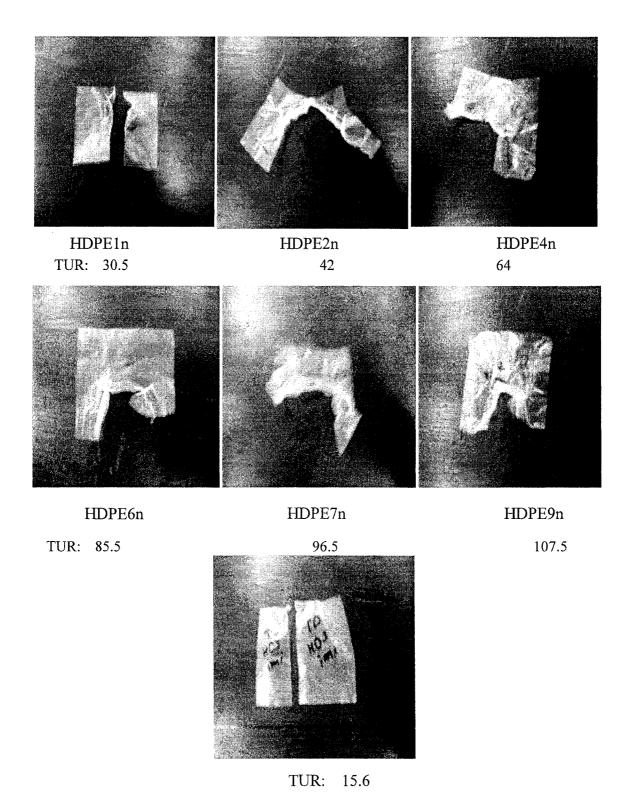
5.5.3. Measured Properties and the effect of process conditions

Tear strength, dart impact strength, tensile properties and haze were evaluated according to ASTM D 882, ASTM D1922, ASTM D1709 and ASTM D 1003 standards respectively. The effect of processing parameters (TUR, BUR, and FLH) on the mechanical properties of the PE films was determined (Table5.3). The tear strength and dart impact are affected by both orientation and crystallinity. In LLDPE films, MD tear increased with an increase in BUR. Increasing BUR would lead to less MD orientation leading to higher MD tear and actually a higher DDR and lower BUR leads to lower MD tear and the most improvement in tear was observed at higher FLH. The results also showed that dart impact increased with an increase in BUR (Higher BUR would lead to more balanced orientation as well as to a higher degree of planar orientation and increasing dart impact). Increasing BUR leads to a better balance of tear strengths in the MD and TD. MD and TD modulus decreased with increasing DDR. MD and TD tear resistance of the films increased with increasing FLH. Stress at maximum load decreased as the cooling rate was decreased.

An interesting feature that was observed for some HDPE samples was that their dart impact strength was almost zero; but they did not tear in transverse direction even using 3200 g standard pendulum (highest capacity of pendulum). This may be due to an increase in the orientation because of increasing of TUR in production of HDPE2n, HDPE4n, HDPE6n, HDPE7n, and HDPE9n. The Lowest TUR was applied for HDPE2n and the highest TUR for HDPE9n.

Figure 5.7 reveals the TD Tear failure in HDPE1n and HDPE3imi that withstood dart impact resistance test (these films are produced at lower TUR), but in other HDPE samples TD tear did not happen.

Investigation of the morphology of the failure regions using SEM showed that dart drop impact resistance of the films was significantly dependent on the lamellar stack structure. However, a good balance in structure and mechanical properties between the MD and TD usually give a high dart impact. The tearing and tensile deformation behavior of the films was also influenced by the orientation distribution of the lamellar stacks. The gloss and haze in PE films can be related to crystal size. If the film is cooled rapidly after extrusion and blowing (decreasing the FLH), the crystals will be smaller and the film will show higher gloss and lower haze. The results showed that the haze is related primarily to the surface roughness and can be reduced by lowering the frost line. The correlations between the properties of PE films and the process conditions and polymer feedstock are summarized in Table 5.4.



HDPE3IMI Figure 5.7. Photographs of the TD tear strength failure samples ((TD \uparrow , MD \rightarrow).

5.5.4. Structural characteristics and the study of the major effects by design of experiment

The structural parameters were obtained from different methods, WAXD pole figure technique was used to obtain quantitative information about crystal orientation and crystal size. The Herman's orientation factors were obtained from WAXD pole figure technique and amorphous orientation functions were calculated by combination with the birefringence results. The percentage of crystallinity was obtained from DSC. SAXS was carried out to determine Long spacing L, the dimensions of the crystallites and the average length of the amorphous layer. The lamellar thickness was determined by calculations from DSC results [18-19].

A statistical design of experiment was used to study the major effects between the microstructural parameters and the properties of the polyethylene films with process conditions. The experiments consisted of 43 test runs (including 10 different samples for LLDPE, 15 samples for LDPE and 18 samples for HDPE) involving 3 independent variables. The independent variables are TUR, BUR and FLH and there are 12 dependent variables (responses) including crystallinity, crystal length, lamellar thickness, crystal size(110), Crystal size(200), roughness, orientation factors for crystalline (a axis, b-axis) phase and amorphous phase in machine and transverse direction. These test data were used to generate equations to describe the factor effects on each of the microstructural parameters.

Table 5.3. Mechanical properties and process conditions for different PE films.

| | Tersile | %strain Tersile | Tersile | %strain | Mbd | S | 36.00 | Se (148) | CO. | mientso% | Ma | S) | | 易「 | | Haze | itty | IIR | TLR |
|----------|-----------|------------------|----------|------------|------|----------|------------|----------|----------|----------|-------|-------|--------|-------|-------|------|------|------|-------|
| | Highans | <u>B</u> | strength | (<u>R</u> | 2 | B | atrength | | strength | | U | | inpact | B | | % | % | | |
| | Yield(ND) | Yield(ND) @Yield | Besk(M | Beak | Man. | AUT | Yield/III) | (a)Yield | Beak(II) | (d) Beak | Min | AUT | 8 | g/m | g/m | | | | |
| 旧田 | 501 | 14.0 | 31.9 | 099 | 236 | 232 | 10.9 | 13.7 | 29.4 | 691/2 | 201.2 | 2559 | 29600 | 1610 | 2819 | 9.7 | 888 | 44.7 | 2 |
| II.HS | \$ 103 | 17.4 | 163 | 466 | 189 | 175 | 9.5 | 15.6 | 152 | 8895 | 224.2 | 223.0 | 32600 | 13.80 | 23.98 | 4.6 | 934 | 44.5 | 21.19 |
| HH | 7 10.1 | 17.6 | 172 | 605 | 121 | 165 | 9.4 | 17.1 | 10.0 | 4553 | 2102 | 204.7 | 741.00 | 15.93 | 21.65 | 43 | 99.4 | 423 | 1692 |
| III | 201 | 182 | 203 | 280 | 211 | 215 | 8.6 | 14.7 | 102 | 518.1 | 243.9 | 239.2 | 33600 | 1807 | 24.05 | 98 | 99.1 | 423 | 1692 |
| III | 4 9.5 | 17.2 | 17.0 | 533 | 190 | 147 | 68 | 167 | 14.1 | 485.7 | 203.0 | 2006 | 70400 | 17.09 | 61.61 | 5.0 | 99.5 | 44.2 | 1524 |
| III | 3 10.1 | 18.7 | 961 | 544 | 185 | 172 | 6.7 | 17.2 | 143 | 477.0 | 24.9 | 2183 | 66200 | 1680 | 22.75 | 53 | 0.66 | 43.8 | 14.6 |
| THE | 2 10.1 | 661 | 164 | 517 | 198 | 167 | 6:6 | 17.1 | 14.9 | 3926 | 232.1 | 224.5 | 434.00 | 1642 | 24.93 | 99 | 0.66 | 43.1 | 1724 |
| ILE | 10.1 | 13.4 | 300 | 109 | 233 | 218 | 10.1 | 126 | 182 | 6366 | 245.7 | 2469 | 33600 | 14.81 | 2723 | 64 | 67.6 | 45.6 | 8 |
| III | 5 10.5 | 13.3 | 23.4 | 622 | 234 | 234 | 10.5 | 14.1 | 671 | 593.1 | 264.3 | 2586 | 480.00 | 1732 | 2422 | 82 | 0.66 | 44.4 | 15 |
| III.PEI(| 501 | 12.0 | 385 | 276 | 241 | 137 | 103 | 10.7 | 20.8 | 687.4 | 277.4 | 2785 | 174.00 | 168 | 29.60 | 52 | 0.66 | 44.2 | 8 |

Table 5.3. Continued.

| HTH. | 4 | 12.5 | | 25 | 7 | 8.5 | 4 | 9 | 5 | 7 | 6 | 9 | 5 | 6 | 7.5 |
|--|---------|---------|----------|---------|---------|---------|---------|--------|--------|--------|--------|-------|-------|-------|-------|
| BUR F | 2.5 | 2.5 | 2.5 | 2.1 | 2 | 2 | 1.7 | 1.5 | 1.64 | 1.6 | 1.47 | 1.5 | 1.29 | 1.92 | 1.7 |
| TURB | 17.48 | 17.44 | 17.04 | 21.05 | 22 | 21.85 | 26.17 | 64 | 42 | 52.5 | 42 | 30.5 | 42 | 70 | 30.5 |
| DDR. | 43.7 | 43.6 | 45.6 | 44.2 | 44.0 | 43.7 | 44.5 | 0.96 | 68.9 | 84.0 | 61.7 | 45.8 | 54.2 | 38.4 | 51.9 |
| Clarity I | 88.1 | 76.2 | 75.0 | 82.5 | 8.89 | 70.9 | 71.8 | 91.2 | 92.0 | 90.3 | 91.9 | 93.7 | 91.0 | 92.4 | 86.4 |
| Haze % | 10.4 | 18.3 | 18.6 | 13.1 | 24.3 | 22.3 | 19.8 | 6.3 | 6.0 | 6.5 | 6.4 | 6.4 | 7.0 | 9.4 | 9.6 |
| | 4.81 | 2.87 | 2.87 | 3.75 | 2.80 | 3.13 | 3.98 | 8.17 | 7.43 | 8.86 | 12.11 | 21.64 | 9.48 | 8.12 | 10.80 |
| Tear strength MD TD glum glum | 3.37 | 9.32 | 69.7 | 10.60 | 12.99 | 13.72 | 12.88 | 7.34 | 9.43 | 7.22 | 9.65 | 28.26 | 12.34 | 4.91 | 8.75 |
| DART impact g | 35.00 | 22.50 | 16.25 | 17.05 | 27.00 | 44.25 | 3.58 | 15.80 | 4.01 | 6.75 | 11.80 | 22.33 | 13.90 | 49.50 | 38.50 |
| | 258.0 | 321.4 | 319.9 | 272.5 | 321.6 | 304.7 | 301.9 | 326.9 | 312.0 | 326.4 | 346.7 | 346.5 | 362.2 | 326.1 | 354.5 |
| Modulus (TD) Man AUT | 259.0 | 322.6 | 319.5 | 272.3 | 318.2 | 303.025 | 298.7 | 329.2 | 312.9 | 324.1 | 349.1 | 347.7 | 361.9 | 333.3 | 354.4 |
| % strain (TD) (@Break | 459.9 | 277.7 | 331.0 | 406.1 | 234.7 | 214.0 | 57.8 | 8.09 | 176.5 | 132.0 | 265.6 | 551.9 | 176.1 | 737.7 | 361.4 |
|) D) | 13.4 | 7.1 | 8.2 | 10.1 | 5.3 | 6.1 | 3.2 | 4.9 | 5.4 | 5.0 | 7.6 | 11.1 | 5.2 | 14.6 | 8.7 |
| % strain Tensile (TD) strength (@Yield Break(T | 11.0 | 9.3 | 0.6 | 8.9 | 8.4 | 9.3 | 7.0 | 4.6 | 6.4 | 8.9 | 8.1 | 9.3 | 7.9 | 11.8 | 9.3 |
| Tensile 9 strength Yield(TD) | 9.6 | 10.1 | 9.6 | 8.9 | 8.9 | 9.3 | 8.7 | 9.1 | 9.5 | 8.6 | 10.8 | 11.2 | 9.01 | 11.9 | 11.3 |
| | 185 | 217 | 208 | 183 | 219 | 213 | 195 | 222 | 201 | 194 | 251 | 222 | 224 | 284 | 217 |
| Na Ma | 216 | 248 | 248 | 220 | 756 | 237 | 573 | 287 | 790 | 726 | 298 | 274 | 290 | 586 | 280 |
| % strain (MD) = Break | 181 | 110 | 104 | 144 | 92 | 81 | 106 | 165 | 991 | 161 | 283 | 442 | 210 | 432 | 354 |
| | 18.6 | 25.7 | 25.1 | 23.0 | 35.5 | 30.2 | 23.4 | 14.5 | 16.3 | 14.2 | 10.1 | 16.4 | 12.8 | 10.3 | 12.3 |
| % strain (MD) (@Yield | 12.3 | 9.8 | 10.3 | 11.2 | 10.0 | 9.3 | 0.6 | 12.1 | 11.9 | 12.4 | 11.9 | 13.2 | 12.6 | 14.6 | 14.1 |
| Tensile | 8.6 | 10.4 | 10.4 | 9.6 | 13.2 | 11.8 | 10.0 | 11.9 | 11.0 | 10.7 | 12.1 | 11.2 | 11.7 | 9"11 | 10.9 |
| | LDPE7im | LDPE6im | LDPESimi | LDPE4im | LDPE3im | LDPE2im | LDPE1im | LDPE13 | LDPE12 | LDPEII | LDPE10 | | LDE | LDFE3 | LDPEO |

Table 5.3. Continued.

| ETH | | 14 | 12.5 | = | 25 | 7 | 8.5 | 4 | 9 9 | 4 5 | 5 7 | 7 9 | 5 6 | .29 5 | 2 9 | 7 7.5 |
|---|-------------------------------------|----------|----------|----------|------------|----------|----------|----------|---------|---------|--------|--------|--------|--------|--------|-------|
| BUR | | 2.5 | 1.25 | 1 2.5 | 2.1 | 7 | 7 | 7 1.7 | 1.5 | 1.64 | 1.6 | 1.47 | 5.1 | 귀 | 1.92 | 5 1.7 |
| <u> </u> | | 17.48 | 17.44 | 17.04 | 21.05 | 22 | 21.85 | 26.17 | 22 | 42 | 52.5 | 42 | 30.5 | 42 | 8 | 30.5 |
| DOR | | 43.7 | 43.6 | 42.6 | 44.2 | 44.0 | 43.7 | 44.5 | 96.0 | 68.9 | 84.0 | 61.7 | 45.8 | 54.2 | 38.4 | 51.9 |
| Clarity DDR % | | 88.1 | 76.2 | 75.0 | 82.5 | 8.89 | 70.9 | 71.8 | 91.2 | 92.0 | 90.3 | 91.9 | 93.7 | 91.0 | 92.4 | 86.4 |
| Haze % | | 10.4 | 18.3 | 18.6 | 13.1 | 24.3 | 22.3 | 19.8 | 6.3 | 0'9 | 6.5 | 6.4 | 6.4 | 7.0 | 9.4 | 9.6 |
| F1000460 00000000000000000000000000000000 | g/um | 4.81 | 2.87 | 2.87 | 3.75 | 2.80 | 3.13 | 3.98 | 8.17 | 7.43 | 8.86 | 12.11 | 21.64 | 9.48 | 8.12 | 10.80 |
| Tear stre MD | g/m | 3.37 | 9.32 | 69.7 | 10.60 | 12.99 | 13.72 | 12.88 | 7.34 | 9.43 | 7.22 | 9.65 | 28.26 | 12.34 | 4.91 | 8.75 |
| DART Tear strength impact MD TD | g | 35.00 | 22.50 | 16.25 | 17.05 | 27.00 | 44.25 | 3.58 | 15.80 | 4.01 | 6.75 | 11.80 | 22.33 | 13.90 | 49.50 | 38.50 |
| | AUT | 258.0 | 321.4 | 319.9 | 272.5 | 321.6 | 304.7 | 301.9 | 326.9 | 312.0 | 326.4 | 346.7 | 346.5 | 362.2 | 326.1 | 354.5 |
| Modulus (TD) | | 259.0 | 322.6 | 319.5 | 272.3 | 318.2 | 303.025 | 298.7 | 329.2 | 312.9 | 324.1 | 349.1 | 347.7 | 361.9 | 333.3 | 354.4 |
| % strain (TD) | @Break Man | 459.9 | 17.17.2 | 331.0 | 406.1 | 234.7 | 214.0 | 57.8 | 8.09 | 176.5 | 132.0 | 265.6 | 551.9 | 176.1 | 737.7 | 361.4 |
| (4.0 | Break(TD) (| 13.4 | 7.1 | 8.2 | 10.1 | 5.3 | 6.1 | 3.2 | 4.9 | 5.4 | 5.0 | 9.7 | | 5.2 | 14.6 | 8.7 |
| % strain Tensile (TD) strength | @Yield E | 01 | 9.3 | 0.6 | 8.9 | 8.4 | 9.3 | 0.7 | 4.6 | 6.4 | 8.9 | | 9.3 | 7.9 | 8.11 | 9.3 |
| Tensile 9 strength | Yield(TD) | 9.6 | 1:01 | 9.6 | 8.9 | 8.9 | 9.3 | 8.7 | 9.1 | 9.2 | 8.6 | 10.8 | 11.2 | 9:01 | 11.9 | 11.3 |
| 92 | Aan AUT | 88 | 217 | 808 | 183 | 219 | 213 | 155 | 222 | 707 | 192 | 151 | 222 | 224 | 284 | 217 |
| Modulus (MD) | Man | 216 | 248 | 248 | 220 | 256 | 237 | 229 | 287 | 09% | 256 | 298 | 274 | 790 | 289 | 780 |
| % strain (MD) | 0 | 188 | 110 | 101 | 141 | 92 | | 106 | 165 | 166 | 197 | 283 | 442 | 210 | 432 | 354 |
| | Yield(MD) (@Yield Break(MD) Break | 18.6 | 25.7 | 25.1 | 23.0 | 35.5 | 30.2 | 23.4 | 14.5 | 163 | 14.7 |] = | 16.4 | 12.8 | 103 | 12.3 |
| % strain Tensile (MD) strength | @Yield | 3 | 86 | 103 | 112 | 90 | 93 | 0.6 | 121 | 011 | 17.4 | 011 | 13.2 | 176 | 146 | 14.1 |
| Tensile strength | /ield(MD) | 8.0 | 10.4 | 10.4 | 96 | 13.2 | 2 = 2 | 0.01 | 11.0 | 110 | 10.7 | 13.7 | 1 2 | 117 | 116 | 10.9 |
| | | I NPF7im | I DPRKim | I DPF5im | T T DF4 im | T NDF3im | I NDF2im | I NPF1im | FINDE13 | יום מרו | 1 DEFI | TAPETA | I NPFK | I NPR7 | I DPF3 | |

| | Response | The state of the s | |
|--|-------------------------------|--|------|
| | MD/TD Elmendorf Tear Strength | Dart drop Impact strength | Haze |
| Polymer | | | |
| Crystalline orientation | √ | | |
| Lamellar stack oriented -MD or TD | ٧ | | |
| -Random orientation | | √ | |
| The balance of mechanical properties (MD & TD) | · | V | |
| Process | | | |
| BUR/ DDR | √ | √ | |
| BUR | V | V | |
| FLH | V | V | √ . |

 $[\]sqrt{\ }$ = property improves.

Table 5.4. Correlation between process conditions and polymer specifications in blown LDPE film.

A stepwise Regression approach was used and each response was regressed against all independent factors. The results of the stepwise regression summary are shown in Table 5.5. It indicates which process variables caused a statistically significant (>95%) effect on the structural parameters of the PE films. The process variables are listed down the left side of the table. The parameters are listed across the top of the table. If a coefficient is listed on the line of a variable, then that variable has a significant effect on the corresponding structural parameter. Table 5.5 shows TUR has significant effect on the majority of microstructural parameters. Increasing TUR resulted in decreased the orientation factors for crystalline (a axis, b-axis) along MD but increased the other microstructural parameters. FLH did not have a significant effect on the orientation factors but BUR can be used to cause a change in the orientation factors for crystalline (a axis, b-axis) phase. Typical relationship between TUR and BUR as process variables and fT_b as microstructural parameter is graphically represented using surface plots (3D XYZ graphs/Quadratic method) in Figure 5.8. It includes the individual and joint factor effects (two level interactions and squared terms).

| | | a profile (2) Supris (2) | F 4 (F) | | Page 1992 Page 1 | Respon | se - | | | rapalit ii | | |
|--------------------|---------------|-----------------------------|----------------------|-----------|--|-----------|-------|------|-------|---------------|----------------|-----------|
| Process Variables | Crystallinity | - | Crystal Size(110) | , | Lamellar Thickness | Roughness | | | | Orien | tation factors | 5 |
| | | ~**** | | 5.24(200) | | | fM_a | fT_a | fM_b | fT_b | fM_amorph | fT_amorph |
| TUR | 0.451 | 0.448 | 0.525 | - | 0.544 | 0.529 | -0.89 | • | -0.32 | 0.40 | 0.853 | 0.779 |
| BUR | • | - | - | - | - | - | -0.66 | 0.66 | 0.58 | -0.56 | - | - |
| FLH | 0.597 | 0.685 | 0.437 | 0.761 | 0.449 | 0.343 | - | - | - | • | - | - |

Table 5.5. The correlation between process conditions and structure parameters of PE blown films using effects chart.

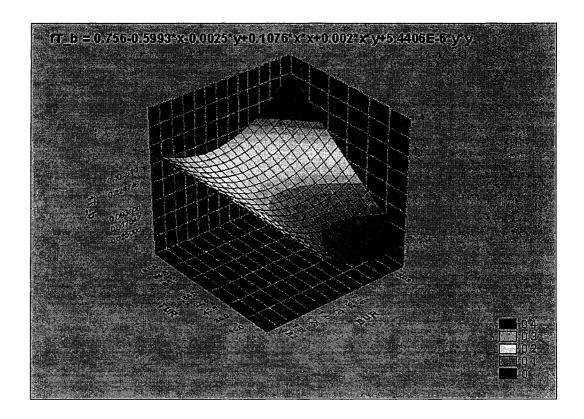


Figure 5.8. Response surface for fT_b; TUR and BUR as independent variables.

5.6. Conclusions

This study has addressed the correlation between morphological features and properties of PE films, with attention to the process conditions. Different structural characterization techniques were utilized to characterize a number of critical aspects of film morphology. The detailed morphological characterization of PE blown films allowed to build a good basis for a fundamental understanding the structure-property relationship of blown films.

Tear strength, dart impact and tensile properties in both MD and TD have been determined and they were influenced by the orientation of the crystalline lamellae. A good balance of lamellar orientation and molecular orientation with no predominant a-axis or c-axis

orientation (well balanced structure) provided for the optimal balance of key film properties. Changes in the blown film process parameters, such as take up ratio, blow up ratio and frost line height have an effect on structural parameters and mechanical properties. As a typical example, it was observed that the structures of HDPE blown films are of the row nucleated type structures with lamellae that have normals oriented in the MD in an amorphous field that has predominant chain axis orientation in the MD. As TUR was increased, the row-nucleated structures became more perfectly aligned in the MD and it has a strong effect on TD tear strength failure. The dart impact strength increased with an increase in BUR (Higher BUR would lead to more balanced orientation as well as to a higher degree of planar orientation and increasing dart impact). Increasing FLH and BUR/DDR have an effect on tear strength and dart impact strength.

5.7. References

- 1 Babel K. A., Nagarajan G., Campbell G. A.: ANTEC, p. 2112 (1996).
- 2 Lu J., Sue H-J.: Journal of Materials Science, 35, p. 5169 (2000).
- 3 Patel M. R., Butler I. T., Walton L. K., Knight W. G: Polymer Engineering & Science, 34, 19, p.1506 (1994).
- 4 Simpson M. D., Harrison R. I.: ANTEC Proceedings, p. 1206 (1993).
- 5 Kim Y-M, Kim C-H, Park J-K, Lee C-W, Min T-I.: Journal of Applied Polymer Science, 63, p. 289 (1997).
- 6 Sukhadia M. A.: ANTEC, p.160 (1998).

- 7 Godshall D., Wilkes G., Krishnaswamy K. R., Sukhadia M. A.: Polymer, 44, p. 5397(2003).
- 8 Lu J., Sue H.: Journal of polymer Science (Physics Edition), 40, p. 507 (2002).
- 9 Ghaneh-Fard A.: Journal of Plastic Film & Sheeting, 15, p. 94 (1999).
- 10 Chai K. C., Selo J-L., Osmont E.: ANTEC Proceedings, p. 331 (2000).
- 11 Lu J., Zhao B., Sue H-J.: ANTEC Proceedings, p. 1768(1999).
- 12 Krishnaswamy K. R., Sukhadia M. A.: Polymer, 41, p. 9205(2000).
- 13 Lu J., Sue H-J., Rieker T. P.: Polymer, 42, p. 4635 (2001).
- 14 Krishnaswamy K. R., ANTEC Proceedings, p. 115 (2001).
- 15 Ajji A., Zhang X.: ANTEC Proceedings, p. 1651 (2002).
- 16 Krishnaswamy K. R., Sukhadia M. A.: ANTEC Proceedings, p. 2395 (2002).
- 17 Zhang X.M., Elkoun S., Ajji A., Huneault M.A.: Polymer, 45,p. 217 (2004).
- 18 Fatahi S., Ajji A. and Lafleur P.G., Journal of Plastic Film & Sheeting, 21,281(2005).
- 19. Fatahi S., Ajji A. and Lafleur P.G., ANTEC Proceedings, 5, 102 (2005).

CHAPTER 6

THIRD ARTICLE

Correlation Between Different Microstructural Parameters and Tensile Modulus of Various Polyethylene Blown Films

Shokoh Fatahi

École Polytechnique de Montréal, Département de Génie Chimique, CREPEC CP 6079, Succ. Centre-ville, Montréal, Québec, H3C 3A7 Canada

Abdellah Ajji

Industrial Materials Institute, NRC, 75 Boul. De Mortagne, Boucherville

Québec, QC, J4B 6Y4 Canada.

Pierre G. Lafleur

École Polytechnique de Montréal, Département de Génie Chimique, CREPEC CP 6079, Succ. Centre-ville, Montréal, Québec, H3C 3A7 Canada

Submitted on the Journal of Polymer Engineering & Science, 2006.

Correspondence concerning this article should be addressed to Shokoh Fatahi.

6.1. Abstract

The objective in this study is to establish a model for the prediction of tensile properties using various types of polyethylene films (LLDPE, HDPE, and LDPE). A series of blown films were produced by varying three process parameters: take-up ratio, blow-up ratio, and frost line height. The tensile properties of the resulting films were investigated in relation to their microstructural characteristics. The microstructural parameters were determined by differential scanning calorimetry, wide angle X-ray diffraction (WAXD) pole figures, SAXS (small angle X-ray diffraction) and birefringence measurements. The orientation parameters of the films were measured by WAXD and birefringence. They were determined for both crystalline and amorphous phases. The crystalline content, lamellar thickness and crystal sizes were obtained from DSC and WAXD. The SAXS technique was used to find the average length of the crystalline and amorphous layers. A model for the tensile modulus is proposed and correlated to some structural parameters including crystalinity, orientation factors for crystalline c-axis and amorphous phase, lamellar thickness, crystal size, the average length of the crystal layer and long spacing period. The measured modulus and the calculated one were compared and a reasonable agreement was found between them for all series of films.

KEY WORDS: modeling, tensile modulus, microstructure, mechanical properties, blown films, PE, LLDPE, LDPE, HDPE, structure-property relation, morphology.

6.2. Introduction

For many years, the dependence of mechanical properties on the morphological structure of the polymer has been the subject of research works. Many investigations have been reported concerning very complex relationships between processing, structure and properties in film blowing [1-4]. The development of molecular orientation and morphology in blown films has been investigated extensively in recent years [5-14]. Numerous studies focused on the influence of processing parameters on mechanical behavior of blown film [15-18]. Some researchers have attempted to correlate the mechanical properties of blown films with the kinematics and dynamics of the process [19]. But from these literature studies, it was found that there is a need for a fundamental comprehensive structure-property relationship; relating the microstructure and morphology to the properties of blown films. It was also noticed that less attention has been paid to the quantitative evaluation of the property- structure concept and no model was developed for polyethylene that can successfully predict the final tensile properties of films.

The elastic tensile modulus is one of the most important mechanical properties of semi crystalline polymers that remain difficult to predict because of its complex dependence on many factors. In literature, the subject of studies on the elastic properties differ in two major aspects; the prediction of modulus as a function of the degree of crystallinity (density) and microstructural morphology. In a study by Janzen et al. [20], the dependence of young's modulus of polyethylene on crystalline content, from a large

collection of data from different sources, was reported. A number of theoretical mixing rules from binary composite micromechanics have been proposed using moduli characteristic of crystalline and amorphous phases to obtain the dependence of modulus of polyethylene on crystalline volume fraction. McCullough et al. [21] reviewed the predictions of PE moduli based upon the percent crystallinity without the use of geometric details of the microstructural features, the theoretical predictions for the moduli of anisotropic polyethylene are in good agreement with values reported in the literature and this result showed that the continued improvements in the longitudinal young 's modulus may be achieved by the controlling the crystalline morphology. The emphasis in this case was on models that involve at least some geometrical parameters describing the microstructural morphology. Another approach presented by Halpin-Tsai which employs a single parameter (aspect ratio) instead of all geometric effects of lamellae [22]. This theory doesn't fit the polyethylene data too well except over a narrow range of crystallinity. All these approaches are based on small strain elasticity theory and cannot predict a stress-strain curve past the linear elastic region. I. M. Ward derived the expressions for the elastic moduli in terms of molecular orientation using an aggregate model for the two cases of continuous stress or continuous strain; in this aggregate model the response matrices (elastic constants and compliance constants) are proposed to be established for a specimen of given crystallinity by comparison of calculated and experimental moduli at various conditions of orientation. Thus crystallinity and separate phase properties do not explicitly appear in the aggregate model [23, 24].

These studies do not provide sufficient data concerning the percent crystallinity, orientation parameters, and geometric details of the microstructural features. The work of Takayanagi et al. [25] is one of the few sources of quantitative structural and mechanical data that can be used as theoretical predictions of mechanical properties, a microcomposite model, in which the crystalline and amorphous components are considered as distinct phases. Takayanagi proposed an explanation in terms of a simple two phase model where the amorphous material is in series with the crystalline phase relative to the draw direction, and in parallel for the transverse case. Later, in the results section, we will discuss the detail of his series and parallel model. But Takayanagi model cannot deal with the orientation of the lamellae and distinguish between the behavior when the lamellar normal's are parallel to the draw direction or at any angle to this direction.

Unfortunately, most of these studies don't develop a clear link between quantitative structural data and mechanical properties, particularly the modulus. It is hence the objective of this work to establish a model that can link microstructural characteristics and tensile modulus.

6.3. Experimental

6.3.1. Materials

A number of polyethylene's, including LLDPE, two different HDPE and LDPE are investigated. The materials were provided by Dow Plastics Company, NOVA Chemicals, Petromont and Union Carbide with the specifications listed in Table 1.

6.3.2 Experimental conditions

Two film blowing equipments were used: A 45 mm Killion single screw extruder with a helical annular die (outer diameter of 63.5 mm and a gap of 3 mm), a dual lip air ring and take up equipments at the École Polytechnique of Montreal; and a multilayer coextrusion line (die diameter of 101.6 mm and die gap of 1.1 mm) from Brampton Engineering equipped with five extruders at the Industrial Materials Institute (IMI) in Boucherville Québec. The mass flow rate was maintained around 2.5 kg/hr by adjusting screw revolution. Various blown films with different structures were produced by changing the three important operating conditions: frost line height (FLH), blow up ratio (BUR), and take up ratio (TUR).

6.3.3. Crystalline content and lamellar thickness measurements

Lamellar thickness is an important morphological characteristic of semi-crystalline polymers. It was derived here from thermal analysis (using DSC techniques) because the melting temperature of polymer crystals is related to the lamellar thickness. The equipment used was a Perkin-Elmer Pyris-7. The weight percentages of crystallinity and melt temperature were obtained from the DSC trace. The heat of fusion of 100% crystalline PE was taken as 289 J/g [28] and the heating rate used was 10° C/min. The Wunderlich equation was used to obtain the lamellar thickness, that is [29]:

$$\ell = 414.2*0.627/(259.7034-T_f) \tag{6.1}$$

 T_f (in K) and ℓ (in nm) are the melt temperature and the thickness of lamellae respectively

6.3.4. Wide & small angle X-ray diffraction

In a polycrystalline polymer, the crystalline regions are composed of crystallites, whose dimensions can be determined from small angle X-ray diffraction measurements

(SAXS) and from analysis of Wide–angle diffraction results (WAXD). The nano-meter scale information is revealed by Small-Angel X-Ray Scattering (SAXS). X-ray diffraction experiments can also yield, in principle, the orientation distribution of the crystal phase. The X-ray diffraction experiments were performed using a Bruker D8 Discover apparatus. The instrument uses a Cu- K_{α} radiation (wavelength of 1.54 Å). For WAXD, films were stacked to a thickness of 3 mm and the source to detector distance was 9 cm. For SAXS, the films samples were prepared by folding the blown films into 80 layers and maintaining the MD of each layer parallel to every other and the source to detector distance was 29 cm.

6.3.5. Mechanical properties measurements

The tensile properties of the films were evaluated according to ASTM D 882-02 standard using an Instron tensile testing machine at room temperature. The mechanical properties in the MD & TD directions such as; tensile elastic modulus, elongation at break, elongation at yield, tensile strength at break and tensile strength at yield were measured.

6.4. Results and discussion

6.4.1. Orientation determination and morphological study of the blown film

WAXD were used to obtain the percentage crystallinity (X_c) of PE blown films. The orientation parameters as well as the average crystallite size in (200) and (110) directions and the average inter crystallite separation (R) in the amorphous region of the films were determined using WAXD. The typical examples of I-2θ WAXD curves for different type of PE films are shown in Figure 1. The scattering pattern of polyethylene usually consists of peaks indexed at (110) and (200) reflections and amorphous halo. The reflections of (110) and (200) are pronounced for all samples. The crystal structure of polyethylene is orthorhombic and the intensity of (110) peak is always higher than that of the (200) peak. In order to accurately determine the lattice constants of the PE crystals, it is convenient to separate the crystalline and noncrystalline contributions to the diffracted intensity. A first straightforward separation of peaks can be performed by using a curve solver (analogue computer designed to resolve an overlapped curve envelope into its component profiles). The data is further refined with help of a least square/curve fitting program. The reflections usually show profiles which are intermediate between Lorentzian and Gaussian. The width (full width at half maximum) and asymmetry of the diffractometer profiles (first peak (110) and second peak (200)), the peak maximum of the profile (2θ) under crystalline peaks ((110) and (200)) and amorphous hump are obtained from diffractometer profiles. The results for some HDPE films are summarized in Table2.

The average inter crystallite separation (R) in the amorphous region of the sample was evaluated from the position of the maximum of the halo [30].

$$R=5 \mathcal{N} (8\sin\Theta) \tag{6.2}$$

The average size of the crystalline regions (P) and the transverse dimension of crystallites (L) (P and L represent crystal size in (110) and (200) planes respectively and a schematic illustration of crystallite that indicates different dimensions is shown in Figure 2) were determined from the broadening of the peaks by using following formula and the results are shown in Table 2 [31]:

$$\wedge^*_{(hkl)} = \frac{\kappa\lambda}{\beta_{(hkl)}\cos\theta} \tag{6.3}$$

Where K is the 0.89 for (110) plane and 0.94 for (200) plane; λ , the applied wavelength; β , the half-width of the reflection; θ_{hlk} , the scattering angle of the (hkl) crystalline plane. The result show that the full-width at half maximum intensity (FWHM) of the first maxima reduced with the orientation of the lamellae or increasing of TUR (process condition for some films is shown in Table3) followed by the increasing of the lateral dimensions (crystal sizes P and L).

The use of wide-angle X-ray pole figures allows one to obtain considerable information regarding the orientation of specific crystalline axes or planes. The pole figures results showed typical features of PE films: a-axis in MD and b-axis in TD-ND plane, with more pronounced effects for HDPE.

SAXS was carried out to determine long spacing period (L) and the length of the crystallites. Long spacing, which is defined as the average repeating distance between the centers of two crystallites, can be determined directly by measuring the distance between the meridional reflection and the primary beam. The length of the amorphous part inside the long spacing represents the difference between the long spacing and the length of the crystallites:

$$I = L - D (nm) \tag{6.4}$$

The SAXS patterns indicated generally that the lamellae were oriented perpendicular to the machine direction. An isotropic (uniform ring) pattern for LLDPE, an elliptic pattern for LDPE and an elongated elliptic shape with a two point pattern for HDPE were observed because of the orientation of the lamellae. These features are all in very good agreement with SEM and AFM images that were reported in our previous studies [32-33].

6.4.2. The relation between tensile properties & structure

In this section, the effects of morphological features of different PE films on tensile properties under various processing conditions were investigated. It was found that the tensile behavior of the films was influenced by the orientation distribution of the lamellar stacks, in addition to many other structural factors, such as degree of

crystallinity, the dimension of crystalline and non-crystalline region and crystallite thickness.

From the measurements of the tensile properties of different blown PE films, it was observed that yield stress was higher in MD. This is attributed to the presence of more tie chains and it took more energy to deform a crystal along the chain direction. Higher yield strain in the MD can be attributed to the relaxed amorphous material in the MD that must be extended before crystal deformation starts (Figure 3).

The results also showed that TD tensile modulus is higher than the MD one (Figure 4). This is because by pulling the polyethylene melt at a high draw down ratio and cooling it as soon as it exits the die, most of the molecular orientation will be in the machine direction. This produces films that are essentially uniaxially oriented so the majority of the lamellae are stacked perpendicular to the MD and gives higher TD tensile modulus than MD. Similar observations were previously reported for LLDPE and HDPE [34-36]. In films with more biaxial orientation, the MD and TD moduli were similar. Conversely when the molecules are uniaxially oriented in the machine direction, it is expected that the tensile strength in MD will be greater than that in TD (Figure 5).

6.4.3. Modeling analysis

Modeling used for predicting tensile modulus includes empirical modeling and fundamental/structure modeling approaches. In fundamental modeling, information on the structure of blown films from microscopic methods is expected to be of great importance.

The empirical approach includes statistical design of experiments and multivariate modeling. A multivariate modeling, with the incorporation of both PE blown films properties and structural parameters was used to develop a predictive model for properties of PE blown films, particularly to identify the most influential structural parameters. In a final stage approach, a combination of statistical modeling technique and fundamental modeling will be used.

For the fundamental/structure modeling approach, there are several steps required in the development of a mathematical model that would predict the properties of the blown films as a function of their microstructure variables. Our Modeling Methodology can be summarized as follows:

• Define the problem

- Development of the model
- o Analyze the structure parameters
- Select suitable notations
- o Specify independent and dependant variables
- Measure variables
- o Formulate the mathematical model:
- Simplify and solve the equations
- Evaluate the model
- Revise the model

6.4.3.1. Statistical modeling

First, the structural parameters were determined by studying the morphology and orientation of different polyethylene films. The orientation, crystalline content, crystal size and lamellar thickness were characterized for the films obtained at different process conditions. The results are presented in Tables 4, 5 and 6.

A statistical model was then developed that showed how each of the structural parameters selected contributes to the magnitude of changes of the tensile properties tested [33, 37]. The equations found following this modeling related the tensile modules to the following structural parameters: the crystalline content, lamellar thickness, crystal length and orientation factors for the crystalline and the amorphous phases along MD & TD. The result of the analysis indicated that lamellar thickness, which is an important morphological characteristic of semi-crystalline polymers; has a major effect on the tensile properties. It was also observed that certain parameters such as crystallinity, and orientation factors have an effect on the majority of film properties measured.

6.4.3.2. Formulation of the structural/fundamental model

Since the mechanical properties of a polymer are dependent on factors such as the arrangement of chains with respect to each other (structure of the molecular chain), the crystalline structure, the molecular orientation and the morphology, two main aspects

should then be considered more seriously in the study of physical structure of polyethylene blown films; orientation and crystallinity.

The crystal structure of polyethylene is shown in Figure 6 and the orthorhombic cell structure: a, b and c crystal axes are illustrated. The planar zigzag carbon chains of the PE macromolecules are parallel to the crystallographic c axis in the orthorhombic unit cell of the crystal. The molecular chains are perpendicular to the lamellar surfaces, that is why the long chain molecules must be folded back and forth many times on a plane perpendicular to the lozenge surface of lamellae, since over 90% of the molecules are many times longer than the lamella thickness. A schematic representation, in which the folds are sharp and regular, is given in Figure 7. The thinnest dimension of the lamellae is along the crystallographic c-axis, the lateral width of the lamellae is along the a-axis, and the b-axis coincides with the longest dimension due to fastest growth rate along this axis during crystallization [38]. Figure 8 illustrates a schematic representation of a possible model for twisted lamellae in spherulitic polyethylene, showing chain-folds and intercrystalline links [39]. Crystalline specimens of polyethylene behave as blocks or lamellae of crystalline material, connected together by tie molecules or crystalline bridges and separated by the amorphous component. These materials can be treated as microscopic composites [40].

In this approach, a laminate composite model was considered for the hard crystalline and soft amorphous phases. The composite theory in the form of a rule of mixtures was used to determine the effect of morphology on modulus. The structure of lamellar texture of polyethylene was considered as a composite solid. For oriented polymers, the

analogy with composite materials was first recognized by Takayanagi, who proposed a series and parallel model for understanding the viscoelastic behaviour of a blend of two isotropic amorphous polymers in terms of the properties of the individual components. He recognized that when one phase is dispersed in the other, there are two limiting possibilities for the stress transfer normal to the direction of tensile stress, such as illustrated in Figure 9 (a); or else there is weak stress transfer across planes containing the tensile stress so that we have the parallel-series model of Figure 9 (b). In Figure 9, the parameter λ expresses the degrees of parallelism and parameter Φ the degree of series connection. For an amorphous phase (A) dispersed in a crystalline phase (C), he devised series-parallel and parallel-series models, with the two extreme possibilities for the stress transfer. For stress transfer perpendicular to the direction of tensile stress we have the series-parallel model in which the overall modulus is given by [25, 41, 42]:

$$E = (1/(\Phi/(\lambda^*E_a + (1-\lambda)^*E_c) + (1-\Phi)/E_c))$$
(6.5)

If the stress transfer across planes containing the tensile stress is weak, we have the parallel-series model, giving a modulus [25, 41, 42]:

$$E = \lambda / (\Phi/E_a + (1-\Phi)/E_c) + (1-\lambda)*E_c$$
(6.6)

Where E represents the modulus, with subscripts a and c referring to the amorphous and crystalline components respectively. However, the Takayanagi model does not account for the crystallite geometry and the orientation parameters [41-43].

In order to consider the role of lamellar orientation, crystal dimensions and lamellar thickness in the tensile properties, such that indicated as important parameters from the statistical analysis, we developed equations to calculate the tensile modulus of the crystalline region E_c, Ea the corresponding modulus in the amorphous region and E_{MD} and E_{TD} the calculated tensile modulus in MD and TD respectively by following Takayanagi model. The emphasis is on a model that involves some important morphological parameters describing microstructural information. The basic assumption we made was to use a series-parallel model for the calculation of MD modulus, for the case in which the force is applied along the molecular axis, and a parallel-series model for the calculation of TD modulus for the perpendicularly applied force to the molecular chain with a continuous fraction of amorphous material (such as illustrated in Figure 10). These assumptions were chosen because our previous work showed that PE blown films have structures with lamellae normal's oriented in the MD in an amorphous field that has predominant chain axis orientation in the MD [32]. According to different analysis that were made to compare the predictions of both models with measurements of tensile modulus in MD and TD, the results showed that parallel-series model is appropriate for calculating TD modulus and series-parallel model for MD one. The volume fractions designated λ and Φ are the volume fractions of crystalline phase parallel and perpendicular respectively to the applied tensile stress as indicated in the figures. The product $\lambda.\Phi$ is equal to the volume fraction of the crystalline phase (v). The calculations of elastic constants for crystalline and amorphous components can be done by combing quantitative considerations on orientation, crystal dimensions and crystallinity. Here, we should mention that Samuels [44] developed an analysis that represented the sonic modulus of an oriented crystalline polymer based on the orientation parameters and crystallinity.

Here we consider that the amorphous phase is continuous, we combine some elements of Takayanagi model and Samuels analysis with our statistical analysis to develop equations for the MD and TD modulus and which are based on all important microstructural parameters:

$$E_{c M} = (E_{ic} * X_c * T_{110} * \ell / T_{200}) / (1 - f_{c M})$$
(6.7)

$$E_{c T} = (E_{ic} * X_c * T_{110} * \ell / T_{200}) / (1 - f_{c T})$$
(6.8)

$$E_{a_M} = E_{ia} / (1 - f_{a_M})$$
 (6.9)

$$E_{a T} = E_{ia} / (1 - f_{a T})$$
 (6.10)

$$E_{MD} = L_c/L^* (1/(\Phi/(\lambda^* E_{c_M} + (1-\lambda)^* E_{a_M}) + (1-\Phi)/E_{a_M}))$$
(6.11)

$$E_{TD} = ((L_c/L)^* \ell/T_{110})^{**}0.5)^* (\Phi/(\lambda/E_{c_T} + (1-\lambda)/E_{a_T}) + (1-\Phi)^*E_{a_T})$$
(6.12)

Where E_{ic} and E_{ia} are the moduli of the PE crystal and the amorphous region respectively and are constant. They were reported in various references [38,45-49]. In this work, the values of 7 GPa and 0.3 MPa were used for the modulus of the polyethylene crystal and amorphous region because these values are well established for

polyethylene at room temperature and were the best average estimation among the different calculated modulus values in the literature. f_{c_M} , f_{c_T} , f_{a_M} and f_{a_T} are crystalline and amorphous orientation functions for polyethylene in MD and TD directions. X_c is the crystal weight fraction and T_{110} , T_{200} and ℓ are the average crystallite size in (110), (200) and thickness of lamellae. L_c and L are the length of the crystallite and Long spacing.

6.4.3.3. Evaluation of the model

The validity of the developed model in predicting tensile modulus was determined by comparing the results of modeling with the experimental (measured) results. It was observed that calculated modulus for the machine and transverse directions have a quite similar trend when compared with the measured one. Comparison of model predictions for the modulus versus the measured modulus are shown in Figures 11 (a), (b), (c),(d). Perfect agreement will lie on the line drawn on the graphs. It can be clearly seen that the there is a good agreement between predicted values by the model and the experimental measurements. A better correlation of measured modulus was obtained as a function of calculated modulus for HDPE samples.

6.5. Conclusions

Different types of polyethylene's; LLDPE, LDPE, and HDPE were blown into films under various conditions and used to establish a model that relates structural parameters to tensile properties. Structural parameters were obtained from different experimental techniques. The tensile properties were measured. The modeling was performed using results from statistical analysis to establish fundamental modeling parameters. It was found that parameters such as crystal size, lamellar thickness, crystallinity, and orientation factors have a significant effect on the tensile properties. Based on Takayanagi composite model, we developed a model to calculate MD and TD modulus and compared it favourably with experiments.

6.6. References

- 1. R. M. Patel, T. I. Butler, K. L. Walton, G. W. Knight, *Polymer Engineering and Science*, **34**, 19, 1506 (1994).
- 2. D. Godshall, G. Wilkes, R. K. Krishnaswamy, A. M. Sukhadia, *Polymer*, 44, 5397 (2003).
- 3. J. Lu, B. Zhao, H-J. Sue, ANTEC Proceedings, 1768 (1999).
- 4. E.J. Dormier, J. M. Brady, W. H. Chang, D. J. Barnes, D. S. Schregenberger, *ANTEC Proceedings*, 696 (1989).
- 5. K. R. Krishnaswamy, M. A. Sukhadia, *Polymer*, 41, 9205 (2000).
- 6. X. M. Zhang, S. Elkoun, A. Ajji, M. A. Huneault, *Polymer*, 45, 217 (2004).

- 7. T. H. Kwack, C. D. Han, M. E. Vickers, *Journal of Applied Polymer Science*, **35**, 363 (1988).
- 8. T-H. Yu, G. L. Wilkes, *Polymer*, <u>37</u>, 21, 4675 (1996).
- 9. A. Gupta, D. M. Simpson, I. R. Harrison, *Journal of Applied Polymer Science*, **50**, 2085 (1993).
- 10. Lu J., Sue H-J., Journal of Materials Science, 35, 5169 (2000).
- 11. K-J. Choi, E. J. Spruiell, L. J. White, *Journal of Polymer Science (Physics edition)*, 20, 27 (1982).
- 12. Lu J., Sue H., Journal of polymer Science (Physics Edition), 40, 507 (2002).
- 13. M. A. Sukhadia, ANTEC Proceedings, 160 (1998).
- 14. K. R. Krishnaswamy, M. A. Sukhadia, ANTEC Proceedings, 2395 (2002).
- 15. M. D. Simpson, R. I. Harrison, ANTEC Proceedings, 1206 (1993).
- 16. A. D. Johnston, G. M. McNally, W. R. Murphy, M. H. Billham, G. Garrett, *ANTEC Proceedings*, 3236 (2003).
- 17. K. C. Chai, J-L. Selo, E. Osmont, ANTEC Proceedings, 331(2000).
- 18. A. Ghaneh-Fard, Journal of Plastic Film & Sheeting, 15, 194 (1999).
- 19. K. A. Babel, G. Nagarajan, G. A. Campbell, ANTEC Proceedings, 2112 (1996).
- 20. J. Janzen, *Polymer Engineering and Science*, **32**, 17, 1242 (1992).
- 21.R. L. McCullough, C. T. Wu and J. C. Seferis, *Polymer Engineering and Science*, **16**, 5, 371 (1976).
- 22. J. C. Halpin and J. L. Kardos, *Journal applied physics*, **43**, 5,2235 (1972).
- 23. I. M. Ward, *Proc. Phys. Soc.*, **80**, 1176 (1962).
- 24. H. Brody and I. M. Ward, Polymer Engineering and Science, 11, 2, 139 (1971).
- 25. M. Takayanagi, K. Imada and T. Kajiyama, *Journal of Polymer Science: Part C*, **15**, 263 (1966).

- 26. K. Seungoh, P. G. Lafleur, P. Sammut and M. A. Huneault, *ANTEC Proceedings*, 361 (2003).
- 27. X. Zhang X., S. Elkoun, A. Ajji, M. A. Huneault, Polymer, 45, 217 (2004).
- 28. D. J. Hoffman, L. R. Miller, *Polymer*, 38, 13, 3151 (1997).
- 29. G.W.H. Hohne, *Polymer*, 43, 4689-4698 (2002).
- 30. P. P. Kundu, J. Biswas, H. Kim, S. Choe, European Polymer Journal, 39, 1585 (2003).
- 31. M. Ziberna Sujica, M. Sfiligoj Smole, *Journal of Applied Polymer Science*, **89**,3383 (2003).
- 32. S. Fatahi, A. Ajji and P. G. Lafleur, *Journal of Plastic Film & Sheeting*, 21,281 (2005).
- 33. S. Fatahi, A. Ajji and P. G. Lafleur, *The Polymer Processing Society (PPS)-America's Regional Meeting, (2005).*
- 34. R. J. Pazur and R. E. Prud'homme, Macromolecules, 29, 119 (1996).
- 35. H. Y. Chen, C. C. Chau, T. Bulter, B. Landes, M. Bishop, D. Bellmore, S. P. Chum and C. Dryzga, *ANTEC Proceedings*, 1401 (2003).
- 36. J. Lu, H-J. Sue and T. P. Rieker, *Polymer*, **42**, 4635 (2001).
- 37. S. Fatahi, A. Ajji and P. G. Lafleur, ANTEC Proceedings, 5, 102, (2005).
- 38. X. Guan and R. Pitchumani, Polymer Engineering and Science, 44, 3 (2004).
- 39. L. Lin, A. S. Argon, *Journal of Materials science*, **29**, 294 (1994).
- 40. L. H. Sperling, *Introduction to physical polymer science*, Wiley-Interscience, New York, (1983).
- 41. I. M. Ward, *Mechanical Properties of Solid Polymers*, Wiley-Interscience, New York, (1983).
- 42. I. M. Ward, *Structure and Properties of Oriented Polymers*, Chapman & Hall, London, (1997).

- 43. J. L. Kardos and J. Raisoni, *Polymer Engineering and Science*, 15, 3 (1975).
- 44. R. J. Samuels, *Structured polymer properties*, Wiley-Interscience New York, (1973).
- 45. B. Crist, J. C. Fisher and P. R. Howard, Macromolecules, 22, 1709 (1989).
- 46. I. Sakurada, T. Ito and K. Nakamae, *Journal of Polymer Science: Part C*, **15**, 75 (1966).
- 47. M. J. Doyle, *Polymer engineering and science*, **40**, 2, 330 (2000).
- 48. J. Janzen, Polymer Engineering and Science, 32, 17, 1255 (1992).
- 49. R. H. Boyd, Journal of polymer science: polymer physics Edition, 21, 493 (1983).

TABLE 6.1: The specification of the materials

| GRADE | MFI 1902.16 (g/10 min) | Density (g/cm3) | Density M w (g/cm3) (kg/mol) | M w/M n | Manufacturer |
|-----------------------|---------------------------|-----------------|--|---------------------|------------------------|
| LDPE 503A | 1.9 | 0.923 | $80900^{26} 5.02^{26}$ | 5.02^{26} | Dow Plastics Company |
| LLDPE-Octene FP 120-A | - | 0.92 | 103200^{27} 3.38 ²⁷ | 3.38 ²⁷ | Nova Chemicals Company |
| HD58A | 0.41 | 0.957 | 193885 ²⁶ 12.94 ²⁶ | 12.94 ²⁶ | Dow Plastics Company |
| LDPE LF-Y-819-A | 0.75 | 0.92 | $189200^{27} 9.10^{27}$ | 9.10^{27} | Nova Chemicals Company |
| HDPE DMDF 6200 | 3.4 | 0.955 | • | 1 | Petromont |

TABLE 6.2: XRD results of HDPE films

| Inter crystallite | separation@Amorphous | $R=5 \mathcal{N} \text{ (8sin\Theta)}$ | 0.5336 | 0.5336 | 0.5279 | 0.5260 | 0.5369 | 0.5269 | 0.5336 | 0.5336 | 0.5336 | 0.5298 |
|-----------------------------|---|--|---------|--------|---------|--------|--------|--------|--------|--------|---------|----------|
| Cristal sizes | $L=0.94\lambda/(\beta\cos\Theta)$ | $\Theta(a)$ | 33.50 | 35.30 | 39.56 | 36.88 | 38.19 | 41.05 | 32:92 | 38:03 | 9E'9E | 38.78 |
| Crista | amorphous P=0.89 λ ($\beta \cos\Theta$) | $\Theta(a)$ | 43.90 | 46.73 | 48.68 | 40.72 | 46.99 | 51.00 | 46.48 | 47.19 | 46.78 | 49.68 |
| 20, the scattering angle of | amorphous | hump | 20.78 | 20.78 | 21.01 | 21.09 | 20.65 | 21.05 | 20.78 | 20.78 | 20.78 | 20.93 |
| scattering | zaks | second | 24.86 | 24.46 | 24.55 | 24.53 | 24.82 | 24.63 | 24.67 | 24.42 | 24.67 | 24.36 |
| 20, the | um crystalline peaks | first | 22.38 | 21.99 | 22.09 | 22.11 | 22.34 | 22.17 | 22.20 | 22.00 | 22.21 | 21.93 |
| M | | second | 1.015 | 0.962 | 0.859 | 0.921 | 0.830 | 0.828 | 0.948 | 0.833 | 0.934 | 0.897 |
| FWHM | Full-width at half maxim | first | 0.730 | 0.685 | 0.658 | 982'0 | 0.682 | 0.628 | 0.689 | 0.678 | 0.685 | 0.644 |
| | | | HDPE 1n | HDPE 1 | HDPE 2n | HDPE4n | S ENDH | U93HQH | WE W | 83-СН | HDPE 9h | HDPE 10n |

TABLE 6.3: Process condition for selected samples

| HDPE9n HDPE10n | 107.5 107.5 | 0.88 0.82 | 6.5 6.5 |
|----------------|-------------|-----------|----------|
| | | 0. | 9 |
| HDPE8 | 107.5 | 6.0 | 7 |
| HDPE7n | 96.5 | 1.08 | 9 |
| HDPE6n | 85.5 | | 9 |
| HDPES | 64 | 0.88 | 5.5 |
| HDPE4n | 64 | 1.25 | 9 |
| HDPE2 | 42 | 1.05 | 5.5 |
| HDPE2n | 42 | 1.15 | 9 |
| HDPE1n | 30.5 | 1.35 | 9 |
| | TUR | BUR | FLH (in) |

TABLE 6.4: The measured structural parameters for HDPE

| HDPE2Imi 68.4 (1.c) spacing (L) Thickness 110 200 fM_c_axis fT_c_axis fM_camorph fT-amorph fT-amorph | | Crystallini ty | Crystal length | Long | Lamellar | Crystal size | Crystal size | H . | lerman's Orien | Herman's Orientation Functions | S |
|--|----------|-------------------|----------------|-------------|-----------|--------------|--------------|-----------|----------------|--------------------------------|-----------|
| 68,4 11,47 17,670 31,7 44,5 42,8 0,041 0,000 0,031 68,4 11,46 17,670 40,9 44,4 41,6 0,006 -0,068 0,017 69,6 11,69 17,670 32,4 45,7 42,3 0,049 0,186 0,018 69,8 11,55 17,670 32,4 42,9 40,7 0,066 0,039 0,018 69,8 11,74 17,670 31,1 44,8 42,5 0,039 0,039 0,029 69,2 11,62 17,670 31,1 44,8 42,5 0,066 0,039 0,029 69,2 11,62 17,670 31,1 44,3 42,1 0,066 0,006 0,009 71,0 11,62 17,670 34,6 39,8 42,1 0,066 0,006 0,019 71,0 11,62 17,670 34,6 39,8 39,4 0,073 0,025 0,012 71,0 | | wt % | (Lc) | spacing (L) | Thickness | 110 | 200 | fM_c_axis | fT_c_axis | fM-amorph | fT-amorph |
| 68,4 11,46 17,670 40,9 44,4 41,6 0,006 -0,068 0,017 68,6 11,169 17,670 32,4 45,7 42,3 0,049 0,186 0,018 68,9 11,155 17,670 29,9 42,9 40,7 0,049 0,186 0,018 69,8 11,174 17,670 31,1 44,8 42,5 0,039 -0,030 -0,009 69,2 11,62 17,670 31,1 44,8 42,5 0,039 0,0136 0,006 71,0 11,62 17,670 31,1 44,3 42,1 0,066 0,006 0,006 71,0 11,62 17,670 34,6 39,8 39,4 0,073 -0,025 0,014 71,0 11,670 34,6 39,8 39,4 0,073 -0,025 0,014 8,6 9,59 14,725 34,7 38,4 0,073 -0,152 0,014 70,2 9,6 14,725 <td>HDPE1imi</td> <td>68,4</td> <td>11,47</td> <td>17,670</td> <td>31,7</td> <td>44,5</td> <td>42,8</td> <td>0,041</td> <td>0,000</td> <td>0,031</td> <td>0,039</td> | HDPE1imi | 68,4 | 11,47 | 17,670 | 31,7 | 44,5 | 42,8 | 0,041 | 0,000 | 0,031 | 0,039 |
| 69,6 11,69 17,670 32,4 45,7 42,3 0,049 0,186 0,018 68,9 11,55 17,670 29,9 42,9 40,7 0,066 -0,030 -0,009 69,8 11,55 17,670 31,1 44,8 42,5 0,036 -0,136 0,009 69,3 11,63 17,670 31,1 44,8 42,5 0,036 0,0136 0,009 69,3 11,62 17,670 31,1 44,3 42,1 0,066 0,006 0,005 71,0 11,63 17,670 34,6 36,4 0,073 0,027 0,012 71,0 11,95 17,670 36,3 49,7 37,9 0,023 0,012 71,0 11,95 17,670 36,3 49,7 37,9 0,023 0,012 68,6 9,59 14,725 37,9 46,8 36,4 0,033 -0,125 0,012 71,3 10,01 14,725 38,9 | HDPE2imi | 68,4 | 11,46 | 17,670 | 40,9 | 44,4 | 41,6 | 0,006 | -0,068 | 0,017 | 0,063 |
| 68,9 11,55 17,670 29,9 42,9 40,7 0,066 -0,030 -0,009 69,8 11,74 17,670 31,1 44,8 42,5 0,039 -0,136 0,029 69,3 11,63 17,670 33,8 42,2 41,3 0,066 0,006 0,005 70,0 11,62 17,670 34,6 39,8 42,1 0,066 0,005 0,012 71,0 11,62 17,670 34,6 39,8 39,4 0,073 -0,025 0,014 72,6 12,26 17,670 36,3 49,7 37,9 0,073 -0,025 0,014 70,2 12,26 14,725 36,9 47,2 38,0 0,297 0,120 0,084 70,2 9,84 14,725 38,9 46,5 36,9 0,297 0,127 0,084 70,2 9,84 14,725 38,9 46,5 36,9 0,146 0,147 0,147 69,3 | HDPE3imi | 9'69 | 11,69 | 17,670 | 32,4 | 45,7 | 42,3 | 0,049 | 0,186 | 0,018 | -0,073 |
| 69,8 11,74 17,670 31,1 44,8 42,5 0,039 -0,136 0,029 69,3 11,63 17,670 33,8 42,2 41,3 0,066 0,006 0,005 69,2 11,62 17,670 31,1 44,3 42,1 0,066 0,006 0,005 77,0 11,95 17,670 34,6 39,8 39,4 0,073 -0,025 0,014 72,6 12,25 17,670 34,6 49,7 37,9 0,269 -0,152 0,014 68,6 9,59 14,725 46,7 46,8 36,4 0,237 -0,127 0,094 70,2 9,84 14,725 38,9 46,5 38,9 0,292 -0,127 0,094 68,7 9,61 14,725 38,9 46,5 38,9 0,248 0,212 0,117 0,184 71,3 10,01 14,725 38,9 40,5 36,9 0,186 -0,116 0,167 | HDPE4imi | 6'89 | 11,55 | 17,670 | 29,9 | 42,9 | 40,7 | 0,066 | -0,030 | 600'0- | 0,051 |
| 69,3 11,63 17,670 33,8 42,2 41,3 0,066 0,006 0,005 69,2 11,62 17,670 31,1 44,3 42,1 0,053 0,027 0,012 71,0 11,95 17,670 34,6 39,8 39,4 0,053 0,027 0,012 72,6 12,25 17,670 35,3 49,7 37,9 0,269 -0,025 0,014 68,6 9,59 14,725 45,7 46,8 36,4 0,297 -0,127 0,094 68,7 9,61 14,725 38,9 46,5 38,0 0,297 -0,127 0,094 71,3 10,01 14,725 38,9 46,5 36,9 0,292 -0,212 0,167 69,3 9,69 14,725 39,9 40,7 38,2 0,186 -0,161 0,041 70,7 9,91 14,725 39,9 40,7 36,9 0,140 0,108 -0,013 -0,032 | HDPE5imi | 8'69 | 11,74 | 17,670 | 31,1 | 44,8 | 42,5 | 0,039 | -0,136 | 0,029 | 0,134 |
| 69,2 11,62 17,670 31,1 44,3 42,1 0,053 0,027 0,012 71,0 11,95 17,670 34,6 39,8 39,4 0,073 -0,025 0,014 72,6 12,25 17,670 35,3 49,7 37,9 0,269 -0,152 0,014 68,6 9,59 14,725 35,9 46,5 38,0 0,297 -0,127 0,094 68,7 9,61 14,725 38,9 46,5 35,9 0,297 -0,127 0,094 71,3 10,01 14,725 38,9 51,0 41,1 0,282 -0,127 0,167 69,3 9,69 14,725 38,9 51,0 41,1 0,248 -0,161 0,135 69,3 9,69 14,725 39,9 40,7 36,9 0,140 -0,161 0,047 70,7 9,91 14,725 36,2 48,7 39,6 0,140 -0,108 0,013 69,5 | HDPE6imi | 69,3 | 11,63 | 17,670 | 33,8 | 42,2 | 41,3 | 0,066 | 900'0 | 900'0 | 0,042 |
| 71,0 11,95 17,670 34,6 39,8 39,4 0,073 -0,025 0,014 72,6 12,25 17,670 35,3 49,7 37,9 0,269 -0,152 0,080 68,6 9,59 14,725 45,7 46,8 36,4 0,297 -0,127 0,094 70,2 9,84 14,725 38,9 46,5 36,9 0,297 -0,127 0,094 68,7 9,61 14,725 38,9 46,5 35,9 0,292 -0,127 0,167 69,3 9,69 14,725 39,9 47,0 38,2 0,186 -0,161 0,47 71,8 10,08 14,725 39,9 47,0 38,2 0,146 -0,116 0,047 70,7 9,91 14,725 36,2 46,7 36,9 0,140 -0,108 0,041 69,5 9,91 14,725 36,2 46,7 36,9 0,140 -0,103 -0,103 69,5 | HDPE7imi | 69,2 | 11,62 | 17,670 | 31,1 | 44,3 | 42,1 | 0,053 | 0,027 | 0,012 | 0,026 |
| 72,6 12,25 17,670 35,3 49,7 37,9 0,269 -0,152 0,080 68,6 9,59 14,725 45,7 46,8 36,4 0,213 -0,220 0,094 0 70,2 9,84 14,725 38,9 46,5 38,0 0,297 -0,127 0,094 0 68,7 9,61 14,725 38,9 46,5 35,9 0,292 -0,127 0,094 0 71,3 10,01 14,725 38,9 51,0 41,1 0,248 -0,161 0,135 0 69,3 9,69 14,725 39,9 40,7 36,9 0,140 -0,108 0,140 0,047 0,083 -0,108 0,041 0,04 | HDPE8imi | 71,0 | 11,95 | 17,670 | 34,6 | 39,8 | 39,4 | 0,073 | -0,025 | 0,014 | 0,076 |
| 68,6 9,59 14,725 46,8 36,4 0,313 -0,220 0,279 70,2 9,84 14,725 37,9 47,2 38,0 0,297 -0,127 0,094 68,7 9,61 14,725 38,9 46,5 35,9 0,292 -0,161 0,167 71,3 10,01 14,725 39,9 51,0 41,1 0,248 -0,161 0,135 69,3 9,69 14,725 40,9 47,0 38,2 0,186 -0,116 0,047 71,8 10,08 14,725 39,9 40,7 36,9 0,140 -0,108 0,041 70,7 9,91 14,725 36,2 48,7 39,6 0,083 -0,073 -0,032 69,5 9,73 14,725 36,2 46,7 35,3 0,102 -0,101 -0,003 69,7 9,76 14,725 37,9 45,9 33,5 0,062 -0,101 -0,107 | HDPE10n | 72,6 | 12,25 | 17,670 | 35,3 | 49,7 | 37,9 | 0,269 | -0,152 | 080'0 | 0,292 |
| 70,2 9,84 14,725 37,9 47,2 38,0 0,297 -0,127 0,094 68,7 9,61 14,725 38,9 46,5 35,9 0,292 -0,212 0,167 71,3 10,01 14,725 39,9 51,0 41,1 0,248 -0,161 0,135 1 71,8 10,08 14,725 39,9 40,7 36,9 0,140 -0,116 0,041 1 70,7 9,91 14,725 36,2 46,7 36,9 0,083 -0,073 -0,032 1 69,5 9,73 14,725 36,2 46,7 35,3 0,102 -0,101 -0,003 1 69,5 9,73 14,725 36,2 46,7 35,3 0,102 -0,101 -0,003 1 | HDPE9n | 9'89 | 69'6 | 14,725 | 45,7 | 46,8 | 36,4 | 0,313 | -0,220 | 0,279 | 0,235 |
| 68,7 9,61 14,725 38,9 46,5 35,9 0,292 -0,212 0,167 71,3 10,01 14,725 39,9 51,0 41,1 0,248 -0,161 0,135 69,3 9,69 14,725 40,9 47,0 38,2 0,186 -0,116 0,047 70,7 9,91 14,725 36,2 46,7 36,9 0,140 -0,108 0,041 69,5 9,73 14,725 36,2 46,7 35,3 0,102 -0,101 -0,003 69,7 9,76 14,725 37,9 43,9 33,5 0,052 -0,101 -0,003 | HDPE8 | 70,2 | 9,84 | 14,725 | 37,9 | 47,2 | 38,0 | 0,297 | -0,127 | 0,094 | -0,048 |
| 71,3 10,01 14,725 39,9 51,0 41,1 0,248 -0,161 0,135 69,3 9,69 14,725 40,9 47,0 38,2 0,186 -0,116 0,047 71,8 10,08 14,725 39,9 40,7 36,9 0,140 -0,108 0,041 70,7 9,91 14,725 36,2 46,7 39,6 0,083 -0,073 -0,032 69,5 9,73 14,725 36,2 46,7 35,3 0,102 -0,101 -0,003 69,7 9,76 14,725 37,9 43,9 33,5 0,052 -0,068 -0,007 | HDPE7n | 2'89 | 9,61 | 14,725 | 38,9 | 46,5 | 35,9 | 0,292 | -0,212 | 0,167 | 0,407 |
| 69,3 9,69 14,725 40,9 47,0 38,2 0,186 -0,116 0,047 71,8 10,08 14,725 39,9 40,7 36,9 0,140 -0,108 0,041 70,7 9,91 14,725 36,2 48,7 39,6 0,083 -0,073 -0,032 69,5 9,73 14,725 36,2 46,7 35,3 0,102 -0,101 -0,003 69,7 9,76 14,725 37,9 43,9 33,5 0,052 -0,068 -0,007 | HDPE6n | 71,3 | 10,01 | 14,725 | 39,9 | 51,0 | 41,1 | 0,248 | -0,161 | 0,135 | 0,208 |
| 71,8 10,08 14,725 39,9 40,7 36,9 0,140 -0,108 0,041 70,7 9,91 14,725 36,2 48,7 39,6 0,083 -0,073 -0,032 69,5 9,73 14,725 36,2 46,7 35,3 0,102 -0,101 -0,003 69,7 9,76 14,725 37,9 43,9 33,5 0,052 -0,068 -0,007 | HDPE5 | 69,3 | 69'6 | 14,725 | 40,9 | 47,0 | 38,2 | 0,186 | -0,116 | 0,047 | 0,141 |
| 70,7 9,91 14,725 36,2 48,7 39,6 0,083 -0,073 -0,032 69,5 9,73 14,725 36,2 46,7 35,3 0,102 -0,101 -0,003 69,7 9,76 14,725 37,9 43,9 33,5 0,052 -0,068 -0,007 | HDPE4n | 71,8 | 10,08 | 14,725 | 39,9 | 40,7 | 36,9 | 0,140 | -0,108 | 0,041 | 0,141 |
| 69,5 9,73 14,725 36,2 46,7 35,3 0,102 -0,101 -0,003 69,7 9,76 14,725 37,9 43,9 33,5 0,052 -0,068 -0,007 | HDPE2n | 7,07 | 9,91 | 14,725 | 36,2 | 48,7 | 39'6 | 0,083 | -0,073 | -0,032 | 0,058 |
| 69,7 9,76 14,725 37,9 43,9 33,5 0,052 -0,068 -0,007 | HDPE2 | 2'69 | 9,73 | 14,725 | 36,2 | 46,7 | 35,3 | 0,102 | -0,101 | -0,003 | 0,109 |
| | HDPE1n | 2'69 | 9,76 | 14,725 | 37,9 | 43,9 | 33,5 | 0,052 | -0,068 | 200'0- | 0,057 |

TABLE 6.5: The measured structural parameters for LLDPE

| | | Т- | Г | | | | | | | | _ |
|--------------------------------|---------------|--------|--------|--------|--------|--------|--------|--------|--------|--------|---------|
| | fT-amorph | 0,025 | 0,024 | 0,034 | 0,033 | 0,036 | 0,021 | 0,038 | 6:00'0 | 0,013 | 0,011 |
| Herman's Orientation Functions | fM-amorph | 0,021 | 0,008 | 0,034 | 0,016 | 0,013 | 0,002 | 0,012 | 0,034 | 0,022 | 0,050 |
| Herman's Orie | fT_c_axis | 0,011 | 900'0- | -0,017 | -0,004 | 0,017 | 0,013 | 800'0 | 0,026 | 0,061 | 0,030 |
| | fM_c_axis | 0,059 | 0,074 | -0,062 | 0,097 | 0,083 | 0,096 | 680'0 | 0,051 | 0,030 | -0,124 |
| Crystal size | 200 | 30,6 | 32,1 | 32,0 | 32,3 | 32,0 | 31,9 | 29,8 | 30,4 | 31,1 | 32,7 |
| Crystal size | 110 | 36,6 | 38,6 | 9'28 | 38,5 | 37,4 | 37,6 | 35,5 | 36,2 | 36,8 | 39,8 |
| Lamellar | Thicknes s | 14,2 | 14,0 | 13,8 | 13,3 | 13,8 | 14,2 | 13,9 | 14,6 | 12,8 | 14,0 |
| Long | spacing (L) | 11,044 | 13,951 | 13,252 | 13,593 | 13,089 | 14,085 | 13,252 | 11,044 | 11,045 | 9,817 |
| Crystal length | (Lc) | 3,77 | 5,39 | 4,86 | 5,10 | 4,88 | 4,78 | 4,86 | 4,16 | 3,98 | 29'8 |
| Crystallinity | wt% | 37,8 | 42,4 | 40,4 | 41,3 | 41,0 | 37,6 | 40,4 | 41,4 | 38,3 | 40,7 |
| | | LLDPE9 | LLDPE8 | LLDPE7 | LLDPE6 | LLDPE4 | LLDPE3 | LLDPE2 | LLDPE1 | LLDPE5 | LLDPE10 |

TABLE 6.6: The measured structural parameters for LDPE

| St | fT-amorph | 0,032 | 0,049 | 090'0 | 0,048 | 0,037 | 0,046 | 0,026 | 0,049 | 0,055 | 0,036 | 0,022 | 0,010 | -0,003 | 500'0- | 0,007 |
|--------------------------------|-----------|--------|--------|--------|--------|--------|--------|--------|--------|----------|----------|----------|----------|----------|----------|----------|
| Herman's Orientation Functions | fM-amorph | 0,032 | 0,019 | 0,051 | 0,013 | 960'0 | 0;030 | 0,017 | 0,023 | 0,111 | 0,137 | 0,100 | 0,038 | 0,040 | 690'0 | 0,055 |
| Herman's Orie | fT_c_axis | -0,055 | -0,124 | -0,046 | -0,100 | 500'0- | -0,034 | 200'0- | -0,058 | 0,084 | 0,131 | 960'0 | 0,029 | 0,138 | 0,169 | 0,151 |
| | fM_c_axis | 0,012 | 0,091 | 0,117 | 0,117 | 0,117 | 660'0 | 0,071 | 0,158 | -0,041 | -0,119 | 0,020 | -0,146 | -0,098 | -0,135 | -0,104 |
| Crystal size | 200 | 31,7 | 30,4 | 32,8 | 32,8 | 33,7 | 31,5 | 32,9 | 32,0 | 30,6 | 31,1 | 9'08 | 31,8 | 32,3 | 31,8 | 31,3 |
| Crystal size | 110 | 40,2 | 34,3 | 37,4 | 36,5 | 40,7 | 39,6 | 36,0 | 36,1 | 36,1 | 35,1 | 35,2 | 37,6 | 39,0 | 37,4 | 35,3 |
| Lamellar | Thicknes | 9,7 | 9,5 | 9,2 | 8,9 | 9,3 | 9,3 | 9,3 | 9,4 | 8,5 | 8,7 | 8,6 | 8,6 | 8,6 | 8,6 | 8,6 |
| Long | spacing(| 9,817 | 9,817 | 9,817 | 11,044 | 11,044 | 11,044 | 9,817 | 11,044 | 12,622 | 11,044 | 11,044 | 11,400 | 11,780 | 11,780 | 12,186 |
| Crystal Iength | (Lc) | 3,55 | 3,60 | 3,48 | 4,24 | 4,14 | 4,14 | 3,76 | 4,18 | 4,23 | 3,60 | 29'8 | 3,91 | 4,05 | 4,03 | 4,10 |
| Crystallinity | wt % | 6'68 | 39,9 | 39,1 | 42,2 | 41,2 | 41,2 | 42,1 | 37,7 | 37,1 | 36,1 | 36,8 | 38,0 | 38,0 | 37,9 | 37,2 |
| | | LDPE13 | LDPE12 | LDPE11 | LDPE10 | LDPE7 | LDPE5 | LDPE3 | LDPE0 | LDPE1imi | LDPE2imi | LDPE3imi | LDPE4imi | LDPE5imi | LDPE6imi | LDPE7imi |

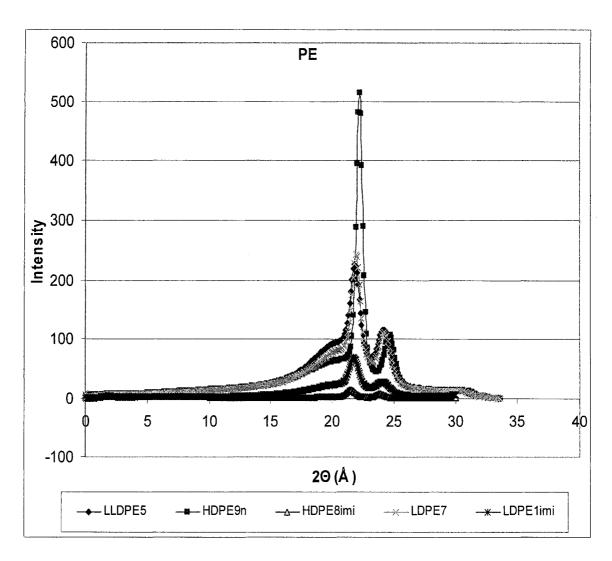


FIG. 6.1. WAXS profiles for PE blown films

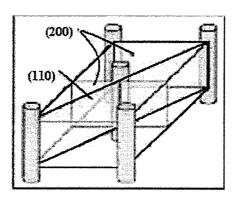


FIG 6.2. Schematic illustration of crystallite

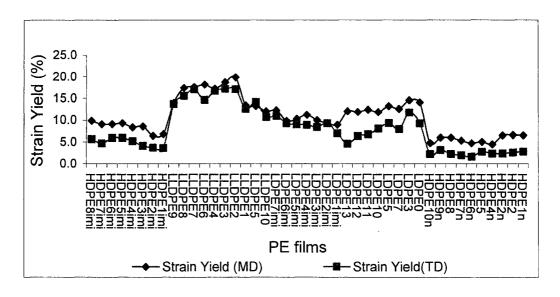


FIG 6.3. Measured strain at yield

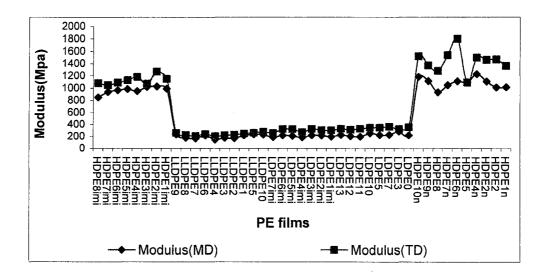


FIG 6.4. Measured tensile modulus

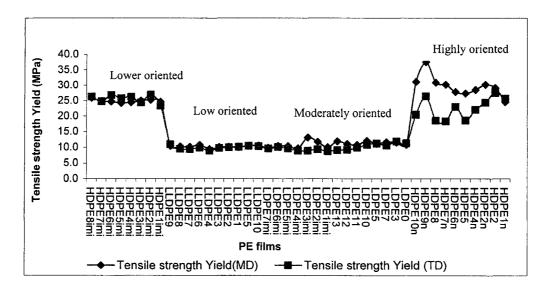


FIG 6.5. Measured tensile strength

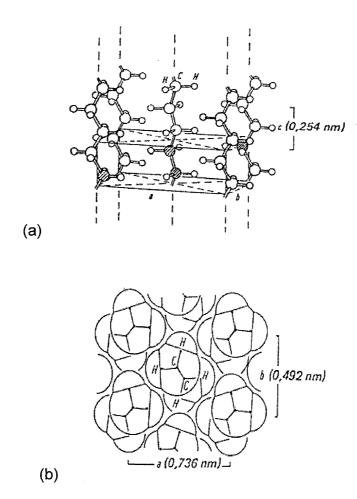


FIG 6.6. Arrangement of the polymer chains in (a) a polyethylene single crystal and (b) View along the C-direction

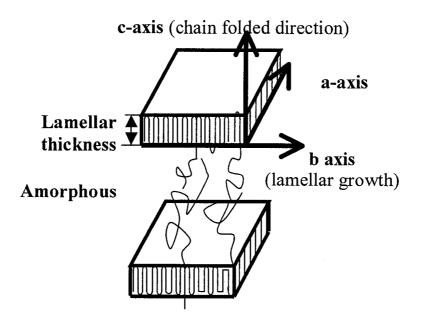


FIG 6.7. The folded chain mode in PE

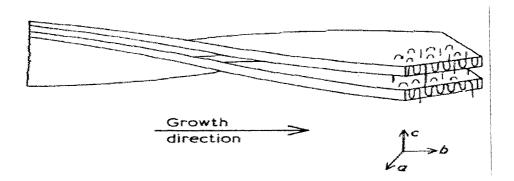


FIG 6.8. Crystalline lamella

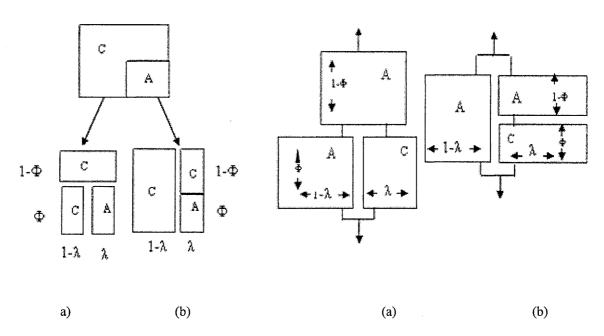


FIG 6.9. Takayanagi models for polymer blends.

FIG 6.10. The series-parallel(a) and parallel-series (b).

The value of λ * Φ is equal to the volume fraction of the amorphous region. (Elements A and C correspond with the amorphous and the crystalline region, respectively.)

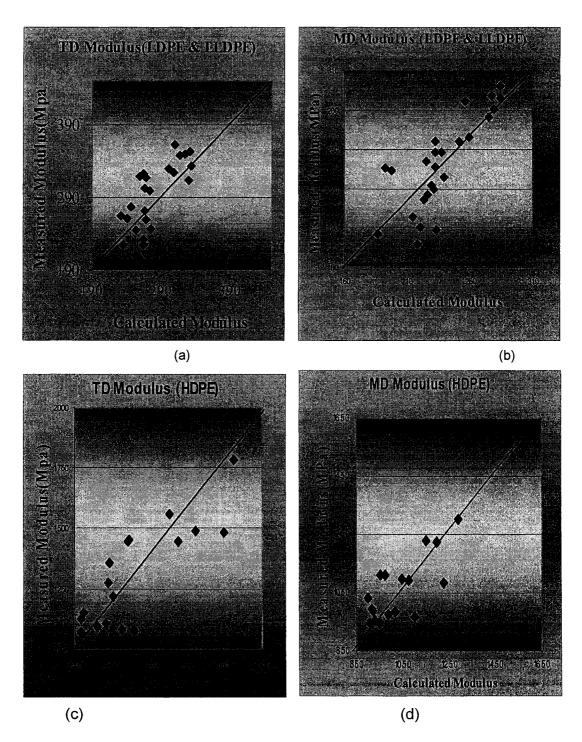


FIG 6.11. Predicted and measured modulus of different PE films

CHAPTER 7

GENERAL DISCUSSIONS

Five PE of different types (HDPE, LDPE and LLDPE) were extruded from two different blown film lines. The effects of three main processing variables (take up ratio, blow up ratio and frost line height) on mechanical and optical properties of the films have been investigated. This part of research work concerned on a better understanding of polymer processing, leading to optimized processes and improved end-use properties. A complete microstructural analysis is performed by SEM and AFM and X-ray diffraction. An important conclusion is that the surface morphology reflects a continuation of the bulk one.

Different techniques were used such as WAXD, pole figure methods, SAXS, DSC, FTIR, birefringence to generate a large quantity of experimental data(44 film samples) thus allowing the understanding of the relations between microstructural parameters and film properties. The important part of this study was to develop models relating detailed structural parameters to performance, providing the means for predicting final films properties.

For the fundamental/structure modeling approach, there are several steps required in the development of a mathematical model that would predict the properties of the blown films as a function of their microstructure variables including statistical modeling, analysis of structure factors, formulation of the structural/fundamental model, simplify and solve the equations, evaluate the model, revise the model.

In statistical modeling, the structural parameters were determined by studying the morphology and orientation of different polyethylene films. WAXS pole figure technique was used to determine the orientation of the crystal phase and the amorphous orientation functions were calculated from the birefringence measurements. The measurement of lamellar thickness, crystal size, the long spacing and the length of the crystallites were accomplished by DSC, WAXD and SAXS techniques.

A linear equation or mathematical model explicitly defining the dependent variables (properties) was used. Then we developed statistical models or equations that show how each of the structural parameters selected contributes to the magnitude of changes of the tensile properties tested. The result of the analysis indicates that lamellar thickness that is an important morphological characteristic of semi-crystalline polymers; has a major effect on tensile properties.

Finally modeling was done by combination of statistical modeling technique and structural modeling. A new model is developed to predict MD and TD modulus and values calculated by the model are in good agreement with experimental data. Since the statistical analysis show that parameters such as crystal size, lamellar thickness, crystallinity, and orientation factors have a significant effect on the tensile modulus, these parameters are considered in the model.

CHAPTER 8

CONCLUSIONS AND RECOMMENDATIONS

8.1 Conclusion

The physical and mechanical properties of polyethylene are known to be strongly influenced by morphological characteristics such as molecular orientation, size and shape of crystalline domains. For example, it has been shown that controlled molecular orientation can result in greatly improved physical and mechanical properties, such as optical property, tensile modulus, impact, and tensile strength. Development of fundamental structure – property (S-P) relationships in PE blown films is also of great importance to blown-film and resins manufacturers. Understanding the S-P relationships will enable film manufacturers to predict the physical and mechanical properties of films and to determine the processing conditions or resin properties required to achieve these properties.

In this work, we focused on the structure and property characterization with the goal to develop a predictive model to relate molecular structure of blown films using different types of polyethylene (LLDPE, HDPE, LDPE) at different process condition, to mechanical and optical properties.

Structural parameters were obtained from WAXD, SAXS, DSC, AFM and, when possible, the results were compared to evaluate the precision of the technique. The crystalline content and the lamellar thickness, obtained respectively from DSC and WAXS technique, were selected for data analysis.

It is believed that the information gained through the statistical study can be used to determine the effects of parameters on each property. It was found that certain parameters such as crystallinity and orientation factors have an effect on the majority of film properties. Based on the statistical technique it was observed that the tensile, optical, and dart impact properties were affected by various structural parameters. The effects chart and response surface show that the modulus in MD, strain at break in MD & TD, strain at yield in MD & TD, tensile strength at yield and also optical property such as haze and clarity correlate well with the crystalline content, orientation parameters for crystalline a-axis along MD & TD, b-axis along MD & TD, amorphous along MD & TD, lamellar thickness and roughness.

SEM images of the films plane surface (MT) and cross section slices in TN and MN planes were made and compared with AFM images. It was observed that the surface morphology reflects a continuation of the bulk morphology for the cases studied.

Changes in the blown film process parameters, such as take up ratio, blow up ratio and frost line height have an affect on structural parameters and mechanical properties. For example, it was observed that the microstructure for HDPE blown films show the row nucleated type structure with lamellae that have normals oriented in the MD in an amorphous field that has predominant chain axis orientation in the MD. As TUR was

increased, the row-nucleated structures became more perfectly aligned in the MD. The dart impact strength increased with an increase in BUR (higher BUR would lead to more balanced orientation as well as to a higher degree of planar orientation).

A model was developed using the results of statistical analysis for the establishment of fundamental modeling parameters. From statistical analysis, it was found that parameters such as crystal size lamellar thickness, crystallinity and orientation factors have a significant effect on the tensile properties. Based on Takayanagi composite approach, we developed a model to calculate MD and TD modulus, which was compared with experiments.

8.2 Recommendations

Based on the research work carried out here, several recommendations can be made for future work.

- To extend the phenomenological model to the prediction of dart impact and haze.
- The film industry has been widely using blends of LLDPE resin with LDPE to facilitate processing and to increase film rigidity, puncture resistance, tensile strength,

Elmendorf tear strength and dart impact strength. It would be interesting for film producers to extend an analysis between structure and properties to blend of this type.

- To analyse the influence of Additives (Calcium stearate, Heat stabilizer, UV stabilizer) on the relationship between structure parameters and their performance.
- To study the influence of molecular parameters of polyethylene polymers, like MW,
 MWD and LCB, on the microstructure and the final properties of blown films.
- To repeat this study for metallocene catalyzed polyethylenes.

CHAPTER 9

SCIENTIFIC CONTRIBUTIONS

This research work contributes to the field of science, more specifically to the field of polymer processing, in various ways. Scientific contributions are listed below:

- It is recognized that the properties of blown films are greatly influenced by structure development during their fabrication. But from the various literature studied on this subject, it was found that this field lacks the fundamental understanding concerning how to relate the molecular structure to the properties of blown films.
- PE films are used in various applications such as food packaging, grocery bags, etc.

 Although the majority of all film markets have different performance requirements, high tensile strength, superior tear and dart impact strength are always desired. PE film manufactures have been aggressive in improving these properties and reducing production cost so that they can be more competitive in the global market. So developing a model to predict final properties of PE films will be interesting for many film producers in commercial process because of high demand for high performance film, economic problems and difficulty in process condition. Thus information

concerning blown film structure and structure-property relationship is important to PE film manufactures.

References:

Aggarwal L. S., Tilley P. G., Sweeting J. O., (1959). "Orientation in extruded polyethylene films". *Journal of Applied Polymer Science*. 1. 91-100.

Ajji, A., and Zhang, X., (2002). "Correlations between orientation and some properties of polymer films and sheets". *ANTEC Proceedings*. 1651-1655.

Ashizawa H., Spruiell E. J., White L. J.,(1984)." An investigation of optical clarity and crystalline orientation in polyethylene tubular film". *Polymer Engineering and Science*. 24:13. 1035- 1042.

Babel K. G., Campbell A. G., (1995). "A model linking process variables to the strength of blown films produced from LDPE and LLDPE". *Tappi Journal*. 78:5. 199-204.

Babel, A.K., Nagarajan, G. and Campbell, G. A. (1996). "Kinematics, structure and properties relationship of polyethylene blown films". *ANTEC Proceedings*. 2112-2119.

Benedikt M. G., (1999)." Metallocene technology in commercial applications". Society of plastics engineering, plastic design library (pdl).137-146.

Boix M. J., Bernabeu E., Barba C.,(2000). "An optical microstructural model for blown polyethylene films". *Journal of Applied Polymer Science*. 75. 1708-1720.

Boyd R. H. (1983)."The mechanical moduli of lamellar semicrystalline polymers".

Journal of polymer science: polymer physics Edition. 21. 493-504.

Brody H. and Ward I.M., (1971)."Modulus of short carbon and glass fiber reinforced composites". *Polymer Engineering and Science*.11:2.139-151.

Butler F. M., Donald M. A., (1998). "Real-time in situ light scattering and X-ray scattering studies of polyethylene blown film deformation". *Journal of applied polymer Science*. 67. 321-339.

Butler T. I., Lai S., Patel P. R., Spuria E. J., (1994). "Blown film frost-freeze Line interactions", *ANTEC Proceedings*. 15-27.

Chai, K. C., Selo, J.-L., and Osmont, E., (2000). "Influence of molecular weight distribution on LLDPE blown film processing conditions and property sensitivity". *ANTEC Proceedings*. 331-335.

Chen H. Y., Chau C. C., Bulter T., Landes B., Bishop M., Bellmore D., Chum S. P. and Dryzga C., (2003)." Orientation and property correlation on LLDPE blown films".

ANTEC Proceedings, 1401-1405.

Choi K-J., Spruiell E. J., White L. J.,(1982)."Orientation and morphology of High Density Polyethylene film produced by the tubular blowing method and its relationship to process conditions". *Journal of Polymer Science(Physics edition)*. 20. 27-47.

Cole, K. C., and Ajji, A.,(2000). Characterization of Orientation in Solid Phase *Processing of Polymers, Ward IM, Coates PD, and Dumoulin MM (Eds.)*. Carl Hanser Verlag. Munich.

Cole, K. C., Legros, N. and Ajji, A., (1998). "Infrared spectroscopic characterization of blown PE films". SPE Conference Proceedings on Orientation of Polymers. 322-334.

Crist B., Fisher J. C. and Howard P. R., (1989)."Mechanical properties of model polyethylenes: Tensile elastic modulus and yield stress". *Macromolecules*. 22. 1709-1718.

Dormier E.J., Brady M. J., Chang H. W., Barnes D. J., Schregenberger D. S., (1989). "Structure/ processing / property relationships for high molecular weight high density polyethylene blown film", *ANTEC Proceedings*. 696-701.

Doyle M. J., (2000)."On the effect of crystallinity on the elastic properties of semicrystalline polyethylene". *Polymer engineering and science*, 40: 2. 330-335.

Fatahi S., Ajji A. and Lafleur P.G., (2005)."Correlation between structural parameters and property of PE blown films". *Journal of Plastic Film & Sheeting*. 21. 281-305.

Fatahi S., Ajji A. and Lafleur P.G., (2005)."Investigation on structure of different PE blown films" *The Polymer Processing Society(PPS)-America's Regional Meeting*.

Fatahi S., Ajji A. and Lafleur P.G., (2005). "Structure-Property Correlations For PE Blown Films". *ANTEC Proceedings*. 5. 102-106.

Fava R., (1973)." Methods of experimental physics: polymers". New York. Academic Press.

Fruitwala H., Shirodkar P.,(1994)."Characterization of blown film morphology", *ANTEC Proceedings*. 2252-2256.

Ghaneh-Fard, A., (1999). "Effects of film blowing conditions on molecular orientation and mechanical properties of polyethylene films", *Journal of Plastic Film & Sheeting*. 15:3. 194-218.

Godshall, D., Wilkes, G., Krishnaswamy, R.K., and Sukhadia, A.M.,(2003). "Processing-structure-property investigation of blown HDPE films containing both machine and transverse direction oriented lamellar stacks". *Polymer*. 44:18. 5397-5406.

Guan X. and Pitchumani R., (2004)." A micromechanical model for the elastic properties of semicrystalline thermoplastic polymers". *Polymer Engineering and Science*. 44:3. 433-451.

Guichon O., Seguela R., David L., Vigier G.,(2003). "Influence of the molecular architecture of Low Density polyethylene on the texture and mechanical properties of blown films". *Journal of Polymer Science*, (Physics Edition). 41. 327-340.

Gupta A., Simpson M. D., Harrison R. I.,(1993)." A morphological study of HDPE Blown films using small angle X-ray scattering ". *Journal of Applied Polymer Science*. 50. 2085-2093.

Gupta A., Simpson M. D., Harrison R. I.,(1993)." Development of crystalline morphology in polyethylene blown films using small angle X-ray scattering (SAXS)". ANTEC Proceedings. 1201-1205.

Halpin J. C. and Kardos J. L., (1972)."Moduli of crystalline polymers employing composite theory". *Journal applied physics*. 43:5. 2235-2241.

Haudin, M. J., Piana, A., Monasse B., and Gourdon B., (2003). "Étude des relations entre mise en forme, orientation et rétraction dans des films de polyéthyléne basse densité réalisés par soufelage de gaine". *Ann. Chim. Sci. Mat.*, 28:1.91-107.

Heuvel, H.M. and Huisman, R.,(1985). "Infrared spectra of poly(ethylene terephthalate) yarns. Fitting of spectra, evaluation of parameters, and applications" *J. Appl. Polym. Sci.*, 30:7. 3069-3093.

Hobbs K. J., Miles J. M., (2001)." Direct observation of polyethylene Shih-Kebab crystallization using in-situ Atomic Force Microscopy". *Macromolecules*. 34. 353-355.

Hoffman, D. J., and Miller, L. R., (1997)." kinetics of crystallization from the melt and chain folding in polyethylene fractions revisited :theory and experiment". *Polymer*. 38:13. 3151-3212.

Hohne, G.W.H., 2002. Another approach to the Gibbs-Thomosn equation and the melting point of polymers and oligomers. *Polymer*, 43:17. 4689-4698.

Holmes R. D., Miller G. R., Palmer P. R., Bunn W. C., (1953). "Crossed amorphous and crystalline chain orientation in polyethylene film". *Nature*. 171. 1104-1106.

Janzen J., (1992). "Crystallite elastic constants and macroscopic moduli of isotropic semicrystalline polyethylenes". *Polymer Engineering and Science*. 32: 17. 1255-1260.

Janzen J.,(1992)."Elastic moduli of semicrystalline polyethylenes compared with theoretical micromechanical models for composites". *Polymer Engineering and Science*. 32:17. 1242-1254.

Johnston A. D., McNally G. M., Murphy W. R., Billham M. H., Garrett G., (2003)."The effect of frost line height changes on blown film using metallocene catalysed polyethylene". *ANTEC Proceedings*. 3236-3240.

Kardos J. L. and Raisoni J., (1975)."The potential mechanical response of macromolecular systems-A composite analogy". *Polymer Engineering and Science*. 15:3.183-190.

Keller A., (1954). "Perpendicular orientations in polyethylene". *Nature*. 174. 926-927.

Keller A., Machin J. M., (1967) "Oriented crystallization in polymers". *Journal of Macromolecular Science (Phys.)*. B1 (1). 41-91.

Kim Y.-M., Kim, C.-H., Park, J.-K., Lee, C.-W., and Min, T.-I.,(1997). "Morphological considerations on the mechanical properties of blown High-Density Polyethylene films". *Journal of Applied Polymer Science*. 63:3. 289-299.

Klug H., Alexander L., (1954). "X-ray diffraction procedure for polycrystalline and amorphous materials". New York. John Wiley.

Krishnaswamy K. R., Lamborn J. M.,(2000)."Tensile properties of Linear Low Density Polyethylene blown films", *Polymer Engineering and Science*. 40:11. 2385-2396.

Krishnaswamy, K. R. (2001). "Structure-property relationships in HMW-HDPE blown films". *ANTEC Proceedings*. 111-115.

Krishnaswamy, K. R. and Sukhadia, A. M. (2000). "Orientation characteristics of LLDPE blown films and their implications on Elmendorf tear performance". *Polymer*, 41:26. 9205-9217.

Krishnaswamy, R.K., and Sukhadia A.M., (2002)."The influence of solid-state morphology on the impact strength of Linear Low Density Polyethylene blown films". *ANTEC proceedings*. 2395-2399.

Kundu P. P., Biswas J., Kim H., Choe S.,(2003)."Influence of film preparation procedures on the crystallinity, morphology and mechanical properties of LLDPE films". *European Polymer Journal*. 39. 1585-1593.

Kwack T. H., Han D. C., Vickers E. M., (1988). "Development of crystalline structure during tubular film blowing of Low Density Polyethylene", *Journal of Applied Polymer Science*. 35. 363-389.

Larena A., Pinto G., (1993)." The effect of surface roughness and crystallinity on the light scattering of polyethylene tubular blown films", *Polymer Engineering and Science*. 33:12. 742-747.

Lin L., Argon A. S., (1994). "Review structure and plastic deformation of polyethylene". *Journal of Materials science*. 29. 294-323.

Lindenmeyer H. P., Lustig S., (1965). "Crystallite orientation in extruded polyethylene film". *Journal of applied polymer science* . 9. 227-240.

Lu J., Sue H-J., Rieker T. P.,(2001)."Dual crystalline texture in HDPE blown films and its implication on mechanical properties". *Polymer* . 42. 4635-4646.

Lu J., Sue H. J., Rieker T., (2000). "Characterization of Dual Crystalline Texture and Process-Structure-Property relationships in HDPE blown films". *ANTEC proceedings*. 1620-1625.

Lu, J. and Sue, H-J. (2000). "Morphology and mechanical property relationship in Linear Low density Polyethylene blown films", *Journal of Materials Science*. 35:20. 5169-5178.

Lu, J., and Sue, H.,(2002). "Morphology and mechanical properties of blown films of a Low Density Polyethylene/Linear Low Density Polyethylene blend". *Journal of polymer Science (Physics Edition)*, 40:6. 507-518.

Lu, J., Zhao, B. Sue H-J.,(1999). "Phase structure characterization and processing-structure-property relationships in Linear Low Density Polyethylene Blown Films". *ANTEC Proceedings*. 1768-1774.

Magill H. J., Peddada V. S., Mcmanus M. G.,(1981)."Crystallization morphology polymer processing correlations for IUPAC Low Density Polyethylenes". *Polymer Engineering and Science*. 21:1. 1-7.

Mandelkern L., (1964)." Crystallization of polymers". McGraw-Hill: New York.

Matthews G. R., Ajji A., Dumoulin M. M., Prud'home E. R., (2000). "The effects of stress relaxation on the structure and orientation of tensile drawn polyethylene terephthalate". Polymer. 41. 7139-7145.

McCullough R. L., WU C. T. and Seferis J. C., (1976)."Predictions of limiting mechanical performance for anisotropic crystalline polymers". *Polymer Engineering and Science*. 16:5, 371-387.

Murakami S., Kohjiya S., Shimamura K.,(2000)."Comparative study of structure and tensile properties of melt-pressed and extruded-blown films of HDPE", *Journal of Macromol. Sci.-Phys.*, B39 (5&6), 645-655.

Pakhomov M. P., Khizhnyak S., Reuter H., Galitsyn V., Tshmel A.,(2003)."Effect of intercrystallite straight chain segments on Young's modulus of gel-spun polyethylene fibers". *Polymer*. 44. 4651-4654.

Patel, R.M., Butler T.I., Walton K.L., and Knight, G.W. (1994). "Investigation of processing-structure-properties relationships in polyethylene blown films", *Polymer Engineering and Science*. 34: 19. 1506-1514.

Pazur J. R., Ajji A., Prud'homme E. R., (1993). "X-ray and birefringence orientation measurements on uniaxially deformed polyethylene film". *Polymer*. 34:19. 4004-4014.

Pazur R. J. and Prud'homme R. E., (1996). "X-ray figure and small angle scattering measurements on tubular blown low-density poly(ethylene) films". *Macromolecules*, 29,119-128.

Pendley W. M., Wobser D. M.,(1992)."Optimization of HMW-HDPE film properties utilizing IBC systems". *Journal of Plastic film & Sheeting*. 8. 48-74.

Sakurada I., Ito T. and Nakamae K., (1966)."Elastic moduli of the crystal lattices of polymers". *Journal of Polymer Science: Part C.* 15. 75 –91.

Samuels R. J., (1973). Structured polymer properties, Wiley-Interscience New York.

Seungoh K., Lafleur G. P., Sammut P., Huneault A. M., (2003). "Effects of molecular structure of polyethylenes on their bubble instabilities in film blowing extrusion". *ANTEC Proceedings*. 2003. 361-365.

Simpson, D.M., and Harrison, I.R., (1993). "The effect of processing parameters on the morphologies and mechanical properties of polyethylene blown films". *ANTEC Proceedings*. 1206-1209.

Smith F. P., Chun I., Liu G., Dimitrievich D., Rasburn J., Vancso J. G.,(1996)." Studies of optical haze and surface morphology of blown polyethylene films using Atomic Force Microscopy", *Polymer Engineering and Science*. 36:16. 2129-2134.

Sperling L. H., (1983). *Introduction to physical polymer science*, Wiley-Interscience, New York.

Stein, R. S., (1963). Newer Methods in Polymer Characterization. Chap. IV. Wiley-Interscience. New York.

Sujica Z. M., Smole S. M.,(2003). "Structure-mechanical properties relationship of polyethylene terephthalate fibers". *Journal of Applied Polymer Science*. 89.3383-3389.

Sukhadia, A.M.,(1998). "The effects of molecular structure rheology, morphology and orientation on polyethylene blown film properties". *ANTEC proceedings*. 160 - 168.

Takayanagi M., Imada K. and Kajiyama T., (1966)." Mechanical properties and fine structure of drawn polymers". *Journal of Polymer Science: Part C*, 15, 263-281.

Wang L., kamal M. R., Rey A. D.,(2001)."Light transmission and haze of polyethylene blown thin films". *Polymer Engineering and Science*. 41:2. 358-372.

Ward I. M., (1962)." Optical and mechanical anisotropy in crystalline polymers". *Proc. Phys. Soc.*, 80. 1176-1188.

Ward I. M., (1983). *Mechanical Properties of Solid Polymers*, Wiley-Interscience, New York.

Ward M. I., (1997)." Structure and properties of oriented polymers". Second Edition. Chapman & Hall. London.

Wong M. C., Shih H. H., Huang J. C., (1998) ."Effect of various polyethylene structures on film extrusion", *Journal of Reinforced Plastics and Composites*. 17: 10. 945-954.

Yu T. H., Wilkes L. G., (1996). "Influence of molecular weight distribution on the melt extrusion of high density polyethylene (HDPE): Effects of melt relaxation behaviour on morphology and orientation in HDPE extruded tubular films". *Journal of Rheology*. 40:6. 1079-1093.

Yu T-H., Wilkes L. G., (1996). "Orientation determination and morphological study of HDPE extruded tubular films". *ANTEC Proceedings*. 2200-2204.

Yu T-H., Wilkes L. G.,(1996)." Orientation determination and morphology study of high density polyethylene extruded tubular films: effect of processing variables and molecular weight distribution". *Polymer*. 37:21. 4675-4687.

Zhang X.M., Elkoun S., Ajji A., Huneault M.A.,(2004). "Oriented structure and anisotropy properties of polymer blown films: HDPE, LLDPE and LDPE". *Polymer*. 45.p. 217-229.

Zhang, X.M., Verilhac, J. M. and Ajji, A., (2001)."Processing- structure-properties relationship of multilayer films. 1.Structure characterization". *Polymer*. 42:19. 8179-8195.

Zhou H., Wilkes L. G., (1998)." Creep behaviour of high density polyethylene films having well-defined morphologies of stacked lamellae with and without an observable row-nucleated fibril structure". *Polymer*. 39:16. 3597-3609.

APPENDICES on CD-ROM:

- 1- Process condition
- 2- The effect of process condition on properties
- 3- SEM images
- 4- AFM images
- 5- FTIR results
- 6- WAXD results
- 7- SAXS results
- 8- Experimental design
- 9- Modeling